Nicotinic regulation of acetylcholine release from rat brain hippocampus

Thorne, Beverley Ann

Award date:
1990

Awarding institution:
University of Bath

NICOTINIC REGULATION OF ACETYLCHOLINE RELEASE

FROM RAT BRAIN HIPPOCAMPUS

Submitted by BEVERLEY ANN THORNE

for the degree of PhD of the

University of Bath

1990

ProQuest LLC
789 East Eisenhower Parkway
P.O. Box 1346
Ann Arbor, MI 48106-1346

FOR DAD AND ME

ACKNOWLEDGEMENTS

I am indebted to my supervisor Dr. Susan Wonnacott for the scientific training I have received and for her help, encouragement and patience during this learning period. I am grateful to Dr. Graham Riley, of Beecham Pharmaceuticals, for his useful discussion and his assistance in the processing of this thesis.

I would like to thank SERC and Beecham Pharmaceuticals for financial support of this project; Dr. Gary Noy for his help with the electrophysiological work; Kate Powell for guidance during the electron microscopy studies; Bob Powell for constructing the constant temperature cabinet and for maintaining the equipment used in these experiments; Bill Moss for helping with the synthesis of bromoacetylcholine and for compiling the chemical structures of the appendix; Bath University animal house for caring for the animals used, in particular Mike Hinton.

Lastly, I would like to thank all the people, past and present, of the nicotine lab and the Bath University Wine Tasting Society for making my stay at Bath enjoyable. I am especially grateful to Jane Irons for typing this report.

SUMMARY

A superfusion system, originally devised to examine dopamine release from striatal synaptosomes, was adapted to study nicotine-evoked acetylcholine release from hippocampal synaptosomes, isolated on sucrose gradients. This evoked acetylcholine release was low. Modifications to the protocol were made to increase this response. An enzymic extraction procedure was devised that showed that most, if not all, the collected radioactivity from the superfusion system was associated with acetylcholine. This is consistent with the observation that 96.6% of the [^{3}H]choline taken up by the synaptosomes was acetylated to acetylcholine.

During the course of these experiments a method for isolating cortical synaptosomes using Percoll was described. This procedure was applied to the hippocampus and the cholinergic nature of the fractions was assessed using the markers: acetylcholinesterase, choline acetyltransferase and [^{3}H]choline uptake. From these experiments, fraction F4 had the highest cholinergic activity. When compared with the sucrose-isolated synaptosomes, fraction F4 had four to five times greater response to nicotine in the superfusion system, which was consistent with the six fold higher [^{3}H]choline uptake. The subcellular content of the fractions from both the sucrose and Percoll gradients were examined by electron microscopy.

Nicotine evoked acetylcholine release, from Percoll fraction F4 synaptosomes, in a dose-dependent manner. This release was Ca^{++} dependent and sensitive to the nicotinic antagonist dihydroβerythroidine indicating that the response was mediated via the nicotinic acetylcholine receptor located on the presynaptic nerve

terminals. In view of their therapeutic use in Alzheimer's disease, the effect of the acetylcholinesterase inhibitors: BW284C51, physostigmine and 9, amino 1,2,3,4-tetrahydroacridine, on basal and evoked acetylcholine release was examined. The results showed that these drugs had more than a purely anticholinesterase action as they appear to interact with either the nicotinic acetylcholine receptor or other ion channels.

Preliminary extracellular electrophysiological recordings from the hippocampal site confirmed that functional presynaptic nicotinic acetylcholine receptors are present.

ABBREVIATIONS

AcCoA	acetyl Coenzyme A
ACh	acetylcholine
AChE	acetylcholinesterase
ANTX	(+)anatoxin-a
ATP	adenosine triphosphate
αBGT	α-bungarotoxin
BSA	bovine serum albumin
BW284C51	1,5 bis(4 allyl dimethylammonium phenyl)dibromide
Ca^{++}	calcium
Ch	choline
ChAT	choline acetyltransferase
ChK	choline kinase
CNS	central nervous system
DHβE	dihydroβerythroidine
DMPP	1,1 dimethyl-4-phenylpiperazinium iodide
DTNB	5,5′ dithiobis(2-nitrobenzoate)
GABA	gamma aminobutyric acid
G protein	guanine nucleotide regulatory protein
HAChT	high affinity choline transporter
HC-3	hemicholinium-3
5HT	5 hydroxytryptamine
K^+	potassium
kDa	kilodaltons
LAChT	low affinity choline transporter
LDH	lactate dehydrogenase
LTP	long term potentiation
mAChR	muscarinic acetylcholine receptor

Mg	magnesium
Na^+	sodium
nAChR	nicotinic acetylcholine receptor
NADH	nicotinamide adenine dinucleotide
NMS	N-methylscopolamine
PPO	2,5 diphenyloxazole
PVP	polyvinylpyrrolidone
QNB	quinuclidinyl benzilate
SDAT	senile dementia of the Alzheimer type
THA	9,amino 1,2,3,4 tetrahydroacridine
TPB	tetraphenylboron

CONTENTS

FIGURES

TABLES

CHAPTER 1. INTRODUCTION

1.1 THE HIPPOCAMPUS

1.1.1 Historical perspective

The hippocampus, situated in the subcortex of the brain was first named by Arantius (1587) who was a student of Vesalius:

> "At the base of these ventricles which face inward toward the median line, an elevation of white substance rises up and, as it were, grows there. This is raised up from the inferior surface like an appendage and is continuous with the psalloid body or hyra. In its length it extends towards the anterior parts and the front of the brain, and is provided with a flexous figure of varying thickness. This recalls the image of a hippocampus, that is of a little sea-horse."
>
> Arantius, 1587.

It took another 200 years before the term hippocampus was adopted. The comparison with a sea horse is confusing as it is not clear which end of the structure represents the animal's head. During this time this brain region was also described as a "stout silk worm", Ram's or Ammon's horn. The comparison with a horn was disputed because horns taper from their roots whereas the hippocampus begins narrow and becomes clubbed. However, it is the sea horse that has survived as the comparable label for this brain region, the hippocampus.

1.1.2 The cholinergic system, learning and memory

1.1.2.1 The cholinergic synapse

The neurotransmitter acetylcholine (ACh) is synthesised from choline (Ch) and acetyl Coenzyme A (AcCoA) by choline acetyltransferase (ChAT; EC:2.3.1.6) in the cytoplasm of nerve terminals. The acetyl moiety comes from glucose and pyruvate which is converted to AcCoA by pyruvate dehydrogenase (PDH; EC:1.2.4.1) in the mitochondria. Several proposals have been put forward to explain how AcCoA crosses the mitochondrial membrane to the cytoplasm for ACh synthesis (see Tucek, 1985). One mode of thought is that AcCoA, together with oxaloacetate, is converted to citrate by citrate synthase (EC:4.1.3.7) and transported by the tricarboxylic acid carrier system to the cytosol where it is converted back to AcCoA by ATP citrate lyase (EC:4.1.3.8). The observation that ATP citrate lyase blockage by (-)hydroxycitrate reduced ACh synthesis by 40% (Endemann & Brunengraber, 1980) shows that citrate is a major source of the acetyl moiety of ACh. Another candidate for an acetyl donor is acetylcarnitine produced in the mitochondria by carnitine acetyltransferase (EC:2.3.1.7). The presence of carnitine acetyltransferase in cholinergic nerve terminals was shown by its reduction, along with ChAT, after lesions in the septal-hippocampal pathway (Tucek, 1985). It has been suggested that AcCoA also crosses the membrane directly, in the presence of high Ca^{++} concentrations which increase the permeability of the mitochondrial membrane (Benjamin & Quastel, 1981). However, the Ca^{++} concentrations (1mM) needed to increase the membrane permeability are too high to be physiologically significant (Ca^{++} 10^{-7}M in cytoplasm). There have also been reports that AcCoA is produced cytosolically by a PDH

complex present on the extramitochondrial membrane (Lefresne et al., 1978) but, so far, no proof of such an extramitochondrial enzyme has been obtained by subcellular fractionation studies. Thus it appears that AcCoA is first converted to another compound which crosses the mitochondrial membrane and is then converted back to AcCoA.

Ch is supplied from dietary intake via the blood, by intracellular hydrolysis of phosphatidylcholine or from the reuptake of Ch after the breakdown of ACh in the synaptic cleft (see fig. 1.1). It was Yamamura & Snyder (1972) who first reported that Ch was accumulated, presynaptically, by two kinetically distinct processes. The high affinity Ch transport system (HAChT; Kt less than or equal to 1μM) is Na^+ dependent, sensitive to hemicholinium-3 (HC-3; which blocks Ch uptake) and is associated with a high degree of acetylation. The low affinity Ch transporter (LAChT; Kt > 30μM) is Na^+ independent, needs high HC-3 concentrations to inhibit uptake and little of it is acetylated to ACh (Yamamura & Snyder, 1972, 1973; Haga & Noda, 1973; Simon et al., 1976). The LAChT has a non-specific distribution in the brain (MacIntosh & Collier, 1976) and is thought to provide Ch for phospholipid synthesis (Meyer et al., 1982). HAChT appear to be specific for cholinergic neurones as high affinity uptake is reduced with neuronal degeneration after septal-hippocampal lesions (MacIntosh & Collier, 1976). HAChT was shown to be specifically located on cholinergic neurones as ACh synthesis was reduced when this uptake system was blocked by low Na^+ or HC-3 (Grewaal & Quastel, 1973; Guyenet et al., 1975). Subsequent reports have indicated that HAChT and Ch acetylation to ACh are coupled (Barker & Mittag, 1975; Burgess & Prince, 1977) suggesting a membrane bound form of ChAT in close association with the HAChT (Benishun &

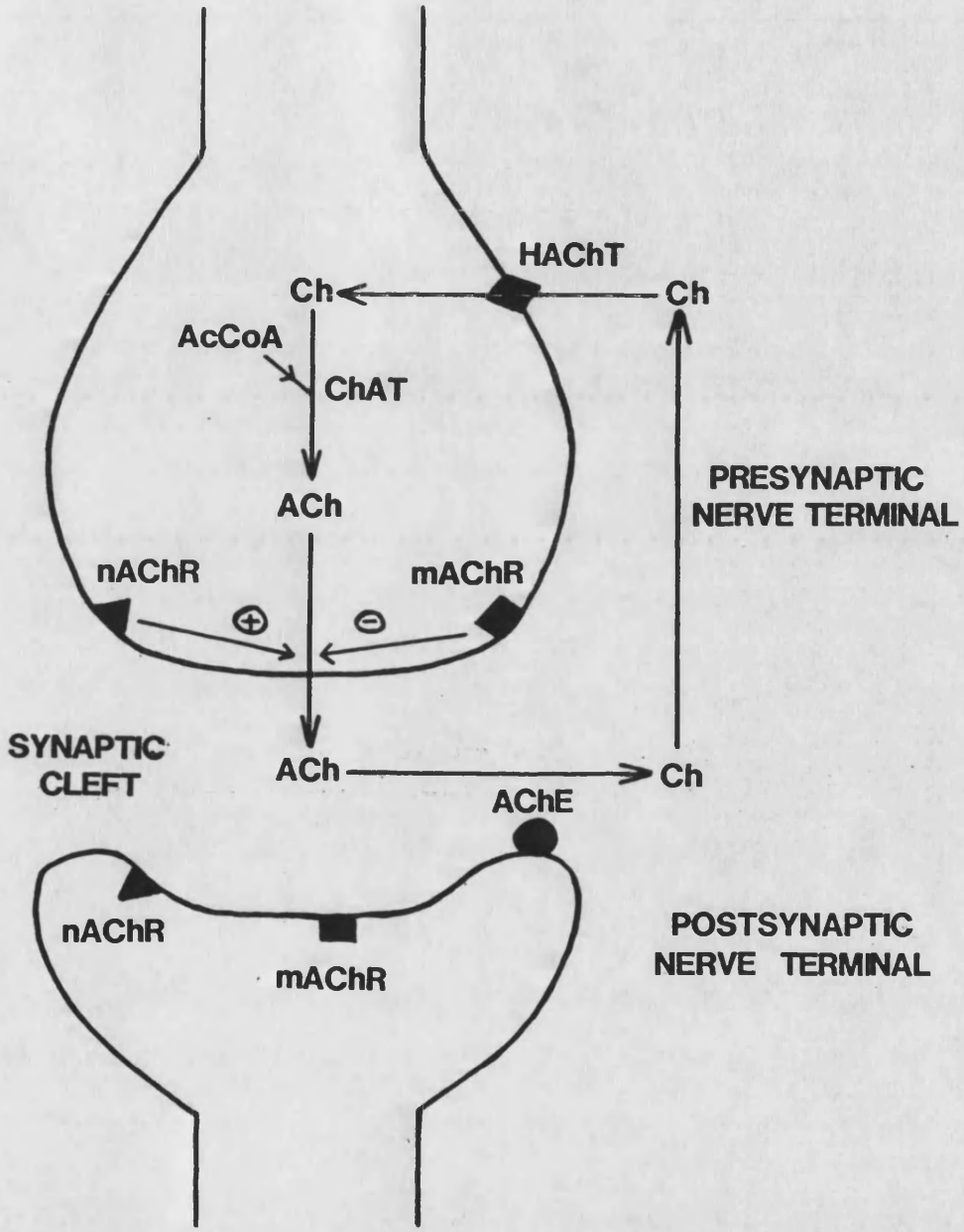

Fig. 1.1. A schematic diagram of a cholinergic synapse depicting Ch uptake, ACh synthesis and release and the ACh receptors. AcCoA: acetyl Coenzyme A; ACh: acetylcholine; AChE: acetylcholinesterase; Ch: choline; ChAT: choline acetyltransferase; HAChT: high affinity choline transporter; mAChR: muscarinic acetylcholine receptor; nAChR: nicotinic acetylcholine receptor.

Carroll, 1981; Meyer et al., 1982).

An influx of Ca^{++} ions into the nerve terminal will evoke ACh release (Miledi, 1973; Crosland et al., 1983). The origin of the released ACh was thought to be the synaptic vesicle, which during Ca^{++} influx would fuse with the plasma membrane releasing its quantum of transmitter. This process has been debated as both vesicular and cytoplasmic ACh pools are present in the nerve terminal (Richter & Marchbanks, 1971). Though quantal release is similar to vesicle exocytosis no morphological proof for this process has been found (Fried & Blaustein, 1978; Dunant, 1986).

Results have shown that newly synthesised cytoplasmic ACh is preferentially released with elevated intraterminal Ca^{++} (MacIntosh & Collier, 1976; Cunnane, 1984) only if the change in Ca^{++} was in the vicinity of the release site (Vizi & Ashley, 1987). Once released ACh interacts with ACh receptors (see section 1.4, fig. 1.1) and is then hydrolysed to Ch and acetate by the extracellular enzyme acetylcholinesterase (AChE; EC:3.1.1.7) in the synaptic cleft (see fig. 1.1). The Ch is then taken up for ACh synthesis to replenish transmitter stores.

1.1.2.2. Cholinergic input

The distribution of cholinergic neurones was first attempted by staining for the marker enzyme AChE (Shute & Lewis, 1963). However, the ubiquitous distribution of AChE, which showed variable densities in staining, suggests a low cholinergic specificity of this enzyme. Indeed, Koelle (1955) reported that AChE was present in adrenergic and other sensory neurones as well as in those cholinergic in nature.

Thus the presence of AChE alone is not sufficient proof of cholinergic innervation (Koelle, 1955; Lehmann & Fibiger, 1979). However, the presence of AChE staining and ChAT activity is specific for cholinergic neurones (Lewis et al., 1967).

Lewis et al. (1967) used this dual marker procedure to show that the hippocampus receives its cholinergic input from the septum. After lesioning the neuronal fibres in the septum there was a marked reduction in both AChE and ChAT activities in the hippocampus. It is now known, from lesion studies, that the cholinergic input into the hippocampus originates from the medial septal nucleus and the nucleus of the diagonal band (Chronister & Whyte, 1975; Pepeu, 1983), see fig. 1.2.

1.1.2.3. Learning and memory

The function of the hippocampus is that of attaining and storage of short term memory (Bartus et al., 1982). When the fibres of the medial septal nucleus are lesioned (Coyle et al., 1983) or when the hippocampus is bilaterally destroyed (Hyman et al., 1984) there is a profound and lasting impairment in learning and memory though long term memory is retained.

The cholinergic involvement, via the muscarinic and nicotinic ACh receptors, in the memory process has been indicated by the fact that administration of the muscarinic ACh antagonist, scopolamine, reduces cognitive intellectual and memory functions in normal humans (Kokman, 1984; Wesnes & Warburton, 1984). These scopolamine induced memory impairments are similar to those seen in senile dementia (Alzheimer's disease; Davies et al., 1978). The cholinergic agonist,

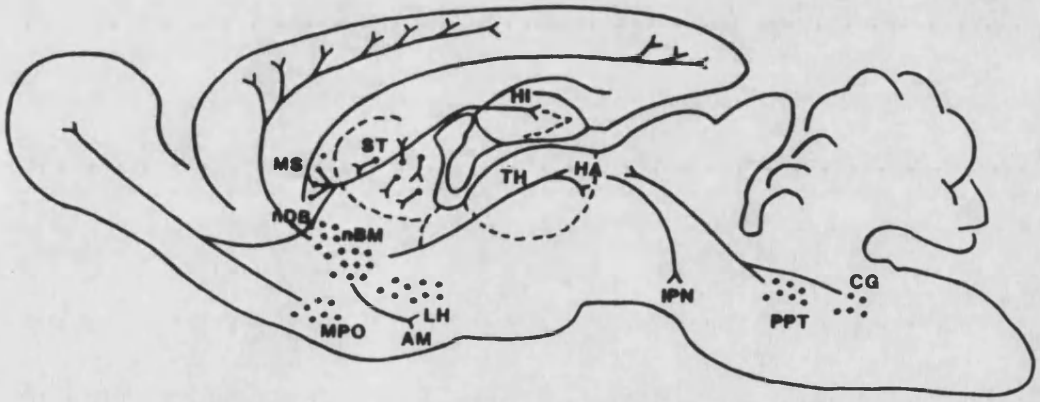

Fig. 1.2. A schematic drawing of the main cholinergic pathways in the rat brain (Pepeu, 1983). AM: amygdala; nBM: nucleus basalis of Meynert; CG: central gray; nDB: nucleus of the diagonal band; HA: habenula; HI: hippocampus; IPN: interpeduncular nucleus; LH: lateral hypothalamus; MPO: magnocellular preoptic nucleus; MS: medial septal nucleus; PPT: peduncolopontine tegmental nucleus; ST: striatum; TH: thalamus.

nicotine, has been shown to prevent this scopolamine induced decline in memory performance (Wesnes & Warburton, 1984).

1.2 ALZHEIMER'S DISEASE

One disease in which loss of recent memory is a major symptom is Alzheimer's disease (Alzheimer, 1907). Historically Alzheimer's disease referred exclusively to presenile dementia, where progressive memory disorders are seen in patients under 65 years, whereas senile dementia applied to older patients (65+ years). As the two conditions are clinically, neurologically, pathologically and biochemically alike they are now considered to be the same disease and routinely referred to as senile dementia of the Alzheimer type (SDAT).

1.2.1 Morphology and pathology

The most pronounced and consistent morphological change that occurs in SDAT is in the cholinergic system resulting in diffuse degeneration of neurones in the neocortex, amygdala and hippocampus, as measured by the reduction (60%) in the presynaptic marker enzyme ChAT. This reduction in neuronal input is due to atrophy in the cholinergic nuclei: the nucleus basalis of Meynert (the origin of cortical innervation) has a severe reduction in ChAT of up to 75% (Whitehouse et al., 1981, 1982; Sitaram, 1984); the hippocampus has its cholinergic origins in the medial septal nucleus and the nucleus of the diagonal band and these structures have shown 55% and 65% reductions in enzyme activity, respectively (Henke & Lang, 1983); see fig. 1.2. The validity of using ChAT activity as a marker for the disease was shown by Perry et al. (1978) who reported that the

reduction in this enzyme was correlated with the extent of intellectual impairment in memory information tests.

The pathology is complex and consists of granulovascular degeneration and the presence of senile plaques and neurofibrillary tangles. Silver staining techniques have shown the senile plaques to be 20-200nm in diameter (Marchbanks, 1982) which consist of abnormal axon terminals (derived from cholinergic, adrenergic and somatatinergic neurones; Perry & Perry, 1985) and dendritic processes, often intermingled with astrocytes and microglial cells, associated with a core of extracellular amyloid (Perry et al., 1978; Marchbanks, 1982; Coyle et al., 1983). The amyloid protein subunit (A4 or β protein), encoded on chromosome 21, is an unsoluble highly aggregating small polypeptide of 4.5 kilodaltons (kDa; Kang et al., 1987) which has a high colocalisation with aluminosilicates (Candy et al., 1986). This has led to the hypothesis that aluminium may be an initiating factor in the disease. However, it is the amyloid protein that entraps the aluminium and so elevated aluminium is probably secondary in the progression of the disease (McGeer, 1984).

The neurofibrillary tangles, particularly in the perikaryon of pyramidal cells, are composed of bundles of tightly packed paired helical neurofilaments (10-12nm in diameter), (Marchbanks, 1982; Coyle et al., 1983). There have been opposing reports on whether the correlation between the severity of dementia (and the reduction in ChAT) is better mapped to the number of senile plaques (Perry et al., 1978; Sitaram, 1984) or neurofibrillary tangles (Wilcock & Esiri, 1982; Wilcock et al., 1982). However, there is a high density of both these pathological features in SDAT brain.

1.2.2. Neurochemistry

The neurochemical changes that take place in SDAT are complex and still not completely defined. Enzymic and metabolic markers of putative neurotransmitters have been measured in brain tissue, obtained from surgical biopsy or autopsy in SDAT and aged matched controls (see Corkin, 1981), to assess what neuronal changes have taken place. Although the presence of dementia and the densities of senile plaques and neurofibrillary tangles correlate best with cholinergic abnormalities, alterations in other transmitter systems have been reported (for a review see Hardy et al., 1985).

Markers for noradrenergic neurones (noradrenalin; dopamine β hydroxylase; 3-methoxy-4-hydroxyphenylglycol, a metabolite) are reduced in the cortex and hippocampus (Adolfsson et al., 1979; Mann et al., 1980; Bondareff et al., 1981; Cross et al., 1981, 1983) due to degeneration of neurones in the locus coerulus (which project to these areas). Reductions in 5-hydroxytryptamine (5HT; serotonin) or its metabolite, 5-hydroxy-3-indole acetic acid, have also been shown in the cortex, hippocampus and caudate nucleus (Adolfsson et al., 1979; Cross et al., 1983; Bowen & Davison, 1986). However, there is no significant correlation between the clinical and neuropathological assessment of the degree of dementia and the monoamine changes, suggesting that these effects may be secondary to alterations in the cholinergic system (Cross et al., 1983).

Using a radioimmunoassay for the neuropeptide somatostatin there was up to 70% reduction in somatostatin-like immunoreactivity in the cortex and hippocampus (Davies et al., 1980; Rossor et al., 1980). The involvement of somatostatin in memory has still to be elucidated

and so the significance of this reduction remains to be determined (McGeer, 1984).

There is no significant change in the GABA-ergic system in SDAT, in the hippocampus or cortex (Coyle et al., 1984).

The bulk of neurochemical work on brain diseases has concentrated on measuring transmitter or metabolite levels and/or enzyme activities for synthesis or metabolism. Using radiolabelled transmitters, agonists or antagonists, changes in receptor densities could also be determined (Davies & Verth, 1978). There are two main types of ACh receptor. Muscarinic ACh receptors (mAChR) and nicotinic ACh receptors (nAChR) so named as muscarine, from the fungus Amanita muscaria, and nicotine, a plant alkaloid from Nicotiana tobacum, were found to stimulate them selectively (Dale, 1914). Thus along with assaying for ChAT activity changes in receptor binding were also examined in SDAT.

Binding experiments using the muscarinic antagonist [^{3}H]QNB (quinuclidinyl benzilate) or [^{3}H]NMS (N-methylscopolamine) have led to mixed results on the changes in the mAChR in SDAT. Nordberg et al. (1986) reported a decrease in receptor binding in the cortex whereas an increase was shown by Nordberg & Winblad (1986). However, using these ligands other groups have indicated no significant change in mAChR density in the cortex and hippocampus, compared with age matched controls (Davies & Verth, 1978; Lang & Henke, 1983; Perry et al., 1986; Kellar et al., 1987). These results suggest that mAChRs are predominantly located on postsynaptic neurones (Yamamura & Snyder, 1974) which are not lost during the disease. Using [^{3}H]oxotremorine-M, a muscarinic agonist, Mash et al. (1985)

reported a decrease in ligand binding in SDAT indicating that a subtype of mAChR (M_2; see section 1.3.1.4.) may be located presynaptically and lost with neuronal degeneration.

Using [^{3}H]nicotine and/or [^{3}H]ACh (in the presence of an AChE inhibitor, to prevent ACh hydrolysis, and atropine, to block the mAChR) there was a marked reduction in nAChR binding sites in the hippocampus and cortex of SDAT patients (Flynn & Mash, 1986; Perry et al., 1986, 1987; Whitehouse et al., 1986, 1988; Kellar et al., 1987; Whitehouse & Kellar, 1987; Nordberg et al., 1988). This loss of nAChR binding sites correlated with the reduction in ChAT (Whitehouse et al., 1986; Kellar et al., 1987; Whitehouse & Kellar, 1987) adding evidence to the suggestion that nAChRs are located presynaptically as these receptors would be lost during neuronal degeneration.

1.2.3. Therapy

As alterations in the cholinergic system are by far the most prominent changes in SDAT, present therapies involve strategies aimed at increasing ACh levels to compensate for losses due to neuronal degeneration.

One procedure is to prevent ACh breakdown by inhibiting AChE. The AChE inhibitor physostigmine (eserine) has been reported to improve memory in recognition tests (Christie et al., 1981; Davies & Mohs, 1982) and reduce the number of inappropriate responses in free-recall tasks in SDAT (Anonymous, 1987). However, for physostigmine to be an effective treatment, individuals need to be carefully titrated to determine the optimal dose as there is a narrow

therapeutic dose range for memory improvement outside of which there may be impairment (Davies et al., 1978; Christie et al., 1981; Hollander et al., 1986). The modest memory enhancement elicited by physostigmine is transient as it has a short half life ($t_{1/2}$ = 30min; Anonymous, 1987).

A more persistent AChE inhibitor is THA (9,amino 1,2,3,4 tetrahydroacridine; $t_{1/2}$ = 6-12 hr; Anonymous, 1987) which has improved memory in SDAT, when given in conjunction with lecithin (Summers et al., 1986). There is, however, considerable excitement and controversy over the therapeutic use of THA as it gives rise to unacceptable side effects such as liver function disorders, diarrhoea, nausea and increased blood pressure (Weintraub & Standish, 1988). The mode of action of THA has still to be completely defined but it is more complicated than a simple AChE inhibitor. At concentrations of 10^{-4} - 10^{-5}M THA interacts directly with K^+ channels (Rogawski, 1987; Stevens & Cotman, 1987), Na^+ channels (Rogawski, 1987) and the nAChR (Perry et al., 1988) and mAChR (Hunter et al., 1989). As these effects are seen at concentrations much higher than therapeutic plasma levels of THA (5-70 ng/ml, 10^{-7} - 10^{-8}M; Park et al., 1986) their relevance to the clinical effects of THA has still to be determined. However, Perry et al. (1988) did report that at therapeutic serum levels THA was still likely to interact with the cholinergic, particularly nicotinic, receptor.

1.3. ACETYLCHOLINE RECEPTORS

An alternative target for therapy is the ACh receptor. The postsynaptic mAChR has been studied but as the receptor is not altered in SDAT its therapeutic use is limited (McGeer, 1984). However, presynaptic receptors whose stimulation would increase ACh release, from the reduced numbers of nerve terminals, could be targetted.

In the periphery the two types of ACh receptor have opposing effects on ACh release from presynaptic nerve terminals. Nicotine and its agonists have an excitatory effect on ACh release, which were inhibited by nicotinic antagonists (Briggs & Cooper, 1982; Wessler et al., 1987) whereas muscarine and its agonists have an inhibitory effect on ACh release which can be blocked by muscarinic antagonists (Briggs & Cooper, 1982). From this Briggs & Cooper hypothesised that the nAChR acts as an accelerator of ACh release, at low ACh concentrations, while the mAChR acts as a brake on release, at high ACh concentrations, thus achieving fine regulation of ACh release. Similar receptor actions have been reported in the CNS (see later). The two ACh receptors differ in structure and mechanism of action.

1.3.1. The muscarinic receptor

1.3.1.1. Structure

By sodium dodecyl sulphate polyacrylamide gel electrophoresis the mAChR gives a single polypeptide of 70-80 kDa (Birdsall et al., 1979; Haga & Haga, 1985; Peralta et al., 1987). Sequence analysis, electron diffraction and limited proteolysis studies have shown the receptor to have a short extracellular glycosylated N-terminal region

which is thought to be associated with the binding site (Hall, 1987), see fig. 1.3a. There are seven hydrophobic regions of 20-25 amino acids which span the membrane (Birdsall & Hulme, 1987; Hall, 1987; Peralta et al., 1987). Intracellularly there is a long cytoplasmic loop between transmembrane regions V and VI that is thought to be the site of interaction with G proteins (see later). The cytoplasmic hydrophilic C-terminal sequence contains serine and threonine residues that can be phosphorylated by protein kinases. This phosphorylation may play an important role in desensitisation and internalisation of the receptor (Birdsall & Hulme, 1987; Hall, 1987). The model (see fig 1.3a) leaves little of the N-terminal structure for selective and stereospecific ligand binding so the binding site may lie in the pocket formed by the transmembrane domains (Kerlavage et al., 1987).

1.3.1.2. Mechanism of action of mAChR

The muscarinic response of the mAChR is slow (latency 100ms and 300-500ms duration; Sokolovsky & Bartfai, 1981) due to its integrated response via three proteins, see fig. 1.3b. The binding of ACh initiates the binding of a guanine nucleotide regulatory protein (G protein) to the mAChR, which acts as a transducer to an appropriate effector system (Bourne, 1986; Hall, 1987). G proteins are a family of heterotrimeric proteins: a common β/γ complex (35kDa and 10kDa, respectively) that is thought to anchor the protein to the cytoplasmic face of the membrane and an α chain (41-45kDa) that binds GTP and determines the specificity of the G protein for receptor and effector (Gilman, 1984; Bourne, 1986).

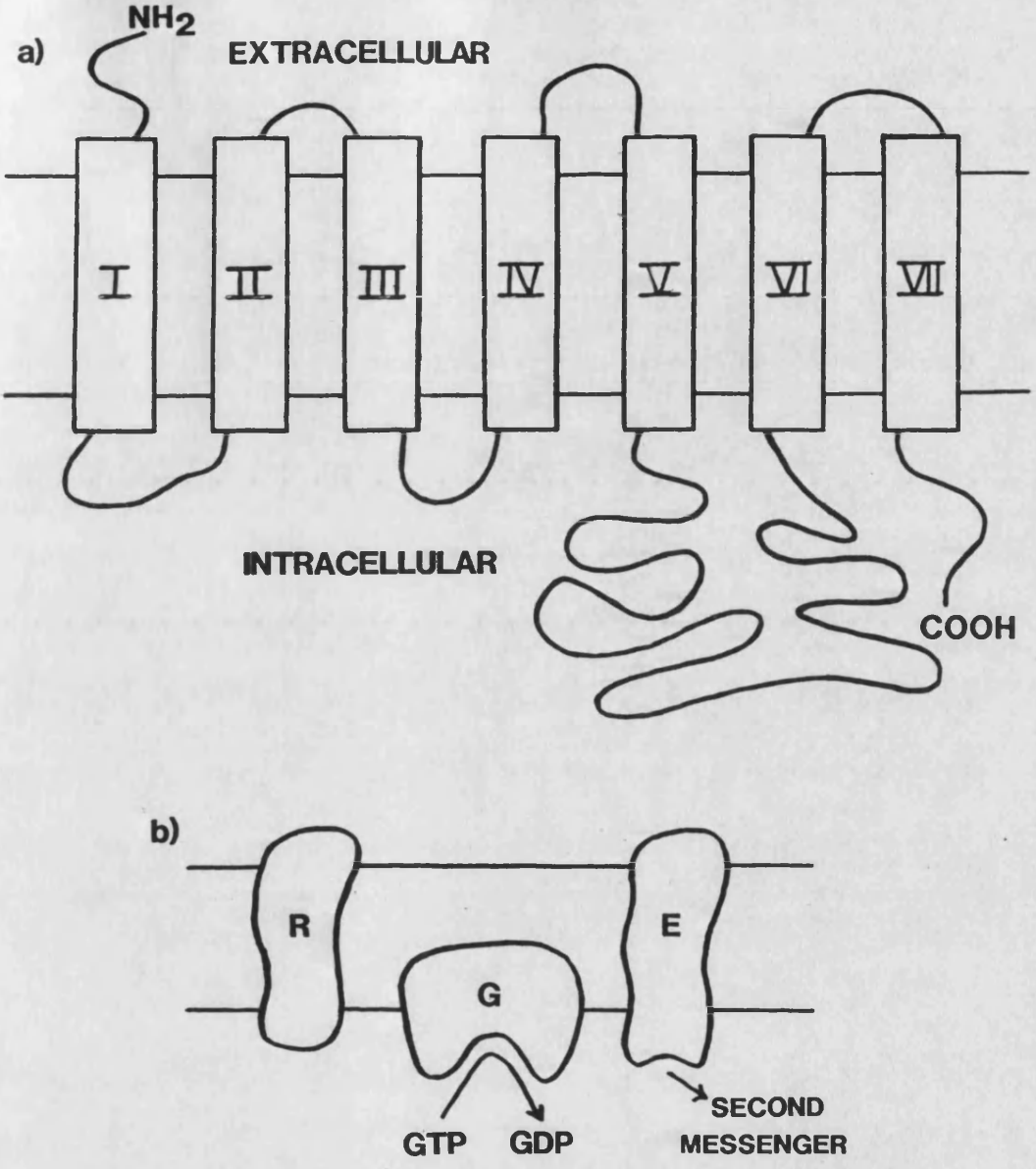

Fig. 1.3 a). The muscarinic receptor arrangement in the lipid bilayer showing seven hydrophobic transmembrane spanning regions (boxes I-VII) and the extracellular N-terminal and intracellular C-terminal.

Fig. 1.3 b). A schematic representation of the arrangement of a second messenger receptor mechanism in a membrane.

R: receptor; G: G protein; E: effector.

Coupling to a receptor causes the G proteins to release GDP and bind GTP. The activated G protein can regulate the function of an effector, hydrolysis of bound GTP to GDP terminates the regulatory effects of the G protein (Bourne, 1986).

The effector that G proteins couple with can be an enzyme: adenylate cyclase (Gilman, 1984) or phosphatidylinositol 4,5 bisphosphate specific phospholipase C (Berridge & Irvine, 1984).

Coupling of G proteins to these enzymes results in the generation of second messengers: either cyclic adenosine monophosphate or inositol triphosphate and diacylglycerol, respectively, which in turn alter the activity of protein kinases (Nestler & Greengard, 1983). Phosphorylation by protein kinases causes receptor desensitisation and alters the open or closed state of a number of ion channels (Christie & North, 1988). Breitweiser & Szabo (1985) showed that G proteins can directly bind to K^+ channels without the intervention of any second messengers (Pfaffinger et al., 1985). In central neurones, activation of mAChR increases the K^+ membrane conductance resulting in hyperpolarisation and so inhibiting ACh release from presynaptic cells due to reduced action potentials (Christie & North, 1988). Alternatively mAChR activation may lead to cell depolarisation due to inhibition of K^+ conductances (M-currents).

1.3.1.3. Location

In the CNS the presynaptic localisation of the mAChR has been well documented based on release studies. Muscarinic agonists (oxotremorine, carbachol) reduced electrically- or high K^+- evoked

release of ACh from synaptosomes (Nordstrom & Bartfai, 1980; Marchi et al., 1981; Raiteri et al., 1984) and slices (Szerb & Somogyi, 1973; Hadhazy & Szerb, 1977) whereas the muscarinic antagonist, atropine, restored or enhanced ACh release. Thus there is a presynaptic mAChR inhibitory effect on ACh release.

However, binding studies with the muscarinic antagonist [^{3}H]QNB suggested there were only postsynaptic mAChR, as there was no reduction in binding after lesions in the medial septal nucleus (Yamamura & Snyder, 1974). In 1982, Bowen & Marek showed that the classic muscarinic antagonists (QNB, atropine and scopolamine) had a 10 fold lower affinity for the presynaptic mAChR than the postsynaptic. This suggests that the low concentration of QNB (1nM) used by Yamamura & Snyder may have been too low to detect a presynaptic mAChR effect. Using [^{3}H]dexetimide, a muscarinic antagonist, Consolo et al. (1984) reported a 20% reduction in receptor binding after septal lesioning supporting the view of a presynaptic mAChR.

1.3.1.4. Receptor subtypes

Initially, binding studies with muscarinic antagonists showed a single class of binding site (Hulme et al., 1978) but binding studies with muscarinic agonists suggested that two major classes of receptors which differed widely in their affinities for potent agonists. In 1980, Hammer et al. reported that the muscarinic antagonist pirenzepine, could discriminate two subclasses of mAChR differing in their affinity for pirenzepine by a factor of 20-40. Those receptors with a high affinity for pirenzepine (M_1) had a low agonist affinity and were located postsynaptically. The M_2 receptor

had a low affinity for pirenzepine, a high agonist selectively and was located both pre- and post-synaptically (Hammer & Giachetti, 1982; Potter et al., 1984). The receptor subtypes also differ in tissue location. M_1 is predominant in the cortex, hippocampus and striatum whereas M_2 is predominant in the superior colliculus, brainstem, heart and smooth muscle (Potter et al., 1984).

The subtypes of receptor differ also in effector function. The M_1 (high affinity pirenzepine site) was shown to mediate phosphatidyl inositol breakdown (Potter et al., 1984; Gil & Wolfe, 1986) which resulted in an accumulation of inositol triphosphate (Kunysz et al., 1988). Stimulation of M_2 (low pirenzepine affinity site) inhibited adenylate cyclase (Potter et al., 1984; Gil & Wolfe, 1986).

The receptor subtypes not only differ in location, binding properties and effector response but also in DNA sequence. Four mAChR sequences have been determined though only two (M_1 and M_2) have so far been expressed (Kerlavage et al., 1987).

1.3.2. The nicotinic receptor

1.3.2.1. Structure

The best characterised nAChR is that obtained from the electric organ of Torpedo californica which is a rich source of these receptors. The receptor is a pentamer (200-250kDa) composed of $\alpha_2\beta\gamma\delta$ subunits which form a Na^+ channel similar to the nAChR of skeletal muscle, see fig. 1.4. Under electron microscopy the receptor has a diameter of 80 angstroms and a channel 110 angstroms protruding on both sides of the membrane (Changeux et al., 1987) which is 6 angstroms wide at the top and 4 angstroms at the bottom (Oiki et al.,

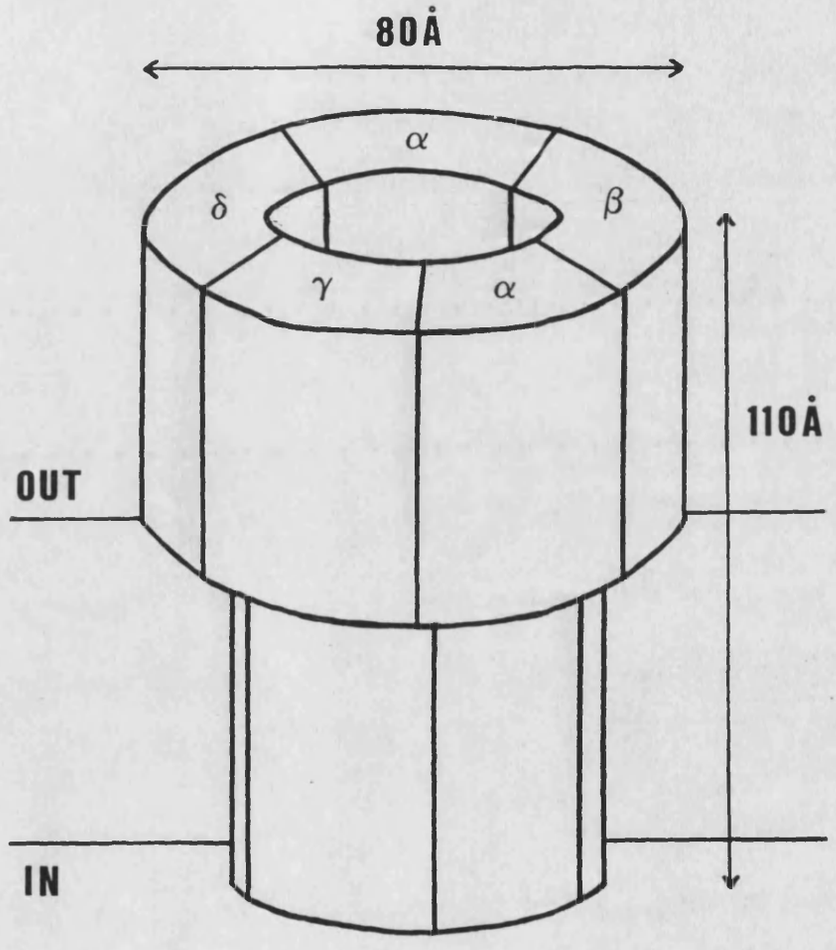

Fig. 1.4. A schematic diagram of the nicotinic receptor in the lipid membrane showing the arrangement of the subunits of the muscle receptor.

1988). Although the individual subunits differ in molecular weight (α, 40kDa; β, 50kDa; γ, 60kDa; δ, 65kDa) and amino acid sequence the overall shape of the folded polypeptide is very similar from one subunit to the next (Barnard & Dolly, 1982; Conti-Tronconi & Raftery, 1982; Noda et al., 1982, 1983; Stevens, 1985).

From cDNA clones of the α subunits the amino acid sequences were determined (Noda et al., 1982). From the sequence there is a large extracellular N-terminal and in the α subunit there are cysteines at positions 192 and 193 which have been shown to be the ACh binding site (Karlin et al., 1986). There are four regions of 20 or more amino acids that are thought to form α helices that span the lipid membrane. Interactions of the hydrophobic groups of the helices with the hydrophobic environment of the lipid bilayer would stabilise the protein in the membrane. Structural models predict that each subunit would donate one transmembrane helix to form the pore lining of the ion channel. Site directed mutations and permeability studies (Dani, 1989) had shown the pore to be composed of the M2 transmembrane region which forms an uncharged channel that is surrounded by a net negative charge. The M2 region is the most conserved, in the subunits sequence (Guy & Hucho, 1987), as expected if it is responsible for nAChR functioning. In the large cytoplasmic loop, between transmembrane regions M3 and M4, there is a stretch of 20 amino acids where every one in four is charged which could twist to form an amphipathic helix (MA; Guy, 1984) but, as yet, its function has not been determined. Between the M3 and MA, of this cytoplasmic region, there is a 20 amino acid stretch of sequence that is rich in serine and threonine residues. Phosphorylation at this site, by protein kinases, is thought to regulate the rate of receptor

desensitisation (Goldman et al., 1987).

1.3.2.2. The putative neuronal nicotinic receptor

The study on neuronal nAChR has not progressed as rapidly as that of electric organ and muscle due to its lower receptor concentration and the concerns about the specificity of α neurotoxins used to specifically label muscle nAChR (Morley et al., 1979).

In 1974, Eterovic & Bennett reported that [^{3}H]αBGT (α-bungarotoxin; a snake venom neurotoxin from Bungarus multicinctus) bound to a crude mitochondrial fraction of rat cerebral cortical membranes. Thus αBGT was adopted to label neuronal ACh binding sites. However, Hunt & Schmidt (1979) showed the αBGT site, though likely to be similar to the nAChR, developed independently of cholinergic input and so the usefulness of αBGT in identifying cholinergic nAChR was questioned.

Using radiolabelled nicotine Romano & Goldstein (1980) showed that ligand binding was stereospecific ((-)nicotine had a 63 fold higher affinity for the receptor than (+)nicotine) and this binding was not inhibited by αBGT suggesting two binding sites. This view was supported by Wonnacott (1986) who reported that the nAChR showed a 88 fold higher affinity for (-)nicotine than (+)nicotine but the αBGT binding site was not stereospecific for nicotine. In the presence of atropine (to block mAChR) [^{3}H]ACh gave a biphasic binding curve indicating the presence of both a high and a low ACh affinity binding site (Reuleuke & Hucho, 1985). Thus it appeared that there were two ACh receptor ion channels which could be preferentially labelled with low concentrations of nicotine or αBGT. Regional distribution of [^{3}H]nicotine or [^{3}H]ACh (plus atropine) and

[^{125}I]αBGT, with binding or autoradiographical studies, has shown independent binding sites with little overlap between αBGT and nicotine (Schwartz et al., 1982; Clarke et al., 1984, 1985) suggesting different locations.

Drugs specific for the high affinity ACh binding site (high affinity nicotine site) are needed to selectively label the neuronal nAChR. One such drug is neuronal bungarotoxin (also known as Toxin F, α-bungarotoxin 3.1 or kappa bungarotoxin) whose binding was inhibited by the nicotinic antagonists DHβE (dihydroβerythroidine) and tubocurarine (Loring & Zigmond, 1988) indicating that binding was to the nAChR.

1.3.2.3. Structure of neuronal acetylcholine receptors

The brain αBGT binding site has four subunits (α, 44.7kDa; β, 52.3kDa; γ, 56.6kDa; δ, 65.2kDa) each encoded on a separate gene and has a similar stoichiometry to that of the muscle nAChR (Conti-Tronconi et al., 1985; Quik & Geertsen, 1988; see section 1.3.2.1).

The neuronal nAChR, that has high affinity for nicotine but no αBGT binding, consists of only two subunits, α (51kDa) and β (79kDa) (Whiting et al., 1987). The heavier subunit was called β because of its slow movement by gel electrophoresis. However, its amino acid sequence revealed cysteines at residues 192 and 193 which is consistent with the binding site for ACh in the α subunit of muscle (Karlin et al., 1986). The stoichiometry of this receptor is not known but microsequencing and binding of monoclonal antibodies indicate that there is more than one copy of each subunit in the

receptor (Whiting et al., 1987).

The non ACh binding subunit in the brain nAChR was identified as β_2 (Deneris et al., 1988) which could substitute for the muscle β_1 to form functional receptors in Xenopus oocytes. Using cDNA cloning techniques α_2 (Wada et al., 1988), α_3 (Boulter et al., 1986) and α_4 (Goldman et al., 1987) subtypes have been isolated and are expressed as functional receptors when co-injected into Xenopus oocytes with the β_2 subunit (Boulter et al., 1986; Wada et al., 1988). Thus the neuronal nAChR is a heterogenous population of subtypes that differ in their distribution as shown by in situ hybridisation (Goldman et al., 1987; Deneris et al., 1988). The neuronal subunits have an insertion in the cytoplasmic loop between M3 and MA (though phosphorylation sites are still present) of varying length and little conservation of sequence between subunits (Goldman et al., 1987). This inserted sequence is thought to be important in directing the cellular location of the receptor and could explain how one subtype (α_4) becomes located presynaptically and another (α_3) postsynaptically. The β_2 subunit is coexpressed with α_2, α_3 and α_4.

1.3.2.4. Mechanism of action of nAChR

The nicotinic response, at the neuromuscular junction, has been well characterised and involves the opening of an ion channel leading directly to cation flux, thus the response is very rapid (approximately 10ms). ACh binds to both the α subunits causing an allosteric conformational change in the receptor which opens the channel to allow cationic influx (Changeux et al., 1984).

In the CNS, electrophysiological studies have shown a physiological response of the nAChR (this is discussed in Chapter 6) which also involves cation influx (Aracava et al., 1987) via an ion channel (Egan & North, 1986). Rowell & Winkler (1984) reported a functional response of the nAChR at the presynaptic nerve terminal of the mouse cortex. Nicotine and the agonist DMPP (1,1 dimethyl-4-phenylpiperazinium) increased the release of newly synthesised ACh and this effect was blocked by the nicotinic antagonist hexamethonium. A similar nicotinic excitatory effect on transmitter release has been reported at the dopamine heteroreceptor in the striatum (Rapier et al., 1988) and at the ACh autoreceptor in the hippocampus, the subject of this study.

For either muscarinic or nicotinic presynaptic receptors to be considered as therapeutic targets in the treatment of SDAT, by increasing ACh release, drugs which act as nicotinic agonists (which evoke ACh release) or muscarinic antagonists (which enhance evoked ACh release by blocking the inhibitory effect of the mAChR) need to be found. Indeed, administration of nicotine has been reported to enhance memory in patients with SDAT (Sahakian et al., 1989) and change in the nAChR correlates better with the density of senile plaques than change in ChAT (Perry et al., 1989). Thus, a better understanding of the pharmacological characteristics of the nAChR may help in the evaluation of the nAChR as a possible therapeutic target in SDAT.

1.4. SYNAPTOSOMES AS A MODEL SYSTEM FOR PRESYNAPTIC STUDIES

When brain tissue is homogenised, in isotonic solution, the plasma membrane of the cells are broken at points of highest stress or least resistance. The nerve terminals are sheared off from their axons. The membrane reseals to form the synaptosome (Whittaker, 1969) containing cytoplasm, with a full complement of glycolytic enzymes, synaptic vesicles and one or two mitochondria. Once formed, synaptosomes maintain their integrity, given the appropriate osmotic conditions, for several hours. They retain most of the structural and functional characteristics of nerve terminals. If in a suitable balanced salt solution containing an energy source (usually glucose) they are metabolically active. They maintain ionic gradients by extruding Na^+ ions and taking up K^+ ions to retain membrane potentials (Heaton & Bachelard, 1973). They take up other substances like putative transmitters (Bogdanski et al., 1970) or their precursors (Dowdall & Simon, 1973) by saturable carrier-mediated, Na^+-dependent processes. Synaptosomes release transmitter in a Ca^{++} dependent manner when depolarised with high K^+ concentrations (Briggs & Cooper, 1982; Rapier et al., 1989) or electrically (DeBelleroche & Bradford, 1973). Thus most synaptic functions are conserved.

1.4.1. Synaptosomal isolation

Synaptosomes are separated from the cellular debris and other subcellular organelles present in the homogenate by differential centrifugation. Most methods for synaptosomal isolation are based on conventional sucrose density centrifugation (DeRobertis et al., 1962; Gray & Whittaker, 1962). First, cell debris and nuclei from the

homogenate are precipitated by a low speed centrifugation (P1 pellet). The supernatant (S1) is then recentrifuged, at higher speed, to sediment myelin, synaptosomes and mitochondria in a P2 pellet. The P2 pellet is resuspended and centrifuged on a three step sucrose density gradient. Myelin fragments are light and so float on 0.8M sucrose. Mitochondria have a rich matrix so when exposed to dense sucrose undergo osmotic dehydration which allows them to penetrate 1.2M sucrose. Synaptosomes are sealed structures and osmotically sensitive but rich in cytoplasm and have a higher water content than mitochondria so equilibrate between 0.8M and 1.2M sucrose.

The hypertonicity of the sucrose causes shrinkage and alteration to the cytoskeletal structure (Whittaker, 1969; Day et al., 1971). The hypertonic sucrose is removed by dilution and centrifugation ready for resuspension in ionic medium containing glucose for maintenance of metabolism. The ionic medium allows rehydration to a more 'natural' appearance.

Many modifications, such as layering the homogenate directly on to a two step sucrose gradient (DeBelleroche & Bradford, 1980) or use of different isolating media have been tried to improve the physiological status of the synaptosomes or their speed of centrifugation. Colloidal silica particles (Ludox) were introduced as gradient media (Mateyko & Kopac, 1963) but these silica solutions were toxic to living cells. Addition of polymers eg polyvinylpyrrolidone (PVP) or polyethylene glycol (PEG) increased the stability of the colloids and decreased their toxic effects (Lagercrantz & Pertoft, 1972). However, the large excess of free

polymer increased osmolarity and viscosity of the media so making it difficult to remove the media from biological membranes.

Hypertonicity of sucrose was overcome by the use of other media such as Ficoll/sucrose (Kurokawa et al., 1965; Abdel-Latif, 1966; Autilio et al., 1968; Cotman & Matthews, 1971). Ficoll is a high molecular weight dextran polymer which is essentially inactive osmotically and forms gradients over the same range as sucrose. Ficoll/sucrose media increase the viability of the synaptosomes due to a shorter centrifugation time. Structural morphology was better preserved due to the isotonic isolating conditions and metabolic activity was increased (Verity, 1972). However, commercially available Ficoll requires extensive dialysis and lyophilisation before use. It is more viscous than sucrose so needs higher centrifugation speeds to fractionate the P2 pellet. Also Ficoll adheres to biological membranes so compromising biochemical studies.

A more recent development is Percoll which is a colloidal suspension of silica particles coated with PVP (Pharmacia, 1982). Percoll is osmotically inactive and produces isotonic gradients of low viscosity enabling more rapid separation with smaller centrifugal forces. Nagy & Delgado-Escueta (1984) used a two step Percoll gradient (4mls each of 16% and 10% Percoll in 0.25M sucrose containing EDTA and HEPES, pH 7.5) to separate the subcellular fractions from the P2 pellet. Dunkley et al. (1987) reported that sucrose brought to a pH of 7.5 with HEPES, PIPES or Tris caused aggregation of membranes thus disrupting normal fractionation so sucrose was brought to the desired pH of 7.4 with dilute acid (HCl) or alkali (NaOH). The advantages of Percoll are that the procedure

is fast, as it does not require long centrifugation times, uses an innocuous medium, so giving metabolically active synaptosomes of good purity, and can be used for small amounts of tissue, an important consideration when working on discrete brain regions such as the hippocampus.

The synaptosome preparation represents a heterogenous population of nerve terminals of mixed origin utilising many different transmitters. Using the Percoll protocol of Dunkley et al. (1987, 1988) it may be possible to further purify the synaptosomes into transmitter subtypes, as synaptosomes are present in four of the five fractions obtained from the four step Percoll gradient (see fig. 4.1).

1.4.2. Superfusion

The principle of superfusion is that synaptosomes, brain slices or minces, preloaded with radiolabelled transmitter or precursor, are continually superfused with a balanced salt solution, containing glucose to maintain metabolic activity. The effect of drugs, introduced into the system, can be monitored by the release of labelled transmitter. Superfusion is a good system to study transmitter release from synaptosomes as re-uptake of transmitter is minimised by prompt removal of the superfusate.

1.5. AIMS OF THIS REPORT

A better pharmacological profile of the presynaptic nAChR is needed before its usefulness as a therapeutic target in SDAT can be determined. The presynaptic hippocampal nAChR was characterised pharmacologically using a superfusion system whereby the receptor

response to drugs was monitored by the level of ACh released. The effect of AChE inhibitors: THA, physostigmine (both used therapeutically in SDAT) and BW284C51, on ACh release via the nAChR was also observed in the superfusion system.

Preliminary extracellular electrophysiological recordings were carried out to see whether the nAChR has a functional role in hippocampal transmitter regulation.

CHAPTER 2. MATERIALS

(^{3}H-methyl)choline chloride ([^{3}H]Ch; 80Ci/mmole) and (^{3}H-methyl)acetyl Coenzyme A ([^{3}H])AcCoA; 3Ci/mmole) were obtained from Amersham International (Amersham, Bucks, UK). The [^{3}H]Ch was stored at -20°C. The [^{3}H]AcCoA was diluted with Triton X-100 buffer (for composition see section 4.2.5) to give a final concentration of 2mM (specific activity 10μCi/μMol) and stored at -20°C in 100μl aliquots.

(-)Nicotine hydrogen(+)tartrate was purchased from BDH Chemicals (Poole, Dorset, UK). Dihydroβerythroidine (DHβE) was a gift from Dr. Benfield, Merck, Sharp & Dohme Research Laboratory (Hertfordshire, UK). (+)Anatoxin-a (ANTX) was donated by Dr. Albuquerque, Department of Pharmacology and Experimental Therapeutics, University of Maryland (Baltimore, USA).

Percoll was obtained from Pharmacia (Sweden).

The acetylcholinesterase inhibitors BW284C51 (1,5 bis(4 allyl dimethylammoniumphenyl)pentan3one dibromide) and physostigmine (eserine) were obtained from Sigma Chemical Company Ltd. (Poole, Dorset, UK). THA (9 amino 1,2,3,4 tetrahydroacridine hydrochloride) was a gift from Dr. Perry, Department of Neuropathology, Newcastle General Hospital (Newcastle-Upon-Tyne, UK).

All other reagents were supplied by either BDH Chemicals (Poole, Dorset, UK), Fisons (Loughborough, Leicestershire, UK) or Sigma Chemical Company Ltd. (Poole, Dorset, UK).

The Krebs buffer, used throughout the experimental procedures, was freshly prepared and had a composition (final concentration, mM: NaCl, 118; KCl, 2.35; $CaCl_2 2H_2O$, 2.40; KH_2PO_4, 1.20; $MgSO_4 7H_2O$, 1.20; $NaHCO_3$, 25; glucose, 10; which was gassed for 1-2 hr, before use, with 95% oxygen/5% carbon dioxide to give a pH of 7.4 at room temperature.

Unless otherwise stated Optiphase 'Safe' scintillant was used for determination of radioactivity in a Packard liquid scintillation counter at 4°C giving a counting efficiency of 35-40%.

Statistical analysis of data was carried out using a two tailed unpaired Student t-test. Significances of 95% or greater were accepted.

CHAPTER 3. DEVELOPMENT OF A SUPERFUSION SYSTEM TO STUDY ACETYLCHOLINE RELEASE

3.1. INTRODUCTION

Hippocampal synaptosomes were isolated as described by Rapier et al. (1988) whereby the homogenate was layered directly onto a two step sucrose gradient. After determining the optimal conditions for labelling the ACh pool with [^{3}H]Ch, the effect of nicotine and other drugs on [^{3}H]ACh release was studied by superfusion as described by Rapier et al. (1988). The released radioactivity was shown to be ACh by an enzymic extraction method.

The synaptosome isolation procedure adopted enabled synaptosomes to be ready for use after a 1 hr ultracentrifugation and a 7 min washing step. Speed of preparation is an important factor, considering the subsequent lengthy superfusion process, as functional activity of the synaptosomes decreases with time. The conventional sucrose gradient centrifugation procedure of Gray & Whittaker (1962) takes 3 hr.

The superfusion protocol was devised to monitor nicotine-evoked [^{3}H]dopamine release from rat brain striatal synaptosomes. Rapier et al. (1987) had, in preliminary studies, already shown that this procedure could be used to measure nicotine-evoked ACh release from hippocampal synaptosomes. However, the response to nicotine was relatively low making differences in response to subsequent stimulations difficult to determine and so the system was adapted in order to study the cholinergic nicotinic effects more clearly.

3.2. METHODS

3.2.1. Synaptosome isolation on a discontinuous sucrose gradient

Male Wistar rats (200-250g) were killed by cervical dislocation and the brain rapidly removed and placed on filter paper, pre-moistened with ice cold 0.32M sucrose (pH 7.4 with dilute NaOH). The hippocampus (100-150mg wet weight) was dissected out and homogenised (10% w/v in 0.32M sucrose, pH 7.4) in a pre-cooled glass-Teflon homogeniser (clearance 0.31mm) by 2 x 6 up and down strokes at 200rpm. The homogenate was diluted to 2ml with 0.32M sucrose and layered on to two discontinuous sucrose gradients, comprised of 1.2M (2ml) and 0.8M (2ml) sucrose, pH 7.4. The gradients were centrifuged at 100,000g for 1 hr at 4°C in a Beckman L5-50B ultracentrifuge using a SW50.1 swing out rotor (Rapier et al., 1988).

The synaptosome fraction at the 0.8M/1.2M sucrose interface (see fig. 3.1) was removed with a pasteur pipette and diluted 1:1 with Krebs buffer (see materials for composition), mixed by gentle pipetting up and down then centrifuged at 1,000g for 10 min at room temperature in a MSE bench centrifuge.

The supernatant was discarded and the pellet gently resuspended in Krebs buffer to 10% w/v of the original wet tissue weight. The protein concentration was 1-1.5mg/ml.

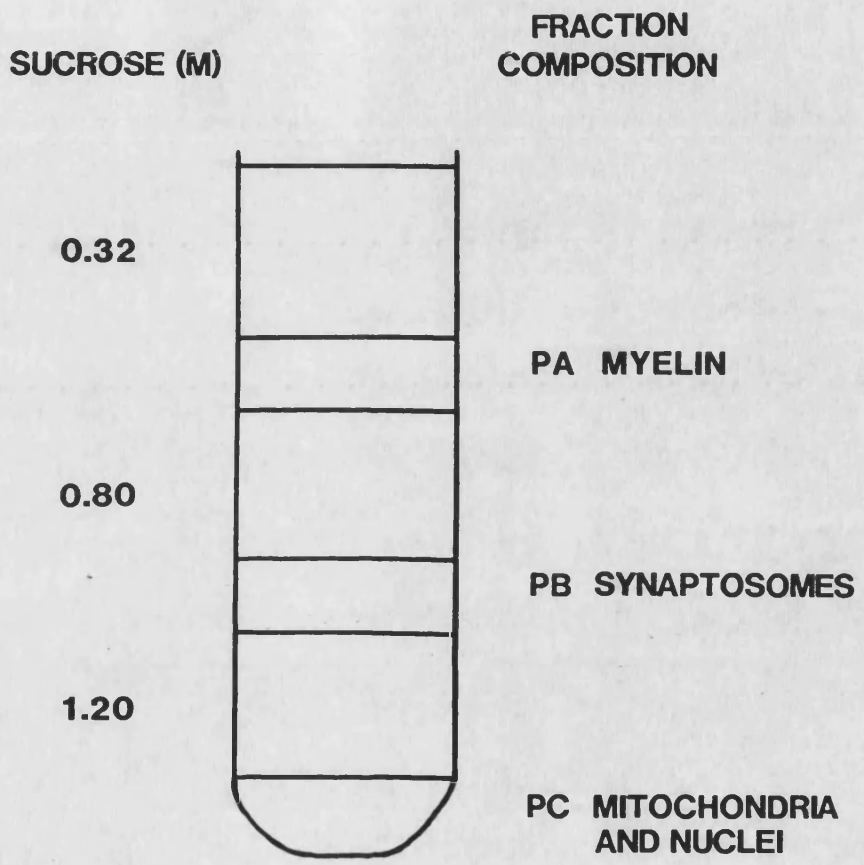

Fig. 3.1. A schematic diagram of the subcellular distribution of hippocampal homogenate on a discontinuous sucrose gradient. The gradient was centrifuged at 100,000g for 1 hr at 4°C in a Beckman L5-50B ultracentrifuge using a SW50.1 swing out rotor.

3.2.2. Lactate dehydrogenase assay

Lactate dehydrogenase (LDH; EC:1.1.1.27) activity was measured in each fraction from the sucrose gradient (see fig. 3.1). LDH is a cytoplasmic enzyme which is released only when the synaptosomal membrane is disrupted (Johnson & Whittaker, 1963). Thus a measure of entrapped (occluded) LDH not only gives an indication of the structural integrity of synaptosomes, it is also a means of assessing the reproducibility of the subcellular fractionation procedure.

Enzyme activity was assessed by measuring the oxidation of NADH in the presence of pyruvate:

$$= -\frac{A}{E} \times \frac{\text{vol in cuvette}}{\text{vol in sample}} \times \frac{1}{p} \times 10^{-3}$$

where A = change in absorbance/min

E = molar absorption coefficient ($6.22 \times 10^{3} Mcm^{-1}$)

l = path length of light (1cm)

p = protein concentration (mg/ml)

The method used was that of Johnson (1960) as modified by Marchbanks (1967) who included the addition of Triton X-100 into the experimental protocol to rupture the synaptosomes, thus giving a measurement of occluded LDH. The measurements obtained were:

Free LDH : absence of Triton X-100

Total LDH: presence of Triton X-100

Occluded LDH = Total LDH - Free LDH

All reagents used for the assay were freshly prepared. Tris-HCl buffer (2.7ml; 0.15M, pH 7.4), sodium pyruvate (0.1ml; 10mM in Tris-HCl buffer) and a sample (0.1ml) from the gradient were placed in a cuvette in a Pye Unicam SP6-450 spectrophotometer, equipped with a chart recorder. The reaction was initiated by the addition of NADH (0.1ml; 2mM in Tris-HCl buffer), followed by rapid mixing. Free LDH was measured by monitoring the oxidation of NADH at 340nm for at least 1 min. Triton X-100 (0.1ml; 10% v/v in Tris-HCl buffer) was then added to the cuvette and the change in absorbance at 340nm monitored for at least 1 min.

3.2.3. Protein determination

Protein concentrations were obtained using the method of Lowry *et al.* (1951). Standard curves were constructed using a freshly prepared solution of bovine serum albumin (BSA) over the concentration range 0-350µg/ml.

BSA standards (0.2ml) or fraction from the gradient (0.2ml sample diluted 1/10 or 1/20 with distilled water) were incubated with alkaline cupric tartrate at room temperature for 10 min. The alkaline cupric tartrate was freshly prepared by diluting 1 vol of 1% (w/v) $CuSO_4 5H_2O$ and 1 vol of 2% (w/v) sodium tartrate with 100 vol of 2% (w/v) Na_2CO_3 in 0.1M NaOH. After incubation, Folin-Ciocalteau's reagent (0.1ml; diluted 1:1 with distilled water) was added to each sample and the colour allowed to develop at room temperature for 40 min. The blanks contained distilled water (0.2ml) in place of protein. The absorbance, at 750nm, was read in a Pye Unicam SP8-100 spectrophotometer.

3.2.4. Characterisation of choline uptake

In order to optimally label the synaptosomal ACh pool the parameters for [^{3}H]Ch uptake were determined.

3.2.4.1. The effect of incubation time

The protocol used follows that described by Marchi et al. (1983) where the synaptosomal fraction from the sucrose gradient was equilibrated at 37°C for 10 min. The [^{3}H]Ch (diluted 1:1 with cold choline chloride, 20µM) was added with mixing to give a final concentration of 0.8µM (31Ci/mmole). At time intervals (0-60 min) samples (0.1ml) were taken and placed on Whatman GFC filters, pre-moistened with Krebs buffer, in a Millipore manifold filtration unit under gentle suction. The filters were immediately washed with 5ml Krebs. A sample (10µl) of the preparation was applied directly on to a GFC filter, without suction or washing, to give an estimate of the total radioactivity present.

Non-specific Ch uptake was determined in the presence of hemicholinium-3 (HC-3; 1µM final concentration). At low concentrations HC-3 is a specific inhibitor of the Na^+-dependent HAChT (Guyenet et al., 1973; Haga & Noda, 1973; Yamamura & Snyder, 1973). Therefore any Ch uptake in the presence of HC-3 will be due to non-specific transport systems and passive diffusion into the synaptosomes.

Radioactivity was measured in the presence of 5ml scintillant. The results were expressed as pmoles Ch taken up/mg protein.

3.2.4.2. The effect of choline concentration

The effect of Ch concentration on Ch uptake was determined by varying the final concentration of [^{3}H]Ch (0.2-2.0μM) added after a 10 min pre-equilibration at 37°C. Samples (0.1ml) were filtered after a 20 min incubation, as described above. Non-specific uptake was determined in the presence of HC-3 (1μM).

Results were expressed as pmoles Ch taken up/mg protein. A direct linear plot (Eisenthal & Cornish-Bowden, 1974) was used to determine the kinetic parameters of Ch uptake: Kt, the concentration for half maximal transport, and Vmax, the maximum transport of Ch.

The conditions adopted for [^{3}H]Ch uptake, in future experiments, were: a 10 min pre-equilibrium period at 37°C followed by a 20 min incubation, at 37°C, with 0.8μM [^{3}H]Ch.

3.2.5. The superfusion system

The effect of nicotinic agonists and antagonists on ACh release was studied using the superfusion system described by Mills & Wonnacott (1984) as modified by Rapier et al. (1988).

The [^{3}H]Ch loaded synaptosomes (20 min at 37°C with 0.8μM [^{3}H]Ch, as above) were washed in an equal vol of Krebs buffer by centrifugation (7 min, 3,000g) in a microfuge. The supernatant was discarded thus removing excess [^{3}H]Ch that had not been taken up by the synaptosomes. The pellet was gently resuspended in Krebs buffer (to original volume for [^{3}H]Ch uptake) and samples (150μl) were taken for superfusion.

Routinely, four superfusion chambers were used. In each case, the synaptosome sample was placed on a Whatman GFF filter, pre-moistened with Krebs buffer, in the superfusion chamber (consisting of a rimmed glass column and a rimmed glass funnel held together with a spring clamp, see fig. 3.2). A Whatman GFD pre-filter was positioned on top of the synaptosomes before tubing, introducing buffer and air pressure, were placed into the chamber. Krebs buffer (37°C, continually gassed with 95% oxygen/5% carbon dioxide) was pumped onto the filter at a flow rate of 9ml/hr. Air pressure (20 p.s.i.) was applied above the filter to ensure rapid flow through of superfusate. Each superfusion chamber was placed over a LKB 2112 Redirac fraction collector and fractions (8 drops; 340µl) were collected directly into minivials. To each fraction 3ml of scintillant was added before the radioactivity was measured.

After a 40 min washout period, the synaptosomes were stimulated at 30 min intervals with a 50µl (40s) pulse of agonist (made up in Krebs buffer); three such stimulations were routinely given before a fourth stimulation with 20mM K^+ was administered. The agonist pulse was separated, on either side, from the Krebs washing buffer by an air bubble (30s), see below. The responses to successive stimulations were designated S1, S2, S3 and S4 and evoked release was quantified by summing the radioactivity in the fractions contributing to a peak of release, after subtraction of baseline. The baseline, due to basal release, was determined by drawing a best fit line through the points, excluding peaks of released radioactivity.

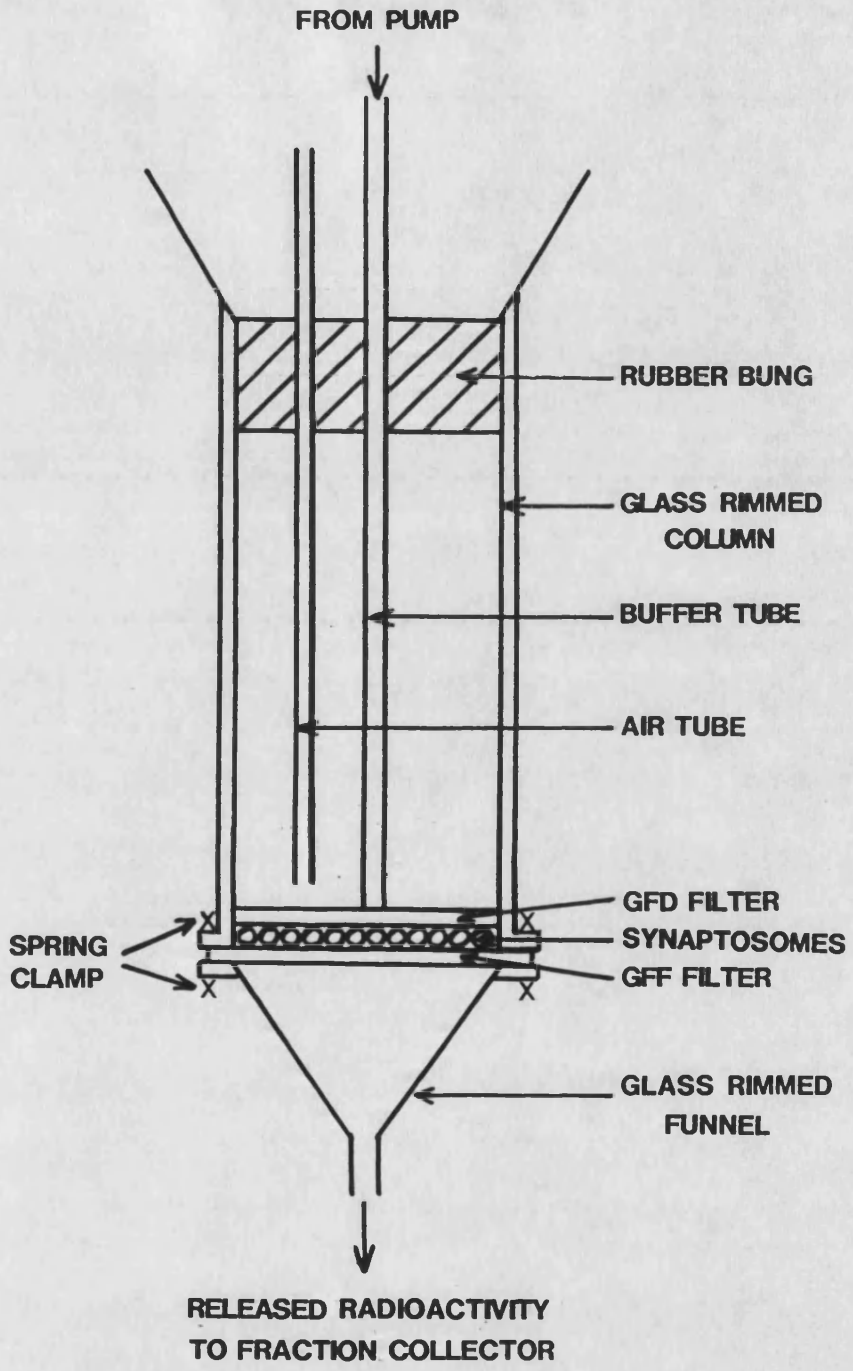

Fig. 3.2. A schematic diagram of a superfusion chamber. This shows the position of the synaptosomes between GFD and GFF filters at the bottom of the chamber.

A schematic representation of an agonist pulse separated from the Krebs washing buffer by two air bubbles in the tubing of the superfusion apparatus.

The effect of antagonists on agonist evoked release was studied by removing the tubing from the normal washing Krebs buffer and placing it into Krebs buffer containing the antagonist (continually gassed as above), 15 min after administration of the S1 agonist pulse. Subsequent stimulations were carried out with agonist and K^+ made up in Krebs buffer containing antagonist.

3.2.6. Enzymic separation of [^{3}H]ACh from [^{3}H]Ch

So far it has been assumed that all the tritium collected from the superfusion system is [^{3}H]ACh. When the synaptosomes are loaded with [^{3}H]Ch it is converted to [^{3}H]ACh by ChAT and it has been suggested that ACh, from this newly synthesised pool of ACh is preferentially released upon stimulation (MacIntosh & Collier, 1976; Cunnane, 1984). However, some of the radioactivity collected could be due to [^{3}H]Ch which:

1. had not been removed during washing
2. had leaked from synaptosomes before it had been acetylated by ChAT
3. was present due to the breakdown of released [^{3}H]ACh by AChE present on the external membranes of synaptosomes (McIntosh & Plummer, 1976).

A method which could be used routinely to differentiate between [^{3}H]ACh and [^{3}H]Ch was devised based on that described by Goldberg & McCaman (1973). This enzymic extraction procedure could be carried out in the minivials in which the superfusion samples were collected.

The basis of the enzymic extraction protocol is as follows and the derivation of its parameters is outlined in the results section 3.3.3.1.

$$[^3H]Ch + [^3H]ACh \xrightarrow[37°C]{ATP,\ ChK}$$

choline acetylcholine

$$P\text{-}[^3H]Ch + [^3H]ACh \xrightarrow{TPB/acetonitrile}$$

phosphorylcholine

$$P\text{-}[^3H]Ch + [^3H]ACh \xrightarrow{Toluene/PPO\ scintillant}$$

aqueous phase organic phase

organic phase $[^3H]ACh$ counted

aqueous phase $P\text{-}[^3H]Ch$ not counted

where ATP = adenosine triphosphate

ChK = choline kinase (EC: 2.7.1.32)

TPB = tetraphenylboron

PPO = 2,5,diphenyloxazole

3.2.7. Synthesis of $[^3H]ACh$

Before determining the parameters of the enzymic extraction procedure $[^3H]ACh$ was synthesised to use as a standard in the protocol. This was accomplished by the acetylation of $[^3H]Ch$ with acetic anhydride, as described by Schuberth & Sundwall (1967).

$[^3H]Ch$ (0.1ml; 100µCi) was evaporated to dryness before acetic anhydride (0.2ml) was added, mixed and incubated at 37°C for 24 hr. Excess anhydride was evaporated and the residue was washed twice with

analar methanol (0.1ml; 95%). The acetic anhydride incubation and the methanol washes were repeated to ensure complete acetylation.

$$(CH_3)_3N^+CH_2CH_2OH + CH_3CO\text{-}O\text{-}OCCH_3 \xrightarrow{37°C,\ 24\ hr} (CH_3)_3N^+CH_2CH_2\text{-}O\text{-}OCH_3 + CH_3COOH$$

choline + acetic anhydride → acetylcholine + acetate

The residue was finally reconstituted in analar methanol (0.1ml) and diluted further, with methanol such that 5µl gave approximately 2 x 10^4 cpm. This was stored at -20°C until needed.

The product was shown to be 96.6% [^{3}H]ACh when run on thin layer chromatography plates (see section 4.3.8 and table 4.2).

3.2.8. The final extraction method and its application to superfusion samples

The enzymic extraction procedure was applied to fractions from two of the four superfusion chambers, in a parallel study, to determine how much of the released radioactivity was [^{3}H]ACh.

To each of the fractions (340µl) NaOH (12µl, 0.02M) was added to bring the pH from 7.4 (the pH of the Krebs buffer) to 8.0, the pH optimum of ChK (Goldberg & McCaman, 1973). ATP (10µl; 1mM final concentration) and ChK (10µl; 0.06mg/ml final concentration) were then added, mixed and incubated at 37°C for 30 min. After incubation TPB/acetonitrile (0.3ml; 3mg/ml) was added with mixing, and the samples were counted in the presence of 3ml toluene/PPO scintillant (25g PPO/5l toluene).

3.3 RESULTS AND DISCUSSION

3.3.1. Lactate dehydrogenase activity

The homogenate was distributed into three fractions on the sucrose gradient (see fig. 3.1) and these were assayed for LDH activity (fig. 3.3). The fraction with the greatest occluded LDH level was designated as the synaptosome fraction, as high occluded LDH indicates greater structural integrity of membrane bound structures containing cytoplasm (Johnson & Whittaker, 1963; Marchbanks, 1967).

The PA fraction contains mainly myelin fragments (Gray & Whittaker, 1962; fig. 4.8A this report) and as expected little of the total LDH activity (approximately 30%) was occluded. The high level of free LDH in this PA fraction was probably a result of LDH released during homogenisation.

As expected the PB fraction being rich in synaptosomes, as seen by electron microscopy (Gray & Whittaker, 1962; fig. 4.8B this report) had the highest occluded LDH activity which accounted for approximately 80% of the total LDH activity in that fraction. It was this fraction that was used in future experiments.

The mitochondrial and nuclear pellet, PC (fig. 4.8C), had relatively low levels of LDH activity consistent with a small synaptosomal content in this fraction. However, only approximately 50% of the total LDH is occluded suggesting that not all the LDH present was purely as a result of synaptosomal contamination. Although LDH is considered to be a cytoplasmic enzyme, there is a tendency for LDH to bind to membranes under certain conditions of pH

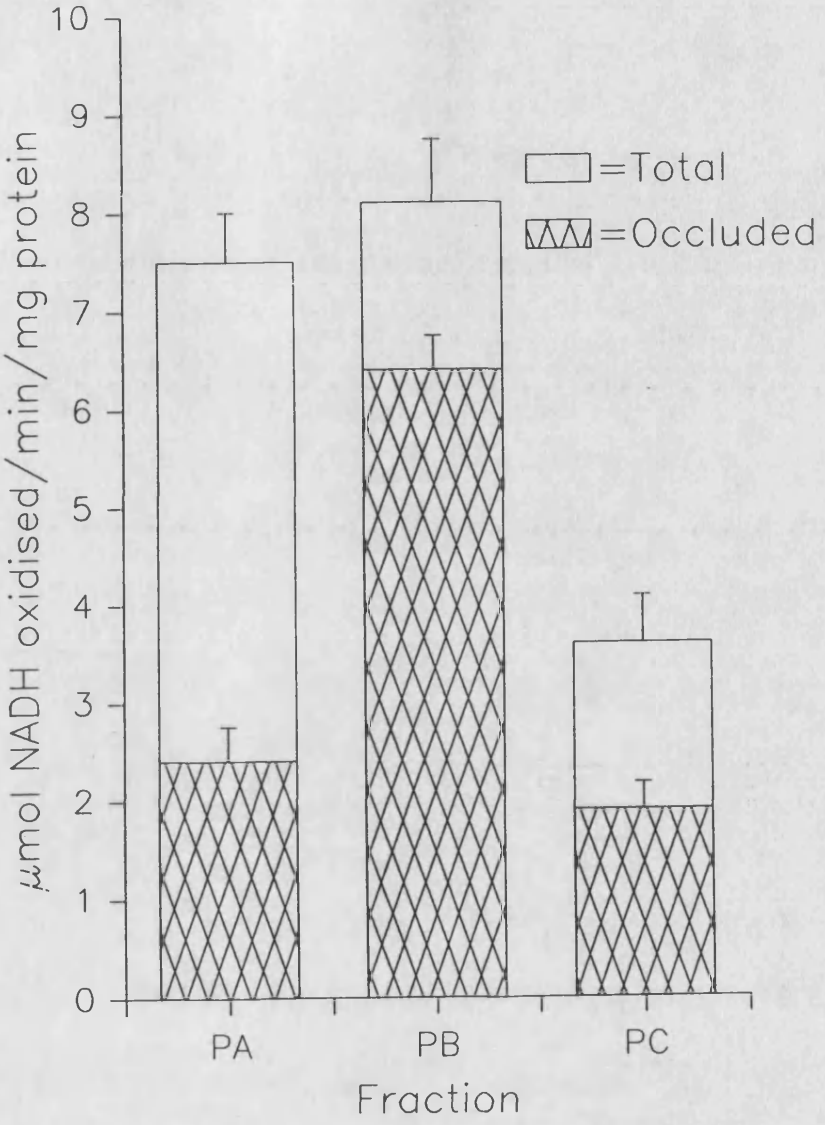

Fig. 3.3. LDH activity in fractions from the sucrose gradient.

Enzyme activity was assessed by measuring the oxidation of NADH at 340nm, with pyruvate as substrate, in the presence (total LDH) and absence (free LDH) of Triton X-100. Occluded levels were calculated as the difference between total and free LDH. Values are the mean ± SEM, n=8.

and ionic strength (Fonnum, 1967) which might account for some of the enzyme activity in this fraction.

3.3.2. Characterisation of choline uptake

To study [^{3}H]ACh release, the synaptosomes were first pre-loaded with [^{3}H]Ch. Specific Na^+ dependent HAChT in the membrane of cholinergic synaptosomes (Jope, 1979) takes [^{3}H]Ch into the synaptosomes where it is acetylated to [^{3}H]ACh by ChAT, in the presence of AcCoA (see section 1.1.2.).

3.3.2.1. The effect of incubation time

The time course of [^{3}H]Ch uptake (0.8μM) was studied over a period of 0-60 min at 37°C. At time intervals samples (0.1ml) were withdrawn, filtered and washed as described in section 3.2.4.1, see fig. 3.4.

Non-specific uptake (determined in the presence of 1μM HC-3) was essentially linear with time and accounted for about 15% of the total [^{3}H]Ch taken up. Specific uptake (the difference between total and non-specific uptake) approached maximal values at 30 min. Thus sufficient labelling of the synaptosomes could be achieved by a 20 min incubation and this was used in future experiments.

3.3.2.2. The effect of choline concentration

The dependence of [^{3}H]Ch uptake on Ch concentration was studied over the range 0.2-2.0μM. After a 20 min incubation at 37°C samples (0.1ml) were taken, filtered and washed as described in section 3.2.4.2, see fig. 3.5(a).

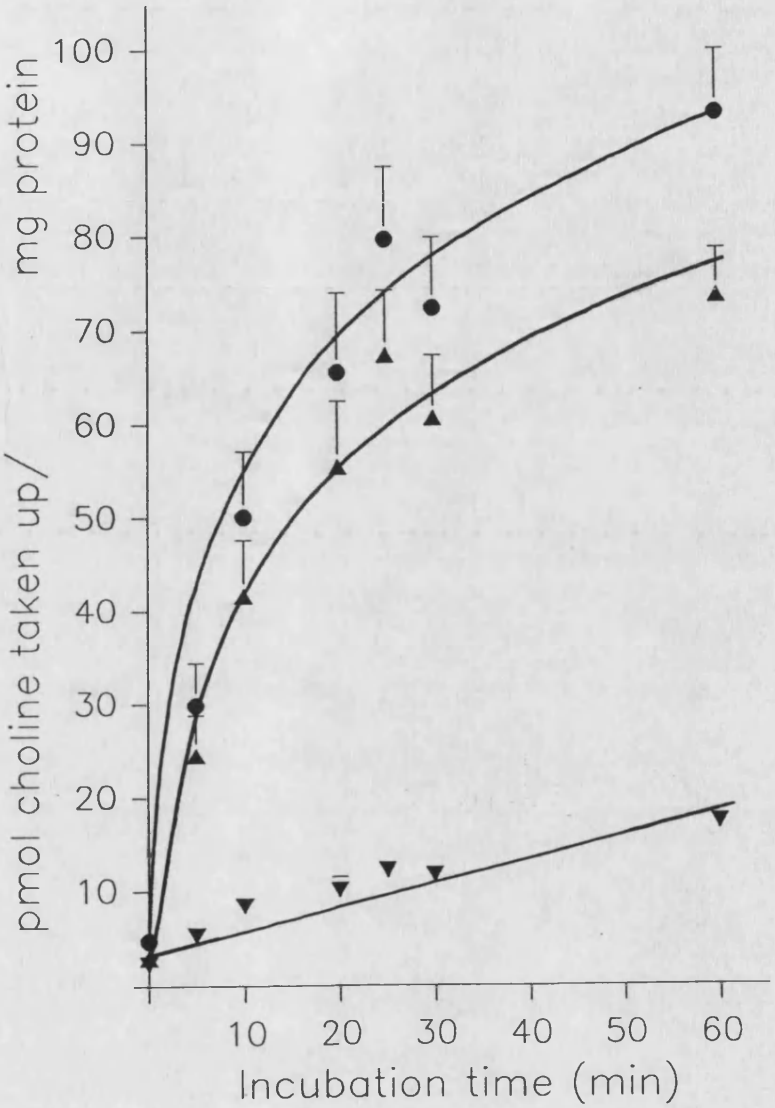

Fig. 3.4. The time course of [^{3}H]Ch uptake by sucrose isolated synaptosomes. After the addition of [^{3}H]Ch (0.8μM), samples were incubated at 37°C and at time intervals (0-60min) 100μl were taken, filtered and washed. Non-specific uptake was determined in the presence of HC-3 (1μM). Values for total (●), specific (▲) and non-specific (▼) uptake are the mean ± SEM, n=5.

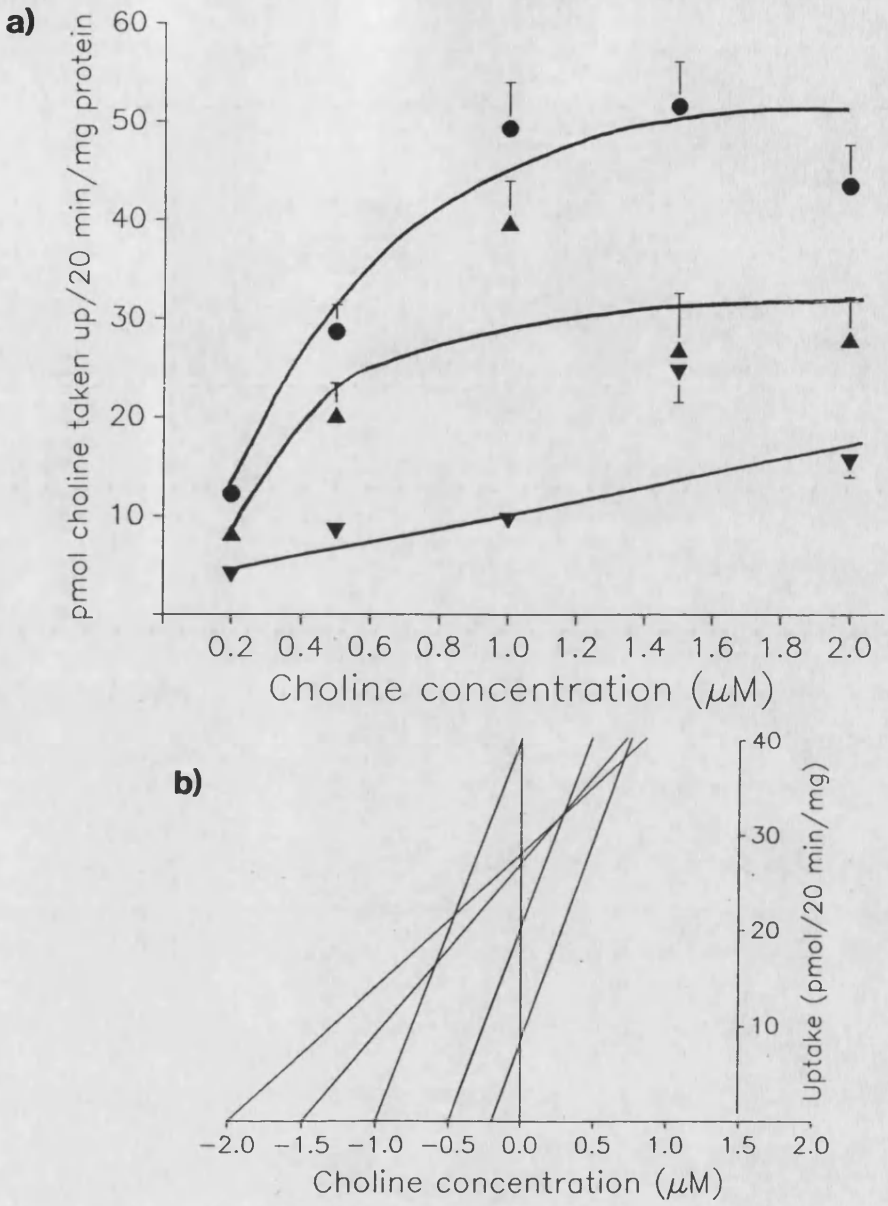

Fig. 3.5 a). The effect of Ch concentration on [^{3}H]Ch uptake by sucrose isolated synaptosomes. Samples were incubated with varying [^{3}H]Ch concentrations (0.1-2.0μM) and after 20 min at 37°C 100μl were taken, filtered and washed. Non-specific uptake was determined in the presence of HC-3 (1μM). The values for total (●), specific (▲) and non-specific (▼) uptake are the mean ± SEM, n=3.

Fig. 3.5 b). A direct linear plot of [^{3}H]Ch uptake against Ch concentration. Values are the mean of 3 experiments. Kt (the concentration of half maximum transport) and Vmax (maximal transport) were derived by determining the mean of the intersections correlating to the x-axis (Kt) and y-axis (Vmax).

Non-specific uptake was essentially linear with concentration. Specific uptake approached saturation at a Ch concentration of 1μM. Thus sufficient labelling of the synaptosomes could be achieved by a [^{3}H]Ch concentration of 0.8μM and this concentration was used in future experiments.

A direct linear lot (fig. 3.5(b)) gave a Kt value of 0.51μM (the concentration for half maximal transport) and a Vmax of 34.5pmol/20 min/mg protein. This Kt value was within the range reported for specific HAChT into hippocampal synaptosomes: 0.43-0.90μM (Sorimachi & Kataoka, 1974; Atweh et al., 1975; Murrin & Kuhar, 1976; Simon & Kuhar, 1976; Simon et al., 1976). These researchers gave Vmax values of 16-56.4pmol/4 min/mg protein, from fig. 3.4 the Vmax value of 26pmol/4min/mg protein is well within this range.

3.3.3. Superfusion

3.3.3.1. Derivation of an enzymic separation of [^{3}H]ACh from [^{3}H]Ch

When monitoring drug effects on radiolabelled ACh release from tissue pre-loaded with the radioactive precursor Ch, a method that will discriminate between the bases is required before changes in transmitter levels can be determined.

The procedure described by Wonnacott & Marchbanks (1976) involved extracting the choline bases into an organic solvent and the subsequent separation of ACh from Ch by thin layer chromatography. The spots were then removed and measured for radioactivity. The enzymic radioassay of Goldberg & McCaman (1973) detailed the phosphorylation of Ch to phosphorylcholine which was then separated

from the labelled substrate ([^{32}P]ATP) on anion exchange columns. The method of Marchi et al. (1983) required the samples to be lyophilised before Ch was phosphorylated. The addition of TPB in an organic solvent would extract ACh into the organic phase, but not phosphorylcholine, the radioactivity of which could then be measured in the presence of an organic scintillant.

However, these methods are lengthy and not easily applied to the large number of samples which are obtained from the superfusion system. Thus an enzymic separation of [^{3}H]ACh from [^{3}H]Ch was devised which could be routinely used in the minivials in which the superfusion fractions were collected.

For these experiments the standards used were: [^{3}H]ACh (5µl; 2.4 x 10 ^{4} cpm; in methanol) and [^{3}H]Ch (5µl; 2.1 x 10 ^{4}cpm; aqueous). Radioactivity of the samples was determined in the presence of toluene/PPO scintillant (3ml), total radioactivity was determined in the presence of 3ml Optiphase 'Safe' scintillant.

3.3.3.1.1. The effect of acetonitrile volume

When [^{3}H]ACh (in methanol) was mixed directly with toluene/PPO scintillant 63% of the total radioactivity was counted (fig. 3.6). When the organic solvent, acetonitrile, was added the amount of radioactivity detected increased with the volume of solvent. Thus the volume of acetonitrile needed to ensure that all the organic phase radioactivity was counted, was determined.

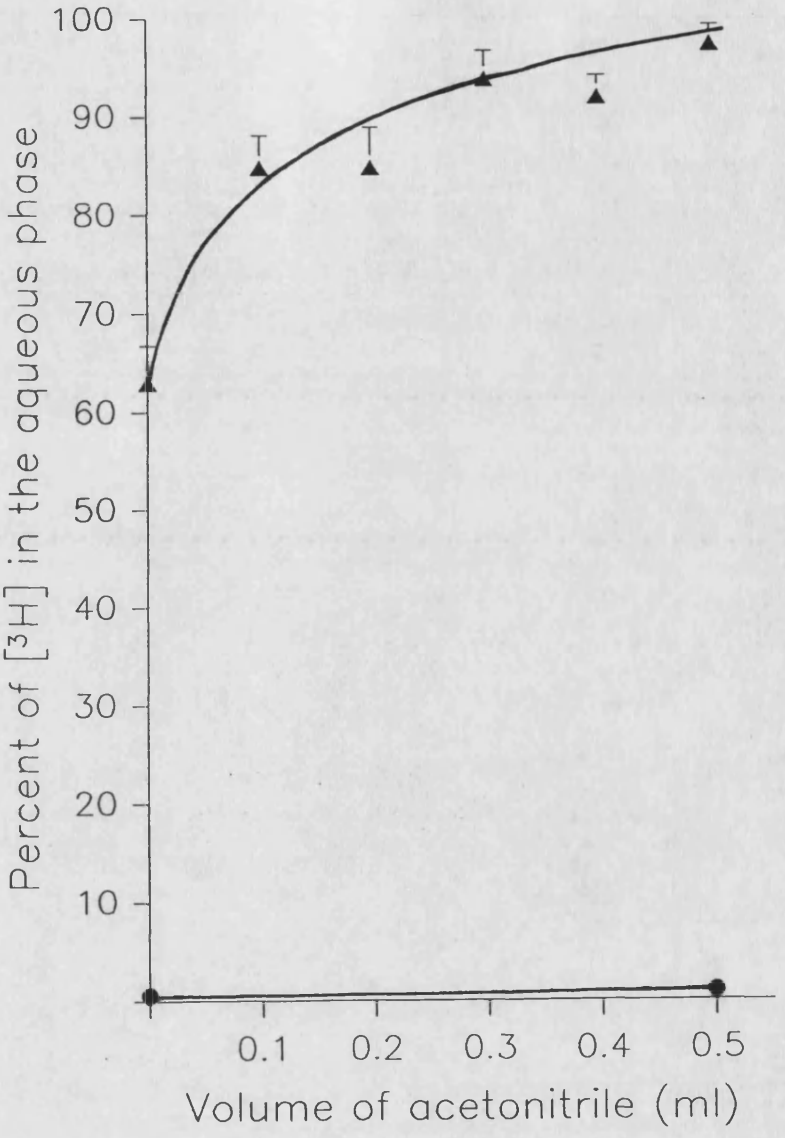

Fig. 3.6. The effect of acetonitrile volume on the counting efficiency of organic phase radioactivity. Values are the mean of 5 experiments, in quadruplicate, ± SEM and samples were counted in the presence of toluene/PPO scintillant. ACh, (▲); Ch, (●).

To [^{3}H]ACh (5µl) varying volumes of acetonitrile (0.1-0.5ml) were added with mixing before being counted in the toluene/PPO scintillant. To ensure that only organic phase radioactivity was counted, [^{3}H]Ch (5µl, aqueous) in Krebs buffer (340µl; the volume of superfusion fractions), was either mixed directly with toluene/PPO scintillant or had acetonitrile (0.5ml) added before being counted in the scintillant. Results were expressed as percent of the total radioactivity counted in the organic phase (fig. 3.6).

With [^{3}H]ACh maximum counts, 97% of total, were achieved in the presence of 0.5ml acetonitrile. Approximately 95% of the total radioactivity was recorded in the presence of 0.3ml acetonitrile and so this volume was used in further experiments.

Little or none of the aqueous [^{3}H]Ch was registered when mixed directly with toluene/PPO scintillant. This rose to approximately 1% of total activity when mixed with 0.5ml acetonitrile. This shows that acetonitrile alone is not sufficient to extract the aqueous radioactivity into the organic phase and that toluene/PPO scintillant will only record radioactivity that is present in an organic medium.

3.3.3.1.2. The effect of TPB concentration

TPB complexes with the positively charged quarternary ammonium group of ACh and Ch forming a precipitate that is only soluble in organic solvents like acetonitrile (Fonnum, 1969).

The effect of TPB concentration, in acetonitrile (0.3ml) on the uptake of aqueous radioactivity into the organic phase was studied over the range 0.1-10mg/ml, fig. 3.7. To ACh or Ch (5µl in 340µl Krebs buffer), 0.3ml of acetonitrile (containing varying

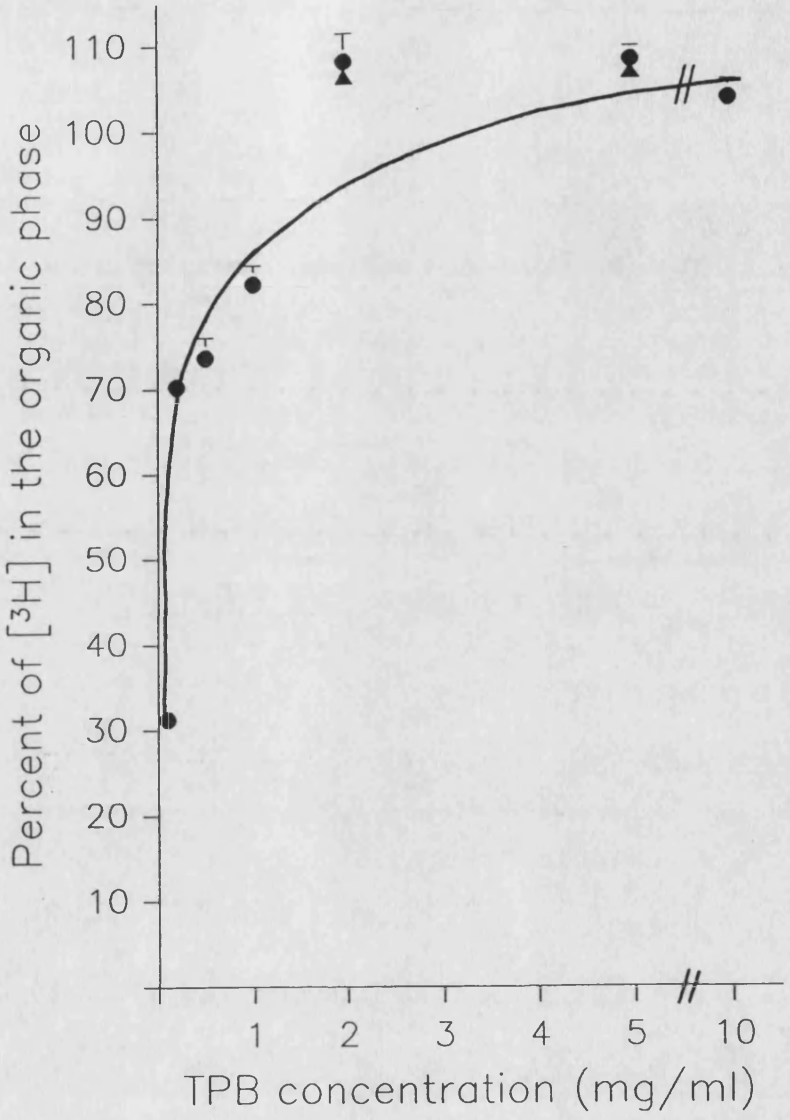

Fig. 3.7. The effect of TPB concentration on the uptake of radioactivity from the aqueous to organic phase. TPB was in 0.3ml acetonitrile and samples were counted in toluene/PPO scintillant. The values are the mean of 3 experiments, in quadruplicate, ± SEM. ACh, (▲); Ch, (●).

concentrations of TPB) was added, mixed and the samples than counted in scintillant, see fig. 3.7.

Uptake of aqueous radioactivity into the organic phase increased with TPB concentration as more complexed with the choline bases. Maximal radioactivity was counted at a TPB concentration of 5mg/ml in acetonitrile. However, over 95% of this radioactivity was obtained in the presence of 3mg/ml TPB in acetonitrile and this concentration was used in further experiments.

This concentration of 3mg TPB/ml acetonitrile was slightly lower than that reported of 10mg TPB/ml butyronitrile (Marchi et al., 1983; Rowell & Winkler, 1984). The lower value probably reflects the smaller superfusate volume used here than by other researchers.

3.3.3.1.3. Enzymic phosphorylation of [^{3}H]Ch

A. The effect of choline kinase concentration

The effect of choline kinase (ChK, EC: 2.7.1.32) concentration on the phosphorylation of Ch, incubated at 37°C for 30 min in the presence of 5mM ATP, was studied over the range 0.01-0.06mg enzyme protein/ml (Marchi et al., 1983; Rowell & Winkler, 1984), see fig. 3.8.

To 5µl samples of [^{3}H]ACh or [^{3}H]Ch, in 340µl Krebs buffer (pH 8.0) containing 5mM ATP, varying concentrations of ChK (10µl; 0.63units/mg) were added to give a final concentration 0.01-0.06mg enzyme protein/ml. After mixing, the samples were incubated at 37°C for 30 min before 0.3ml TPB/acetonitrile (3mg/ml) was added and then counted in scintillant, see fig. 3.8.

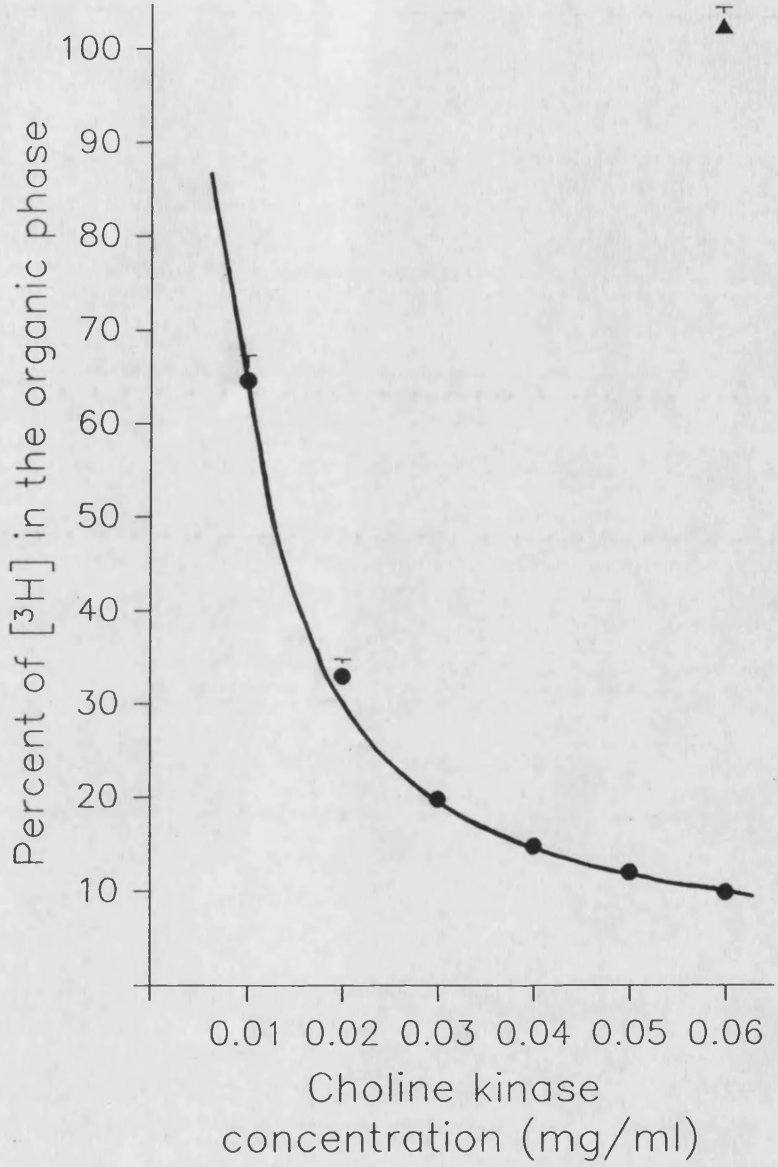

Fig. 3.8. The effect of choline kinase concentration on Ch phosphorylation. Samples were incubated for 30 min at 37°C with 5mM ATP and varying concentrations of choline kinase, then extracted with TPB/acetonitrile (0.3ml; 3mg/ml) and counted in toluene/PPO scintillant. Values are the mean of 4 experiments, in quadruplicate, ± SEM. ACh, (▲); Ch, (●).

The phosphoryl group on phosphorylcholine prevents complex formation with TPB and so [^{3}H]Ch radioactivity, present as phosphorylcholine, remains in the aqueous phase and so is not counted. As ChK concentration increased, so less [^{3}H]Ch was counted consistent with increasing phosphorylation of Ch. Maximal phosphorylation, 90%, was obtained with 0.06mg/ml ChK, in the presence of 5mM ATP, and so this concentration was used in further experiments. The acetyl group on ACh prevents its phosphorylation by ChK and so it will complex with TPB and be taken into the organic phase (fig. 3.8).

B. The effect of ATP concentration

Varying concentrations of ATP (10µl; 0.2-10mM final concentration) were added to samples containing Krebs buffer (340µl; pH 8.0), [^{3}H]ACh (5µl) or [^{3}H]Ch (5µl) and ChK (10µl; 0.01mg/ml). These were mixed, incubated at 37°C for 30 min then extracted with TPB/acetonitrile (0.3ml; 3mg/ml) and counted.

A suboptimal ChK concentration was used so that the effect of ATP concentration on Ch phosphorylation could be seen more clearly. Results were expressed as the percent of radioactivity remaining in the aqueous phase, fig. 3.9.

Ch phosphorylation increased with ATP concentration up to a maximum of 1mM ATP, then decreased. ChK requires magnesium, Mg, for phosphorylation as it is via a Mg-ATP complex that Ch is phosphorylated. When ATP concentrations are greater than those of Mg (Mg is 1.2mM in the Krebs buffer) then a less active Mg-$(ATP)_2$ complex forms and so ChK is less efficient at Ch phosphorylation.

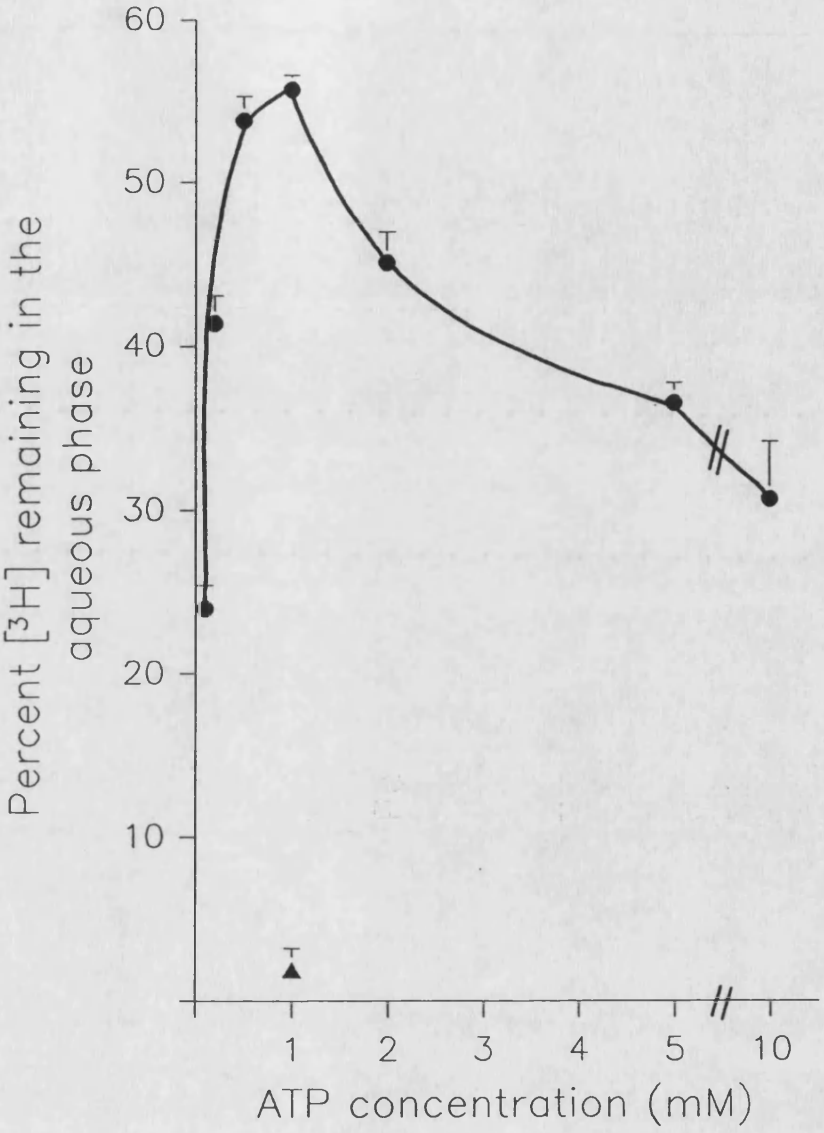

Fig. 3.9. The effect of ATP concentration on Ch phosphorylation. Samples were incubated at 37°C for 30 min with 0.01mg/ml choline kinase and varying ATP concentrations, then extracted with TPB/acetonitrile (0.3ml; 3mg/ml) and counted in toluene/PPO scintillant. Values are the mean of 4 experiments, in quadruplicate, ± SEM. ACh, (▲); Ch, (●).

This Mg-$(ATP)_2$ complex formation could explain why at ATP concentrations greater than 1mM Ch phosphorylation decreases so that more [^{3}H]Ch is taken into the organic phase.

Maximal phosphorylation, 55%, was achieved with 1mM ATP and so this was used in further experiments. Ch phosphorylation was lower than that reported in section 3.3.3.1.3B, fig. 3.8, as the ChK concentration was lower in these experiments.

A similar ATP concentration was used by Goldberg & McCaman (1973). The higher ATP concentration of 10mM used by Marchi et al. (1983) and Rowell & Winkler (1984) was counterbalanced by the addition of 10mM $MgCl_2$.

C. The effect of Ch concentration

To ensure that the enzymic conditions, of 30 min incubation at 37°C with 0.06mg/ml ChK and 1mM ATP, were sufficient to phosphorylate all the Ch that may be present in the superfusate the Ch concentration was increased from 0.165µM (present in 5µl) to 0.465µM by the addition of 20µM Ch.

Varying ATP concentrations (10µl; 0.2-5.0mM final concentration) were added to either 0.165µM or 0.465µM Ch in Krebs buffer (340µl; pH 8.0) with ChK (10µl; 0.06mg/ml). These were mixed, incubated at 37°C for 30 min before TPB/acetonitrile (0.3ml; 3mg/ml) was added and the samples were counted for radioactivity, see fig. 3.10.

Phosphorylation increased with ATP concentration and there was no significant difference when Ch concentration was increased. Maximal phosphorylation, 95% with optimal ChK concentration of

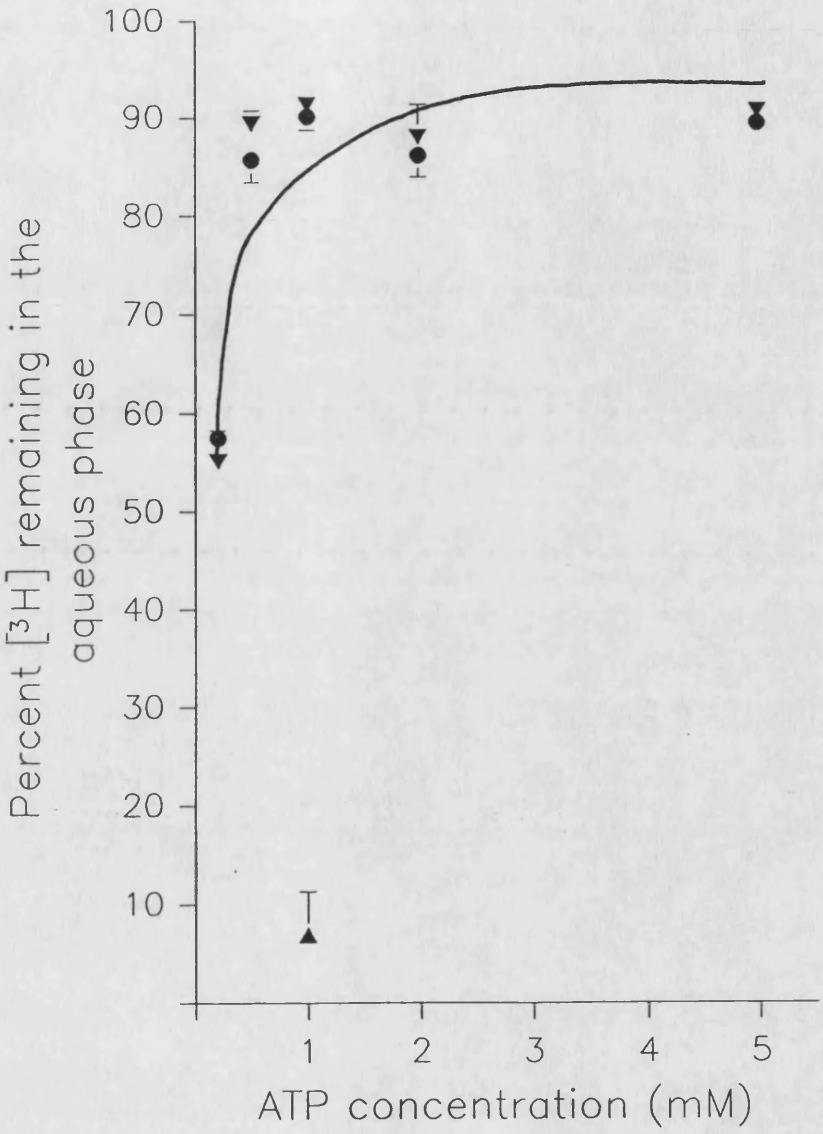

Fig. 3.10. The effect of ATP concentration on the phosphorylation of Ch, at two concentrations. Samples containing either 0.165 or 0.465μM Ch were incubated at 37°C for 30 min with 0.06mg/ml choline kinase and varying ATP concentrations, then extracted with TPB/acetonitrile (0.3ml; 3mg/ml) and counted in toluene/PPO scintillant. Values are the mean of 2 experiments, in triplicate, ± SEM. ACh, (▲); 0.165μM Ch, (●); 0.465μM Ch, (▼).

0.06mg/ml, was obtained with 5mM ATP (a similar result was seen in section 3.3.3.1.3A). However, approximately 90% phosphorylation was achieved with 1mM ATP (which also gave the maximal results in section 3.3.3.1.3B, fig. 3.9) and so it was this concentration that was used in further experiments.

D. The effect of incubation time

Having defined the optimum concentrations of the assay constituents, the effect of incubation time on the enzymic phosphorylation of Ch was examined.

To 5µl samples of [^{3}H]ACh or [^{3}H]Ch, Krebs buffer (340µl; pH 8.0 with 12µl 0.02M NaOH), ATP (10µl; 1mM) and ChK (10µl; 0.06mg/ml) were added and mixed. These were incubated at 37°C for varying lengths of time before TPB/acetonitrile (0.3ml; 3mg/ml) was added and the samples counted for radiactivity, see fig. 3.11.

Ch phosphorylation increased with time reaching a maximum of 95% after 60 min. Sufficient phosphorylation, 92%, could be achieved after a 30 min incubation at 37°C and so this was used in further experiments. This incubation time of 30 min at 37°C was within the range (15-45 min) reported (Goldberg & McCaman, 1973; Marchi et al., 1983; Rowell & Winkler, 1984).

3.3.3.1.4. Application of the enzymic extraction to superfusion samples

The final enzymic extraction procedure of adding NaOH (12µl; 0.02M), ATP (10µl; 1mM) and ChK (10µl; 0.06mg/ml) then incubating at 37°C for 30 min was applied to fractions collected from two of the

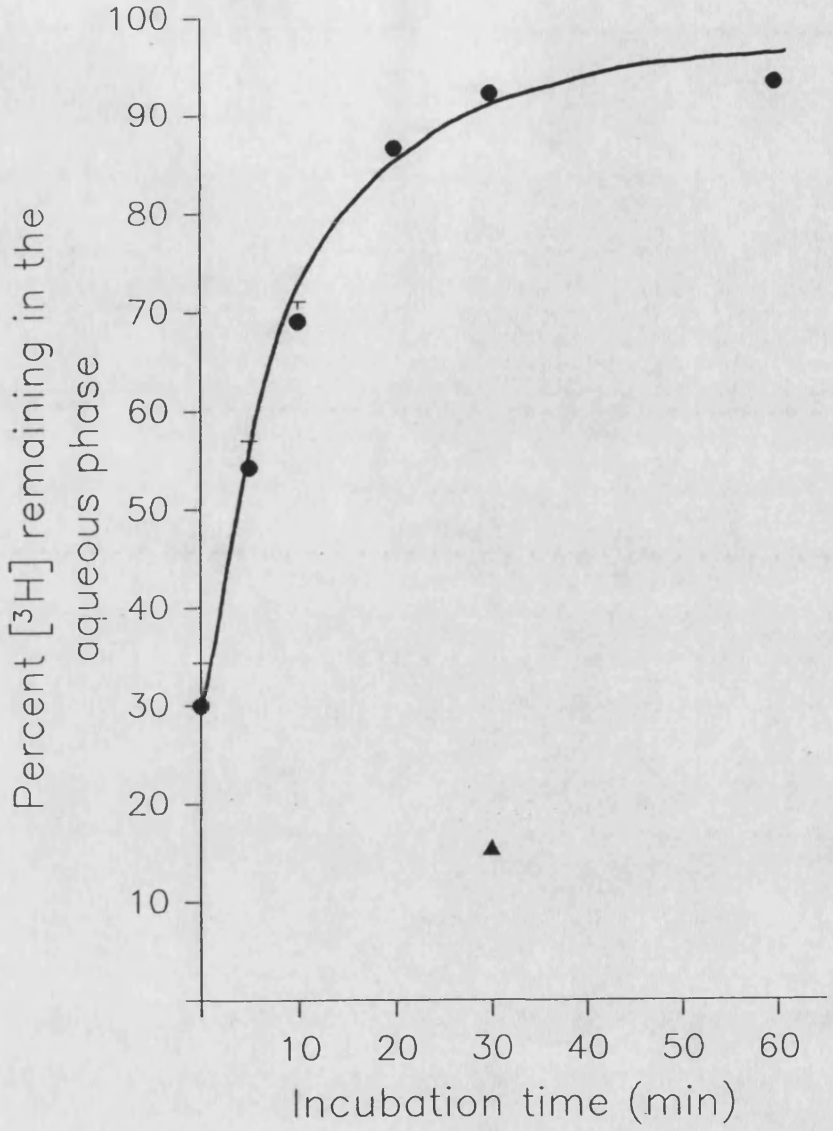

Fig. 3.11. The time course of Ch phosphorylation. Samples were incubated at 37°C for varying amounts of time with 1mM ATP and 0.06mg/ml choline kinase, then extracted with TPB/acetonitrile (0.3ml; 3mg/ml) and counted in toluene/PPO scintillant. Values are the mean ± SEM of 4 experiments, in quadruplicate. ACh, (▲); Ch, (●).

four superfusion chambers. After incubation, the [^{3}H]ACh was extracted from the aqueous phase by TPB/acetonitrile (0.3ml; 3mg/ml) and the samples were counted for radioactivity in the presence of toluene/PPO scintillant (3ml), see fig. 3.12b; table 3.1.

Fractions from the other two superfusion chambers were counted for radioactivity, directly, in the presence of Optiphase 'Safe' scintillant (3ml), see fig. 3.12a, table 3.1.

From fig. 3.12 it can be seen that there is no decrease in basal release of radioactivity in the presence of the enzymic extraction suggesting that this is leakage of [^{3}H]ACh from the synaptosomes. Fig. 3.12 and table 3.1 show that there is no significant difference in response to stimulation with 50μM nicotine as the amount of [^{3}H] released was equivalent whether in the presence or absence of the enzymic extraction. Thus most, if not all the released radioactivity was [^{3}H]ACh and this compares well with the results of Rowell & Winkler (1984) who reported that 87% of the nicotine-evoked tritium released, from cortical synaptosomes, was associated with ACh.

3.3.3.1.5 Summary of the extraction procedure

The results have shown that the enzymic extraction procedure can separate [^{3}H]ACh from [^{3}H]Ch in an aqueous solution. When applied to samples collected from the superfusion system there was no observed change in basal or nicotine evoked release of tritium to that seen when no extraction was applied. This indicates that most, if not all, the released radioactivity was [^{3}H]ACh and so the routine use of this procedure was not necessary. It also indicates that [^{3}H]ACh was removed in the superfusate before it was hydrolysed by any AChE that

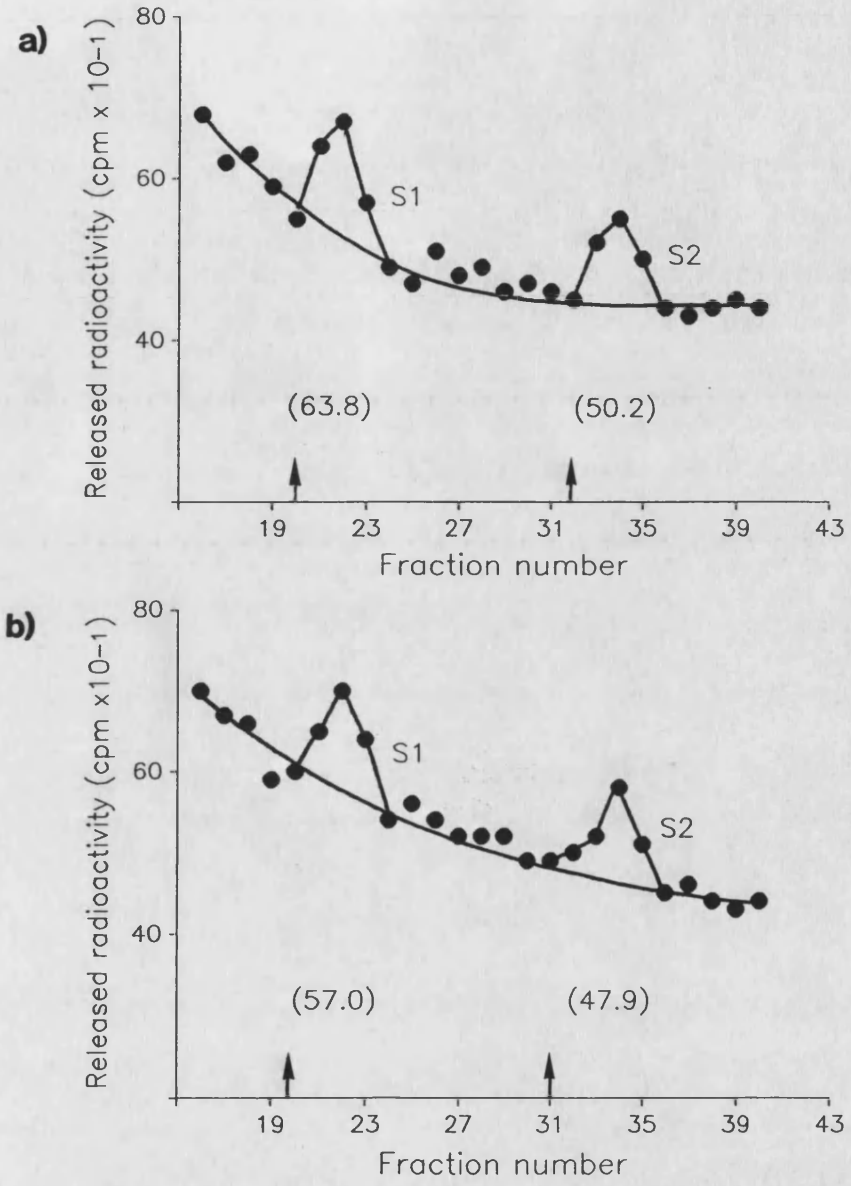

Fig. 3.12. Superfusion profiles of ACh release in (a) the absence and (b) the presence of the enzymic extraction procedure. The synaptosomes were subjected to successive stimulations of nicotine (50µM; S1, S2) after a 40 min washout. Samples were extracted with TPB/acetonitrile (0.3ml; 3mg/ml) after incubation at 37°C for 30 min with 1mM ATP and 0.06mg/ml choline kinase. ↑ Indicates pulse arriving at the synaptosomes. Numbers in brackets are fmol ACh released/mg protein.

AGONIST	ENZYMIC EXTRACTION	S1	S2
NICOTINE 50μM	-	59.0 ± 2.0	49.9 ± 3.3
NICOTINE 50μM	+	56.1 ± 3.3	48.2 ± 2.6

Table 3.1. The effect of the enzymic extraction on the level of [^{3}H]ACh released by nicotine stimulation. Release by successive stimulations of nicotine (50μM; 40s agonist pulse, 30s air bubble) were expressed as fmol [^{3}H]ACh released/mg protein ± SEM, n=4 separate experiments.

may be present.

This result correlates well with the observation that 98% of the loaded [^{3}H]Ch was converted to [^{3}H]ACh (see section 4.3.8) and so a high [^{3}H]ACh content was expected.

3.3.3.2. The nicotinic nature of evoked ACh release

Rowell & Winkler (1984) were one of the first groups to show that nicotine evoked ACh release from the CNS, using synaptosomes isolated from the cerebral cortex of mice, after pre-loading with [^{3}H]Ch. This nicotine response was blocked by the nicotinic antagonist hexamethonium suggesting the effect was via a nAChR.

The nicotinic nature of ACh release from rat hippocampal synaptosomes was studied using successive pulses of nicotine (50μM; S1, S2 and S3) followed by a K^+ pulse (20mM; S4) in the presence and absence of the nicotinic antagonist DHβE (Eccles et al., 1954; Krnjevic, 1974; 1μM), see fig. 3.13 and table 3.2.

It can be seen in fig. 3.13 and table 3.2 that with successive stimulations with nicotine there was a reduction in evoked release (S2/S1 = 84%; S3/S1 = 75%, see table 3.4) which could be due to a decrease in synaptosome responsiveness with time.

In the presence of DHβE there was a marked reduction in nicotine evoked release (S2/S1 = 44%; S3/S1 = 34%, see table 3.4) which was equivalent to approximately 50% of the nicotine evoked release of the control (in the absence of DHβE; $p<0.001$). As DHβE blocks the nicotine-evoked [^{3}H]ACh release it suggests that nicotine stimulated release is via a nAChR. DHβE had no effect on ACh release induced by

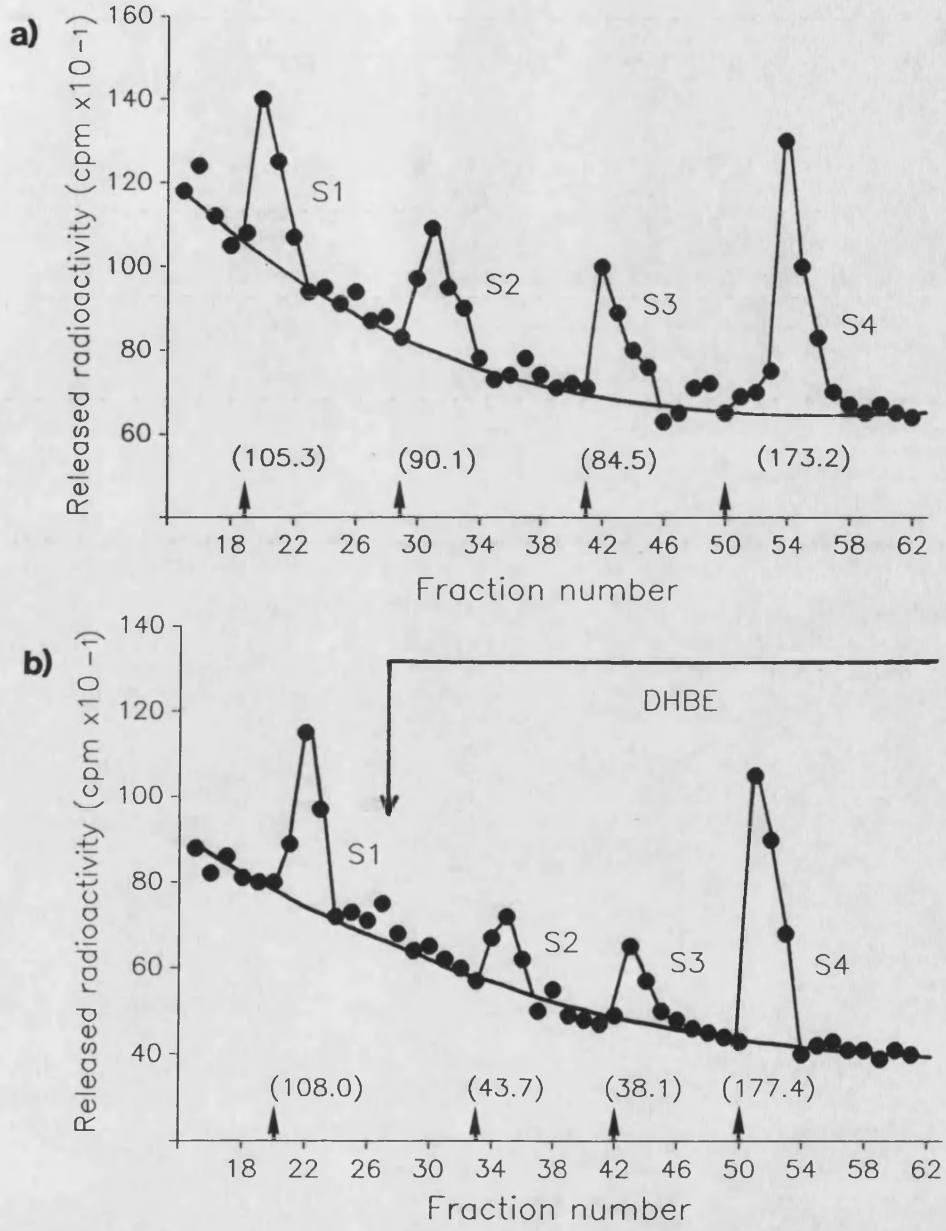

Fig. 3.13. Superfusion profiles of nicotine evoked ACh release in (a) the absence and (b) the presence of DHβE. Synaptosomes were stimulated with nicotine (50μM; S1, S2, S3) and K^+ (20mM; S4) after a 40 min washout. DHβE (1μM) was introduced 15 min after the S1 pulse. ↑ Indicates pulse arriving at the synaptosomes. Numbers in brackets are fmol ACh released/mg protein.

S1 Nicotine 50μM	DHβE 1μM	S2 Nicotine 50μM	S3 Nicotine 50μM	S4 K^+ 20mM
111.7 ± 8.8 (n=9)	-	95.8 ± 5.7	83.4 ± 6.8	179.2 ± 8.4
109.9 ± 6.9 (n=4)	+	48.5* ± 5.7	37.8* ± 4.8	188.8 ± 7.4

Table 3.2. The effect of DHβE on ACh release evoked by successive stimulations with nicotine and K^+. Nicotine (50μM; S1, S2 and S3) and K^+ (20mM; S4) stimulated release in the presence and absence of DHβE, introduced 15 min after S1,were expressed as fmol ACh released/mg protein ± SEM. Significantly different from control (no DHβE), * $p<0.001$.

K^+ depolarisation as was expected as K^+ depolarisation is independent of the nAChR.

3.3.3.3. The effect of (+)anatoxin-a on ACh release

(+)Anatoxin-a (ANTX) is an exotoxin isolated from a filamentous, freshwater, blue-green algae Anabaena flosaquae (Carmichael et al., 1975). It has been found to be a potent stereospecific agonist at the nicotinic synapses in frog muscle and Torpedo (Swanson et al., 1985). Though it has been used in [^{3}H]nicotine binding studies in rat brain (MacAllan et al., 1988) its functional effects in the CNS have not been studied.

3.3.3.3.1. The nicotinic nature of (+)anatoxin-a evoked ACh release

In order to examine the nicotinic nature of the effect of (+)ANTX on ACh release successive pulses of (+)ANTX (10μM; S1, S2 and S3) were administered in the presence and absence of DHβE, as described in section 3.2.5, see fig. 3.14 and table 3.3.

As seen with nicotine stimulation (fig. 3.13, table 3.2) there was a successive reduction in evoked release when stimulated with (+)ANTX (S2/S1 = 90%, S3/S1 = 80%; see table 3.4) and this is probably due to a decline in synaptosome responsiveness with time.

In the presence of 1μM DHβE (table 3.3) there was no significant decrease in ANTX-evoked ACh release (S2/S1 = 90%; S3/S1 = 77%; see table 3.4). However, when the DHβE concentration was increased to 10μM there was a reduction in ANTX stimulated ACh release (S2/S1 = 61%; S3/S1 = 40%; see table 3.4) which was equivalent to

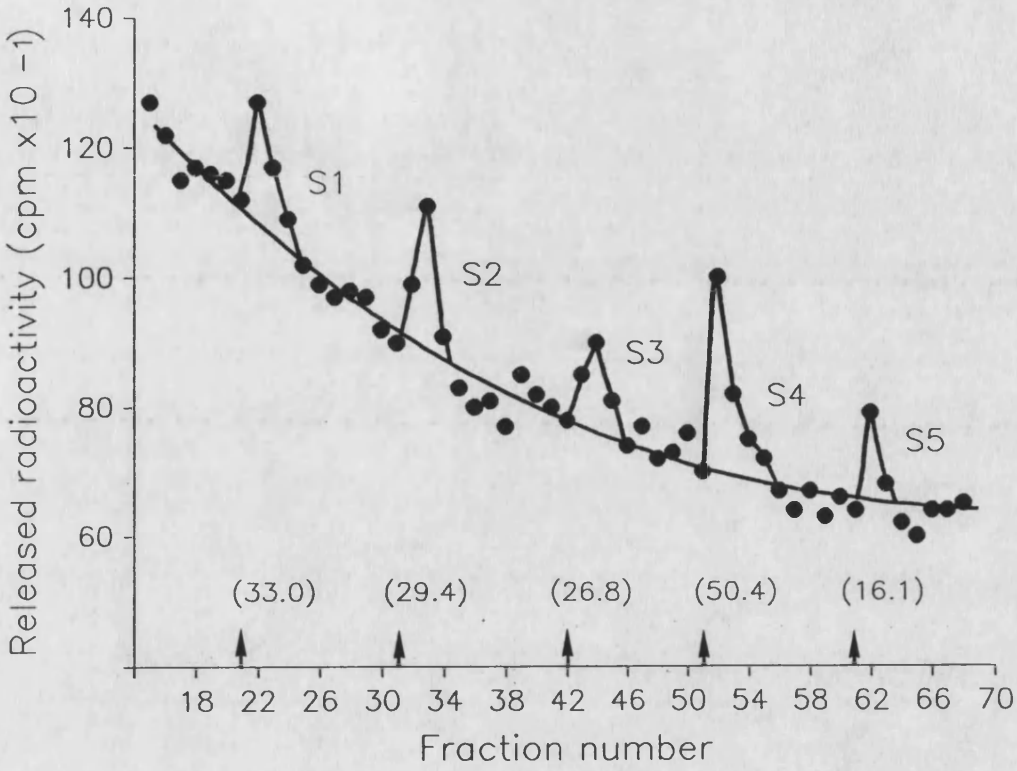

Fig. 3.14. A superfusion profile of successive stimulations of ANTX on ACh release. ANTX (10μM; S1, S2, S3), K^+ (20mM; S4) and Krebs buffer (S5) pulses were administered at 30 min intervals after a 40 min washout. ↑ Indicates pulse arriving at the synaptosomes. Numbers in brackets are fmol ACh released/mg protein.

S1 ANTX 10μM	DHβE μM	S2 ANTX 10μM	S3 ANTX 10μM	S4 K^+ 20mM	S5 KREBS BUFFER
32.1 ± 2.1 (n=6)	-	28.9 ± 0.9	25.8 ± 2.2	48.8 ± 2.4	15.5 ± 1.6
30.8 ± 2.7 (n=2)	1	27.7 ± 0.2	23.7 ± 1.1	50.6 ± 1.2	-
31.8 ± 2.4 (n=3)	10	19.5* ± 3.1	12.6** ± 2.8	47.5 ± 3.0	-

Table 3.3. The effect of DHβE on ACh released by successive stimulations with ANTX and K^+. ANTX (10μM; S1, S2 and S3) and K^+ (20mM; S4) stimulated release in the presence and absence of DHβE, introduced 15 min after S1, were expressed as fmol ACh released/mg protein ± SEM. Significantly different from control (no DHβE), * $p<0.05$, ** $p<0.02$.

approximately 50% of the evoked release of the control (no DHβE present). Thus 10μM DHβE inhibited 10μM ANTX evoked release by approximately 50%. As before DHβE had no effect on K^+ depolarisation. These results indicate that ANTX has an excitatory effect on ACh release which is blocked by DHβE suggesting it acts via a nAChR.

3.3.3.3.2. Problems with the superfusion system highlighted by these experiments

A. Temperature fluctuations

ACh release evoked by K^+ depolarisation was greater in table 3.2 than table 3.3 suggesting a problem with the system. The lower response could be due to reduced experimental temperatures of the laboratory (see section 3.3.3.4.4.) where decreases in external temperatures correlated with a decline in synaptosomal responsiveness.

Indeed, a decrease in the laboratory temperature could explain why ANTX stimulated ACh release (table 3.3) was lower than that elicited by nicotine (table 3.2). It was expected that ANTX effects on ACh release would be equal or greater than those of nicotine, as [^{3}H]nicotine binding studies, to rat P2 membranes, has shown ANTX (Ki = 3.4×10^{-10}M) to be approximately 50 fold more potent than nicotine (Ki = 1.5×10^{-8}M), MacAllan et al. (1988).

When the response to agonist is quantified (Sn/S1; table 3.4) there appears to be a similar decrease with successive stimulations of agonist (in the absence of DHβE) with both nicotine and ANTX. The response to K^+ stimulation, as a percent of S1, was essentially

AGONIST	DHβE	STIMULATION AGONIST		K^+
	μM	S2/S1	S3/S1	S4/S1
NICOTINE 50μM	-	84%	75%	160%
NICOTINE 50μM	1	44%	34%	172%
ANTX 10μM	-	90%	80%	152%
ANTX 10μM	1	90%	77%	164%
ANTX 10μM	10	61%	40%	149%

Table 3.4. Comparison of successive stimulations of nicotine, ANTX and K^+. Nicotine (50μM; S1, S2 and S3) or ANTX (10μM; S1, S2 and S3) and K^+ (20mM; S4) stimulation in the presence and absence of DHβE, introduced 15 min after S1, expressed as a percent of the S1 response.

identical throughout all the experiments (160% ± 4.1).

Nicotine stimulation was blocked, by 50%, in the presence of 1μM DHβE whereas 10μM DHβE was required to show a similar inhibition of ANTX evoked release. This 10 fold greater requirement for DHβE suggests that ANTX could be a more potent agonist than nicotine as it needs higher concentrations of the competitive antagonist to block its effects. However, although ANTX appears to be a more potent agonist than nicotine (when quantitatively comparing antagonist effects) parallel experiments where agonist is administered under the same temperature conditions need to be carried out before functional potency can be determined.

B. Air bubble effect

When a pulse of Krebs buffer was given as a control there was, surprisingly, a significant amount of tritium released (S5: fig 3.14; table 3.3), which represented almost 50% of agonist evoked release. This effect was probably due to the air bubble, which separates the pulse from the washing buffer, causing some kind of mechanical effect on the synaptosomes provoking [^{3}H]ACh release. This was probably as a result of re-introduction of buffer after the air bubble has passed (see diagram in section 3.2.5) and highlights another limitation of the superfusion protocol, which was examined further in section 3.3.3.4.1.

The influence of the air bubble artefact was illustrated in the determination of the concentration dependence of ANTX on ACh release.

This was studied by varying the ANTX concentration (1-50μM) in the S2 agonist pulse, see fig. 3.15.

Evoked release reached maximal at a concentration of 20μM. When the effect of the air bubble was taken into account, a curve of similar shape was obtained but 1μM ANTX had little or no effect above this non-specific release. A direct linear plot of ACh release (after the air bubble effect had been deducted) against ANTX concentration (not shown) gave an EC50 (concentration to give half maximal effect) of 7.5μM and a Vmax (maximum effect) of 23.9 ± 3 fmol ACh released/40s/mg protein.

3.3.3.4. Modifications made to the superfusion protocol

The experiments carried out so far have highlighted some limitations to the superfusion protocol used to study ACh release. One such problem was that the air bubble, which separates the agonist pulse from the washing buffer, appears to provoke tritium release from the synaptosomes. Another was that the responsiveness of the synaptosomes was temperature sensitive. Both of these effects were examined as outlined below.

3.3.3.4.1. The air bubble effect

A. Size dependence

As a 30s air bubble provoked 50% of the agonist evoked release (see fig. 3.14, table 3.3), was the effect dependent on the size of the air bubble? This was investigated by administering 40s pulses of nicotine (50μM) or Krebs buffer, separated from the washing buffer by increasing sizes of air bubble (10s-30s), see fig. 3.16 and

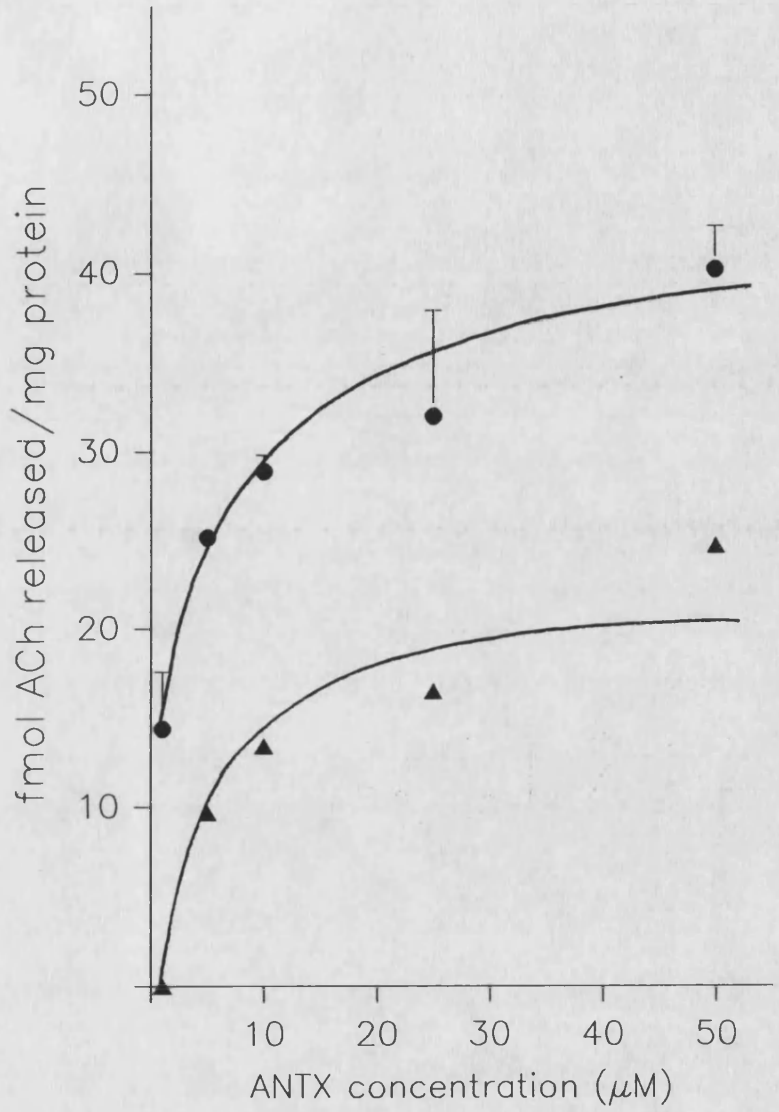

Fig. 3.15. The effect of ANTX concentration on ACh release. The concentration of ANTX in the S2 pulse was varied, and the values are the mean ± SEM, n = 2. (●) Indicates evoked release (▲) represents evoked release after deduction of the air bubble.

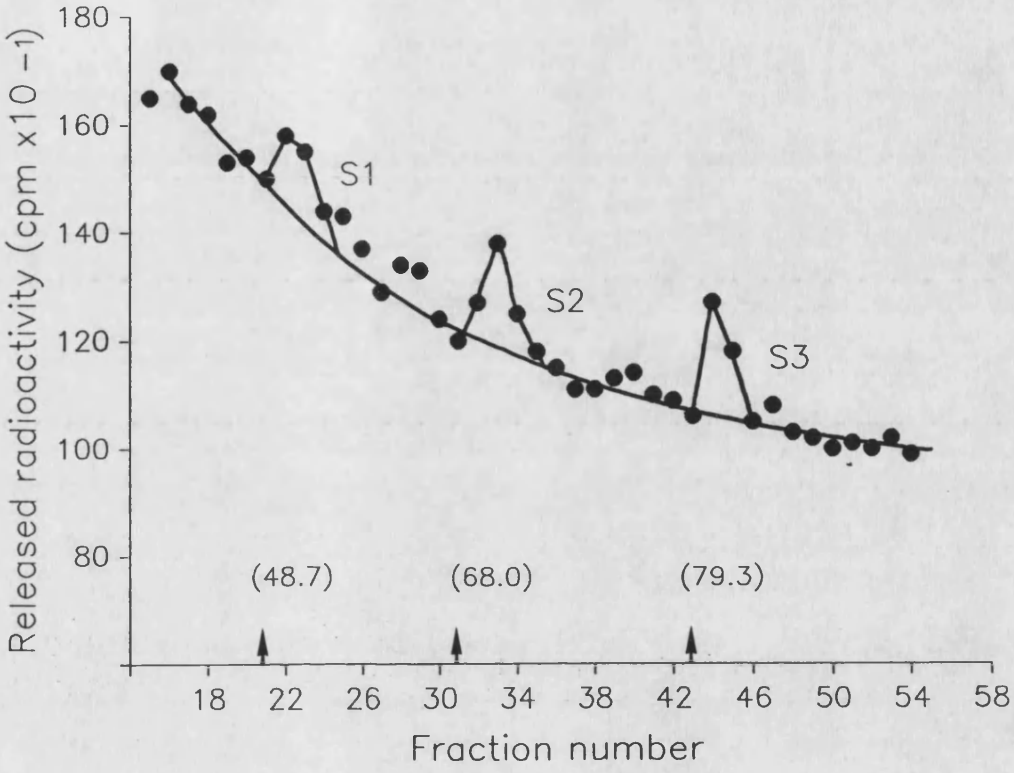

Fig. 3.16. A superfusion profile showing the effect of increasing air bubble size on nicotine evoked ACh release. Air bubble size was increased with successive stimulations of nicotine (50μM; S1: 10s; S2: 20s; S3: 30s). ↑ Indicates pulse arriving at the synaptosomes. Number in brackets are fmol ACh released/mg protein.

table.3.5.

From fig. 3.16 and table 3.5 it can be seen that there is an increase in tritium release with increasing air bubble size. When the amount of release (fmol/mg protein) was plotted against air bubble size (fig. 3.17) effect due to air bubble was linear with respect to size. When the release provoked by air bubble was deducted from that evoked by nicotine the response was constant indicating that the increase in ACh release, with subsequent stimulations of nicotine (50μM), was due to an increase in air bubble size.

When the air bubble was 5s duration, not shown, the pulse was not retained as a discrete volume as the air bubble became lost in the tubing. Thus an air bubble of 10s duration was used in further experiments as it had the smallest effect on tritium release but was still large enough to retain a discrete pulse throughout the tubing of the superfusion system.

B. The need for an air bubble

As an air bubble provokes tritium release is it necessary to have an air bubble when introducing an agonist?

To investigate this, a 40s pulse of a dye was introduced into the superfusion tubing in the presence and absence of a 10s air bubble. Benzoquinonium chloride was used as it is dark pink/red in colour and so its passage could be followed through the tubing. The length of the pulse was measured when it was first introduced and again just prior to reaching the filter support in the superfusion chamber (a distance of 143cm). The change in pulse length was noted

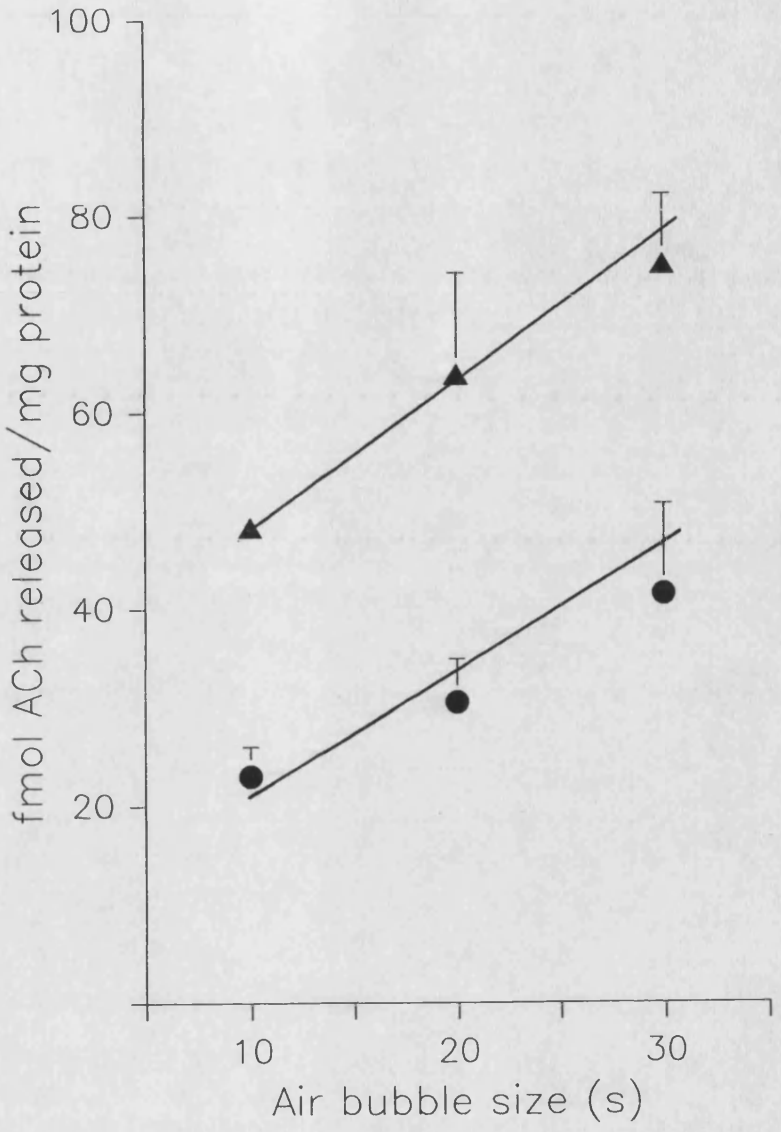

Fig. 3.17. The effect of air bubble size on tritium release.

Air bubble size was increased with successive stimulations with 50μM nicotine (▲) or Krebs buffer (●). Values are the mean ± SEM, n = 4.

	AIR BUBBLE SIZE		
	S1	S2	S3
	10s	20s	30s
NICOTINE 50μM	48.3 ± 0.3	63.9 ± 4.2	75.1 ± 3.6
KREBS BUFFER	22.8 ± 0.7	30.5 ± 2.2	41.5 ± 3.7

Table 3.5. The effect of air bubble size on release of tritium. Air bubble size was increased with successive pulses of nicotine (50μM) or Krebs buffer. Values are fmol tritium released/mg protein ± SEM, n=4.

in table 3.6.

As shown in table 3.6 there was no increase in the pulse length when it was separated from the washing buffer by an air bubble. However, without an air bubble there was considerable diffusion of the pulse resulting in a six fold increase of pulse length from start to finish.

Thus an air bubble was required to retain a discrete pulse of known concentration and prevent agonist diffusion which would prolong synaptosome stimulation.

C. Use of an injection pump

If the agonist pulse, without air bubble, was introduced closer to the synaptosomes there would be less distance for diffusion. A three way injection pump, attached to the top of the superfusion chamber (see fig. 3.2), was used to investigate this as agonist, present in a known concentration and volume in the pump, could be administered by diverting the washing buffer through the pump and on to the synaptosomes.

A superfusion profile showing the effect of nicotine (100µl; 50µM) stimulation on ACh release, via a three way injection pump, was shown in fig. 3.18. It can be seen that there are no clear peaks of evoked release (n = 5). The baseline was quite erratic which could be due to diffusion of the agonist, even in the short length of tubing from the top of the chamber to the synaptosomes resulting in prolonged agonist stimulation of unknown concentration.

TUBE	AIR BUBBLE 10s	PULSE SIZE AT START (mm)	PULSE SIZE AT FINISH (mm)
A	+	28.5	28.5
B	-	61.0	383.5

Table 3.6. The change in pulse length through the superfusion tubing, in the presence and absence of air bubble (n=2).

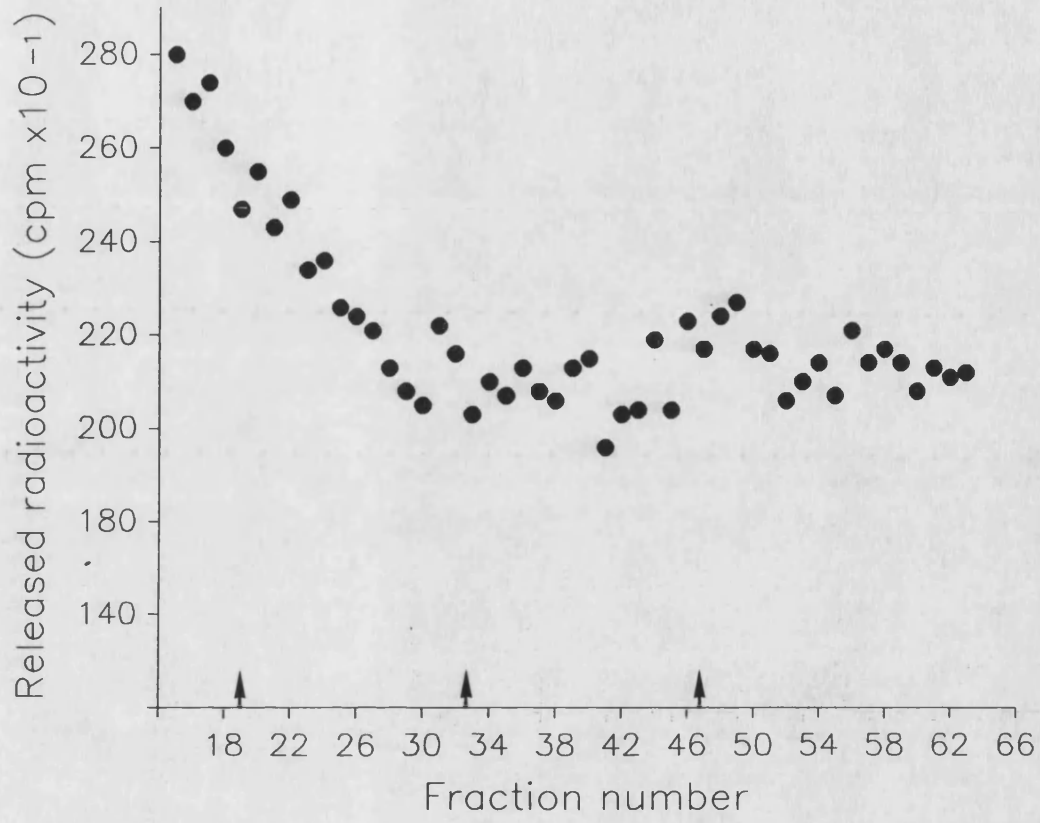

Fig. 3.18. A superfusion profile of ACh release when nicotine was administered via a three way injection pump. Nicotine (50µM; 100µl) was given at 30 min intervals after a 40 min washout period. ↑ Indicates pulse arriving at the synaptosomes.

Thus from these results it was clear that an air bubble was required to retain a discrete pulse of agonist stimulation of known concentration and duration. As a 10s air bubble was the minimum size for retaining the agonist pulse, the response to nicotine was studied to determined if it could be increased by manipulating the volume of agonist administered.

3.3.3.4.2. The effect of agonist pulse size

It has been reported that nicotine could desensitize the receptor which would reduce the response to nicotine (Egan & North, 1986; Clarke et al., 1985). Thus a pulse size of 40s duration with 50μM nicotine could be long enough to cause desensitisation. This was studied by varying the pulse size (20s-40s duration) of a known concentration of either nicotine (50μM), DMPP (the nicotinic agonist 1,1,dimethyl-4-phenylpiperazinium, 50μM) or K^+ (20mM) separated from the washing buffer by a 10s air bubble, see fig. 3.19 and table 3.7.

The release in response to buffer was not dependent on the size of the pulse indicating that Krebs buffer alone does not provoke tritium release but the increase above basal, was due to the air bubble.

When DMPP or K^+ was given as a pulse there was a trend towards an increase in ACh evoked release, though not significant, with increasing pulse size i.e. the more agonist present the greater the evoked release. However, the response to nicotine decreased with increasing pulse size suggesting that desensitisation may have occurred.

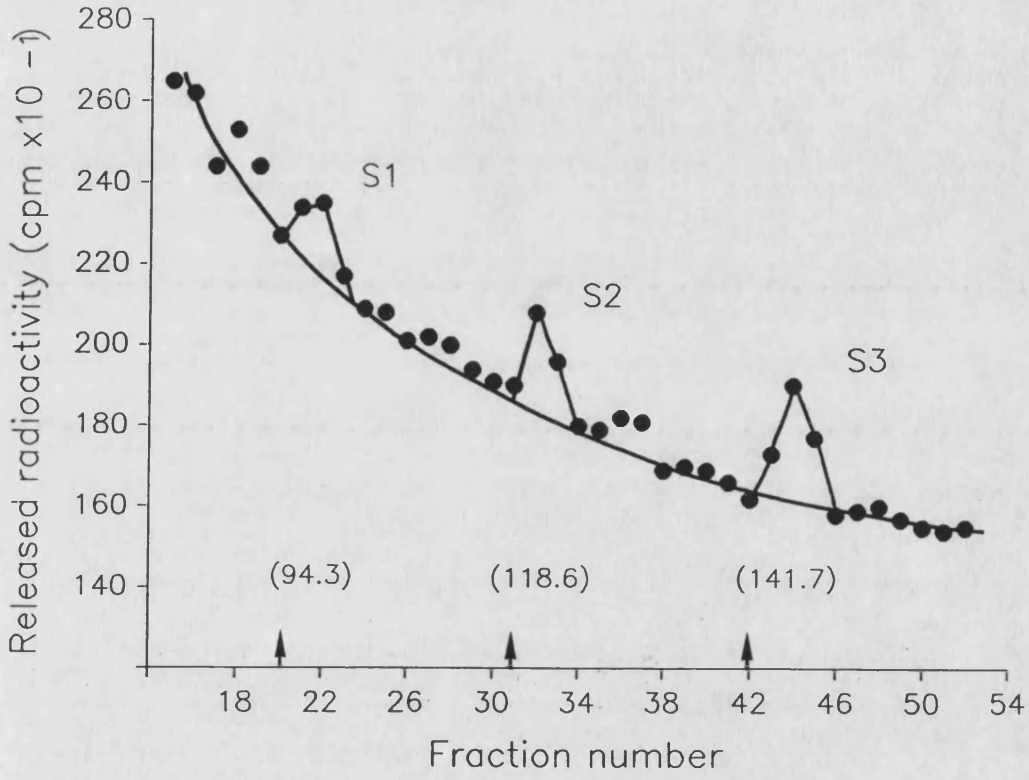

Fig. 3.19. A superfusion profile showing the effect of increasing pulse size on evoked ACh release. The pulse size was increased with successive stimulations with DMPP (50μM; S1: 20s; S2: 30s; S3: 40s). ↑ Indicates pulse arriving at the synaptosomes. Numbers in brackets are fmol ACh released/mg protein.

	PULSE SIZE		
PULSE	S1	S2	S3
	20s	30s	40s
KREBS BUFFER (n=3)	26.5 ± 1.3	24.2 ± 2.0	21.2 ± 2.6
NICOTINE 50μM (n=4)	85.7 ± 4.4	65.0 ± 3.8	50.8 ± 2.0
DMPP 50μM (n=2)	92.8 ± 2.6	116.7 ± 4.1	139.4 ± 3.4
K^+ 20mM (n=3)	184.7 ± 1.4	200.9 ± 2.9	219.4 ± 4.6

Table 3.7. The effect of varying pulse size on ACh release. Pulse size was increased with successive stimulation with Krebs buffer, nicotine (50μM), DMPP(50μM) or K^+(20mM). Values are fmol ACh released/mg protein ± SEM.

The maximum response to nicotine (50μM) was achieved by a 20s agonist pulse separated from the washing buffer by a 10s air bubble and it was these conditions that were used in further experiments.

3.3.3.4.3. The effect of nicotine concentration

Nicotine concentration may also have an effect on desensitisation. To investigate this, the effect of successive stimulations of nicotine (10μM or 50μM) was studied using a 20s agonist pulse and a 10s air bubble, see table 3.8.

From table 3.8, 50μM nicotine evoked approximately 30% less ACh than 10μM nicotine. A similar reduction in ACh release, with increasing agonist concentration, was reported by Lapchak et al. (1989) when using the nicotinic agonist methylcarbamylcholine. This suggests that the higher nicotine concentration (50μM) may be causing some receptor desensitisation thus reducing the level of ACh released.

The effect of the air bubble was equivalent in the two experiments. However, the response to air bubble amounted to approximately 25% of that evoked by 10μM nicotine (S3/S1) as opposed to 35% of that evoked by 50μM nicotine (S3/S1). This reduction in the air bubble effect probably reflects the increase in response to the lower nicotine concentration.

The conditions of a 20s pulse of 10μM nicotine, separated from the washing buffer by a 10s air bubble, was observed as giving the maximal response and so these conditions were adopted in further experiments.

NICOTINE μM	S1	S2	S3 KREBS BUFFER
10	118.2 ± 6.2	92.2 ± 4.8	28.5 ± 3.5
50	81.8* ± 4.0	69.8** ± 3.0	28.5 ± 3.9

Table 3.8. The effect of nicotine concentration on ACh release. Values are fmol ACh released/mg protein ± SEM, n=6. Significantly different from the response to 10μM nicotine, * $p<0.001$, ** $p<0.005$.

3.3.3.4.4. The effect of temperature

As discussed in section 3.3.3.3.2.A the response to agonist could be temperature sensitive. This was illustrated in fig. 3.20 where superfusion profiles of ANTX evoked ACh release were compared when the laboratory temperature was either 18°C or 25°C.

At 18°C (fig. 3.20a) there was no significant response to agonist above baseline whereas there were discrete peaks of evoked release at 25°C (fig. 3.20b). Such variation in agonist response due to changes in laboratory temperature makes the comparison of different preparations difficult. Thus a constant temperature cabinet (fig. 3.21) was constructed to eliminate this problem.

The temperature cabinet was a perspex box enclosing the entire superfusion apparatus with sliding doors for access. Inside the cabinet was a fan heater attached to a cut-off thermometer, to maintain a constant temperature and a conductor fan to circulate the air, see fig. 3.21. Although the optimum temperature would have been 37°C this was difficult to maintain in the air heated cabinet so a constant temperature of 32°C was used in further experiments.

3.4. Summary

These experiments have shown that nicotine evoked tritium release from hippocampal synaptosomes, after optimal labelling with [^{3}H]Ch, could be monitored in a superfusion system. An enzymic extraction method was developed which showed that most if not all the tritium released was ACh. Inhibition of nicotine-evoked ACh release by the competitive antagonist DHβE suggests that release was via a nAChR.

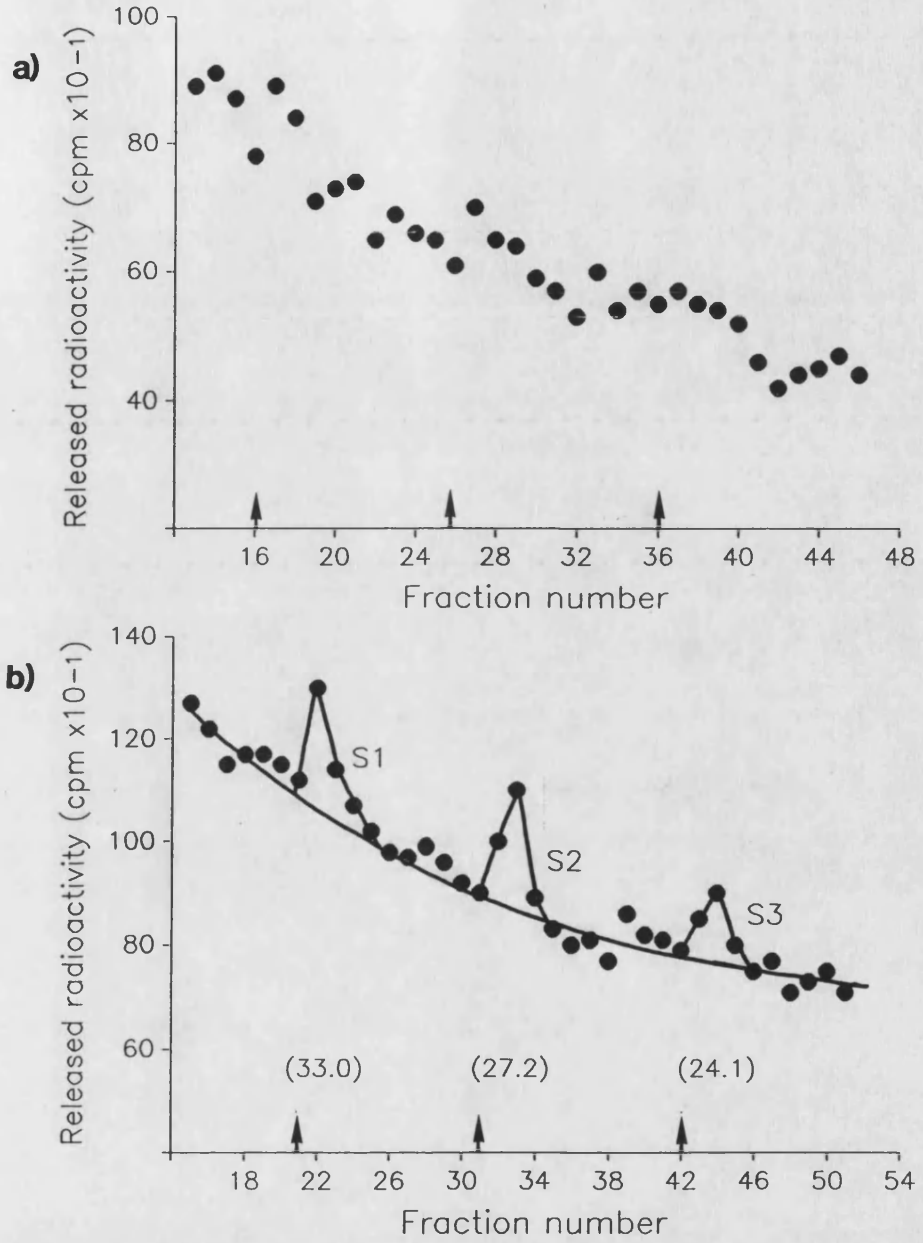

Fig. 3.20. Superfusion profiles of ANTX evoked ACh release at (a) 18°C and (b) 25°C. Synaptosomes were subjected to successive stimulations with ANTX (10μM; S1, S2, S3) after a 40 min washout period. ↑ Indicates pulse arriving at the synaptosomes. Numbers in brackets are fmol ACh released/mg protein.

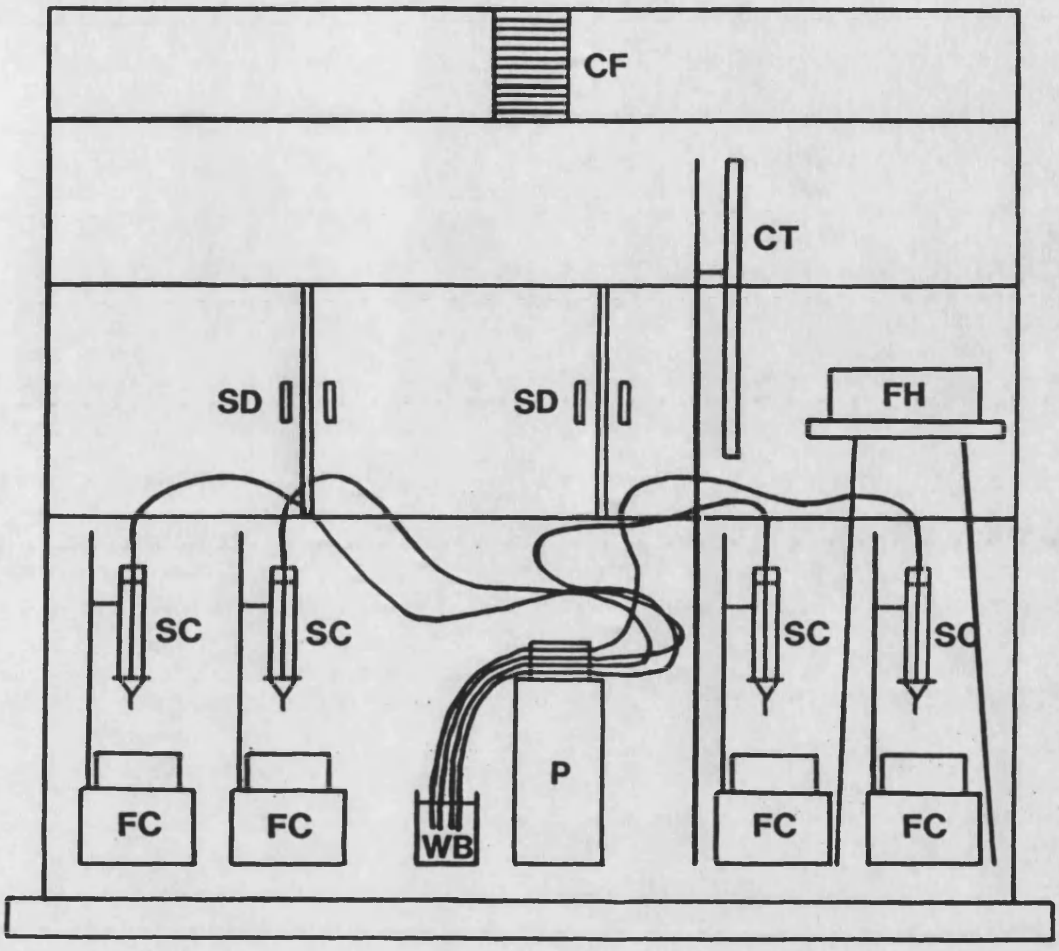

Fig. 3.21. A schematic diagram of the superfusion constant temperature cabinet. CF: conductor fan; CT: cut off thermometer; FC: fraction collector; FH: fan heater; P: pump; SC: superfusion chamber; SD: sliding door; WB: washing buffer.

However, some limitations of the superfusion protocol, of Rapier et al. (1988), for studying nicotine-evoked ACh release have been highlighted. To reduce day to day fluctuations in synaptosomal responsiveness, due to changes in laboratory temperatures, subsequent superfusion experiments were carried out in a constant temperature cabinet (32°C), fig. 3.21.

The response to nicotine was maximised by reducing the concentration and pulse size of agonist given, thus decreasing receptor desensitisation. Therefore 10μM nicotine in a 20s pulse was routinely administered in further experiments.

Results have also shown that air bubble provoked tritium release in a size dependent manner. The requirement for an air bubble has been shown to be necessary to retain a discrete agonist pulse of known concentration. The effect of air bubble was minimal at 10s duration and so was used in further experiments.

The adapted superfusion protocol was that a 20s agonist pulse was administered, separated from the washing buffer by a 10s air bubble. All superfusions were carried out in a 32°C constant temperature cabinet. The effect due to the air bubble was continually monitored, by giving a pulse of buffer, and this value was routinely deducted from the agonist evoked release to determine the response due to the drug.

CHAPTER 4. CHARACTERISATION OF THE FRACTIONS FROM THE PERCOLL GRADIENT

4.1. INTRODUCTION

During the course of these experiments Dunkley et al. (1987) reported that subcellular fractionation of a S1 supernatant, on a discontinuous Percoll gradient, produced an enrichment of synaptosomes for the study of noradrenaline release from the cortex. This protocol was adopted to determine whether subcellular fractionation of the hippocampus on Percoll gradients, would produce a purer synaptosomal preparation to study ACh release. This was undertaken as the response of sucrose isolated synaptosomes to nicotine evoked ACh release was small and differences between agonist effects were difficult to determine. Thus it was thought that an enriched population of cholinergic synaptosomes would enable the nicotinic modulation of ACh release to be better characterised.

4.2. METHODS

4.2.1. Synaptosome isolation on a discontinuous Percoll gradient

The subcellular fractionation of hippocampal S1 supernatant on discontinuous Percoll gradients was as described by Dunkley et al. (1987, 1988).

Male Wistar rats (200-250g) were killed by cervical dislocation, the brain was removed and the hippocampus dissected out. The hippocampi from six rats (600-650mg wet weight) were homogenised (10% w/v in 0.32M sucrose, pH 7.4) in a pre-cooled glass-teflon homogeniser (clearance 0.31mm) by 2 x 6 up and down strokes at 200rpm. The homogenate was then centrifuged at 1,000g for 10 min at 4°C in a MSE 18 centrifuge using a 16 x 15ml fixed

angle rotor. The supernatant, S1, made up to 8ml with 0.32M sucrose, was layered on to four Percoll gradients using a peristaltic pump set up with a large bore needle (19G x 1.5 inch; running speed 1ml/min).

To make the gradients, Percoll was first filtered using a Millipore AP15 pre-filter, to remove aggregates which otherwise sediment during washing. Then the gradients, comprising 2ml of 23%, 15%, 10% and 3% Percoll (v/v in 0.32M sucrose, pH 7.4) were layered using a peristaltic pump set up with a fine bore needle (25G x 15/16 inch; running speed 1ml/min). The gradients were stored at 4°C for up to 24 hr before use.

After layering the S1 supernatant, the gradients were centrifuged at 32,000g for 5 min at 4°C in a MSE 18 centrifuge using a 16 x 15ml fixed angle rotor. Centrifugation time was important because this non-equilibrium procedure separates subcellular particles on the basis of size as well as density, in contrast to conventional isopycnic gradients, and so did not include acceleration and deceleration. Centrifugation times of less than 3 min results in incomplete movement of subcellular particles. Whereas prolonged centrifugation beyond 5 min disrupts normal fractionation of the organelles, as Percoll particles are not of uniform size, and so gradients would form within each Percoll step.

After centrifugation five major subcellular fractions were obtained (interfacial fractions F1-F4 and a pellet F5, see fig. 4.1).

Each fraction F1-F5 was taken, using a pasteur pipette, and washed twice with Krebs buffer (10ml) by centrifugation at 15,000g for 15 min at 4°C in a MSE 18 centrifuge using a 16 x 15ml fixed

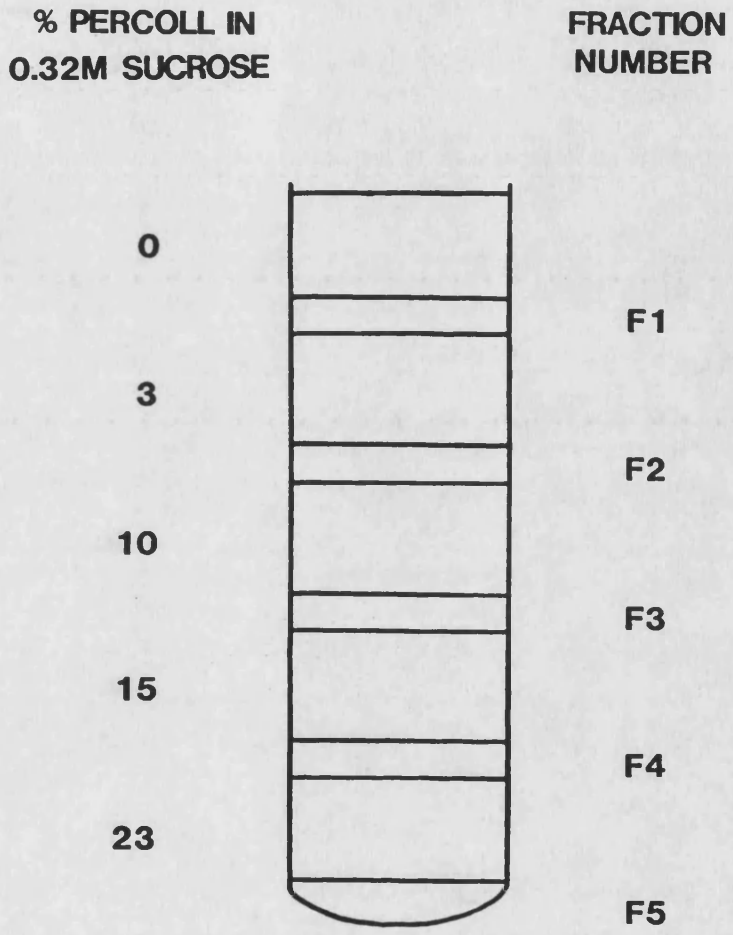

Fig. 4.1. A schematic diagram of the subcellular distribution of the hippocampal S1 supernatent on a discontinuous Percoll gradient. The gradient after centrifugation at 32,500g for 5 min at 4°C in a MSE 18 centrifuge using a 16x15ml fixed angle rotor.

angle rotor. The fractions were finally resuspended in Krebs buffer (F1-F4, 1.5ml; F5, 0.7ml) using a pasteur pipette.

4.2.2. Protein determination

4.2.2.1. Standard Lowry

The protein content of each fraction (S1, F1-F5) was determined using the method of Lowry et al.,(1951) as described in section 3.2.3.

4.2.2.2. Modified Lowry for samples containing detergent

Protein concentrations of samples containing detergent were determined using the method of Markwell et al.,(1978). A standard curve was constructed using a freshly prepared solution of BSA in Triton X-100 buffer (for composition see section 4.2.5.) over the concentration range of 20-100µg/ml.

To 0.1ml of BSA standard or sample (diluted in Triton X-100 buffer: S1, 1/10, 1/20; F1-F5, 1/4, 1/8) 1ml of reaction mixture was added, mixed and incubated for 10 min at room temperature. The reaction mixture consisted of 100 vol of solution A (2% Na_2CO_3, 0.4% NaOH, 0.16% sodium tartrate and 1% sodium dodecyl sulphate) mixed with 1 vol solution B (4% $CuSO_4 5H_2O$). After incubation, 0.1ml Folin-Ciocalteau's reagent, diluted 1:1 with distilled water, was added to each sample with mixing and the colour allowed to develop for 45 min at room temperature. Blanks contained 0.1ml of Triton X-100 buffer in place of protein. The absorbance was read at 750nm in a Pye Unicam SP8-100 spectrophotometer.

4.2.3. Lactate dehydrogenase assay

LDH activity of each fraction (S1, F1-F5) was determined using the method of Johnson (1960) as modified by Marchbanks (1967); this was outlined in section 3.2.2.

4.2.4. Acetylcholinesterase assay

When ACh is released from the presynaptic nerve terminal it is hydrolysed by AChE. Thus AChE activity gives an indication of the possible cholinergic nature of neurones but because of its ubiquitous distribution it is a non specific plasma membrane marker.

The levels of AChE can be assayed by allowing the enzyme to hydrolyse thiocholine esters, following the protocol of Ellman et al. (1961). The thiol produced exchanges with 5,5'-dithiobis (2 nitrobenzoate) (DTNB) in situ, producing 5-mercapto-2-nitrobenzoate. This is yellow in colour and so the rate of reaction can be measured by following the change in optical density at 412nm with time.

The reaction is as follows:

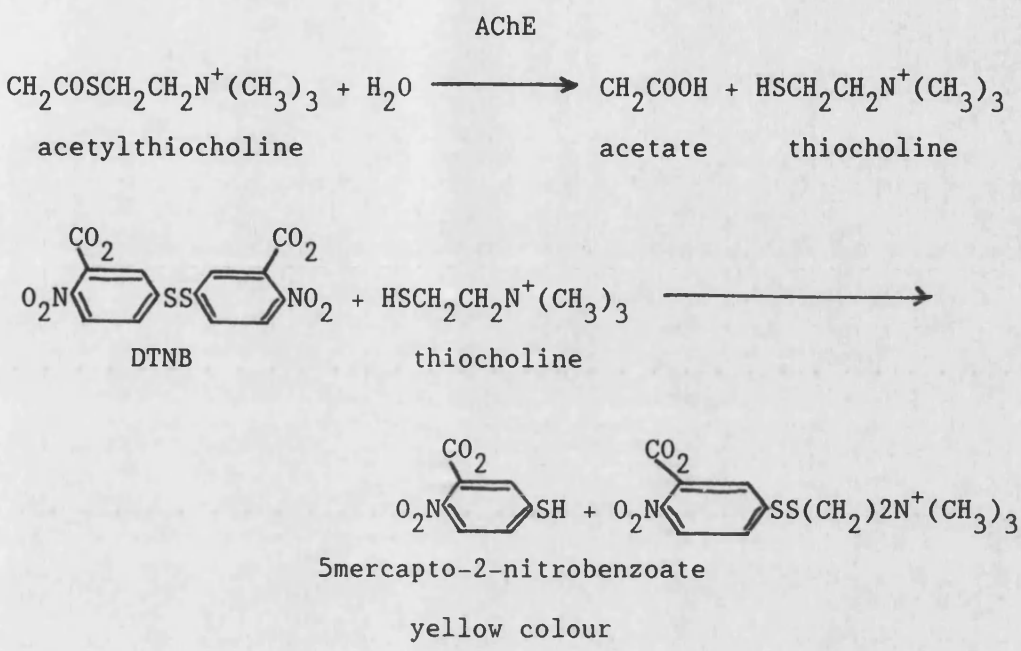

Samples (0.1ml, S1; 0.5ml, F1-F5) of the fractions from the Percoll gradient were added to 0.1M phosphate buffer (2.7ml; 0.1M KH_2PO_4: 0.1M Na_2HPO_4, pH 8.0) and incubated at 37°C for 30 min. Then the samples were cooled to room temperature before being placed in a cuvette (3ml). To these 0.1ml DTNB solution (0.01M DTNB, 15mg $NaHCO_3$ in 0.1M phosphate buffer, pH 7.4) was added followed by 0.1ml of 0.015M acetylthiocholine iodide (in 0.1M phosphate buffer, pH 8.0). This was stirred rapidly and the change in absorbance at 412nm was recorded for a few minutes.

The results were expressed as µmoles of acetylthiocholine hydrolysed/min/mg protein:

$$-\frac{A}{E} \times \frac{\text{vol in cuvette}}{\text{vol in sample}} \times \frac{1}{p} \times 10^{-3}$$

where A = change in absorbance/min

E = molar absorption coefficient ($1.34 \times 10^{4} Mcm^{-1}$)

l = length of light path (1cm)

p = protein concentration (mg/ml)

ACh hydrolysis, by AChE, is undesirable when studying the effects of drugs on ACh release, especially when using more complex models like the hippocampal slice (see section 6.3). To estimate the concentration of the AChE inhibitor, BW284C51, needed to block AChE activity the AChE assay, described above, was repeated using the S1 supernatant (0.1ml) in the presence of varying concentrations of BW284C51 (10^{-4} - 10^{-10}M in 0.1M phosphate buffer, pH 8.0). The S1 fraction was used as it gives a better representation of the AChE activity in the hippocampal slice than any one of the fractions from the Percoll gradient.

4.2.5. Choline acetyltransferase assay

The cholinergic nature of the fractions from the Percoll gradient was further investigated by assaying for the cholinergic marker ChAT.

The protocol used was based on the liquid cation exchange procedure described by Fonnum (1975). The washed fractions from the gradient were resuspended in Triton X-100 buffer (comprising: 0.05M phosphate (KH_2PO_4, Na_2HPO_4), 0.2M NaCl, 1mM EDTA and 0.5% Triton X-100) such that the protein concentration was approximately 1mg/ml

(see section 4.2.2.2., modified Lowry for samples containing detergent). For each fraction the following reaction mixtures were set up in duplicate:

Total activity = 20µl assay buffer + 10µl sample
Assay blank = 20µl assay buffer + 10µl sample + 20µl formic acid

The assay buffer was freshly prepared on the day of use and comprised: 12.5mM choline chloride, 0.1mM neostigmine bromide, 0.2mM [^{3}H]AcCoA (specific activity 10µCi/µmol) and 5mg/ml BSA in Triton X-100 buffer.

The reaction mixtures were incubated at 37°C for 10 min before the reaction was stopped by the addition of 20µl formic acid. To each sample 0.3ml tetraphenylboron(TPB)/heptan2one (15mg/ml) was added, shaken vigorously and centrifuged in a microfuge for 3 min at high speed (12,000g). A sample (150µl) of the upper organic phase was taken and added to 5ml of scintillant. Vials were cooled at 4°C overnight, to reduce chemiluminescence, before being counted.

The standards used were:

150µl TPB/heptan2one

150µl TPB/heptan2one + 10µl assay buffer

This latter standard was used to determine the counting efficiency.

Specific ChAT activity (the difference between total activity and assay blank) was expressed as μmoles [^{3}H]ACh produced/min/mg protein:

$$\frac{\text{specific ChAT activity} \times 2 \times 1 \times 30}{\text{c.e.} \times 2.2 \times 10^6 \times 10 \times 10} \times \text{mg/ml}$$

where 2 = dilution factor, counted 150μl from 300μl

1 = assumed 100% extraction

30 = 10μl sample in 300μl extraction mixture

c.e. = counting efficiency

2.2×10^6 = dpm/μCi

10 = specific activity of [^{3}H]AcCoA (μCi/μmole)

10 = incubation time (min)

mg/ml = protein concentration

4.2.6. Bromoacetylcholine synthesis

In the presence of AcCoA the mitochondrial enzyme carnitine acetyltransferase (EC: 2.3.1.7) will acetylate carnitine to acetylcarnitine. When carnitine levels are low carnitine acetyltransferase will use Ch as an alternative substrate producing ACh (White & Wu, 1973; Tucek, 1985). To ensure that the radioactivity measured in the above assay was ACh produced by ChAT and not by carnitine acetyltransferase an inhibitor was synthesised. This inhibitor was bromoacetylcholine which acts as a competitive substrate for ChAT (Morris & Grewaal, 1971; Kasa & Morris, 1972; Roskoski et al., 1974). Thus any radioactivity measured in the presence of bromoacetylcholine would be due to carnitine acetyltransferase activity.

The synthesis of bromoacetylcholine follows that described by Chiou & Sastry (1968) and produced the perchlorate salt.

To 4.60g choline bromide (0.025moles) placed in an Erlenmeyer flask, cooled in ice water, 6.06g bromoacetylbromide (0.03moles) was added with stirring. The reaction product (a viscous mass) was dissolved in 3.75ml ice cold absolute ethanol before 2.81ml of 70% perchloric acid was added. A white precipitate separated which was filtered and recrystallised from acetone-ethylacetate.

To determine non-specific acetyltransferase activity the following reaction mixture was set up in duplicate:

non-specific acetyltransferase activity = 20µl assay buffer + 10µl sample + 10µl bromoacetylcholine (0.1mM)

After a 10 min incubation at 37°C the reaction was stopped by the addition of 20µl formic acid. ACh was extracted into TPB/heptan2one, centrifuged and then counted in the presence of scintillant, as described above.

4.2.7. Choline uptake by fractions from the Percoll gradient

The parameters used for [^{3}H]Ch uptake by the fractions, from the Percoll gradient, were those determined for uptake by the sucrose gradient synaptosome fraction (see section 3.2.4.2.).

The fractions were pre-equilibrated at 37°C for 10 min before [^{3}H]Ch (0.8µM final concentration) was added and the samples incubated for a further 20 min at 37°C. A sample (100µl) was then

taken, filtered and washed with Krebs buffer (5ml) and counted in the presence of 5ml scintillant. Non-specific uptake was determined in the presence of HC-3 (1μM). Results were expressed as pmoles choline taken up/mg protein.

4.2.8. Characterisation of choline uptake by fraction F4

The parameters used for [^{3}H]Ch uptake, above, were optimal for choline uptake by sucrose isolated synaptosomes. The conditions for uptake were examined to determine if these parameters were also optimal for [^{3}H]Ch uptake by fraction F4 from the Percoll gradient.

4.2.8.1. The effect of incubation time

At time intervals (0-60 min) samples (100μl) were taken, filtered, washed and counted in 5ml scintillant, as described in section 3.2.4.1. Non specific uptake was determined at 4°C.

4.2.8.2. The effect of choline concentration

The effect of varying choline concentration (0.1-2.0μM) on choline uptake was determined as described in section 3.2.4.2. Non-specfic uptake was determined at 4°C.

The final [^{3}H]Ch loading conditions used were 0.8μM [^{3}H]Ch incubated for 20 min at 37°C after a 10 min pre-equilibration period.

4.2.9. Acetylation of [^{3}H]Ch by fraction F4 synaptosomes

Having established the optimum [^{3}H]Ch loading conditions by fraction F4 synaptosomes, above, the percent acetylation of this accumulated [^{3}H]Ch was determined to give an indication of the proportions of radioactivity associated with Ch and ACh in the

synaptosome preparation, used in the superfusion system. ACh was separated from Ch by thin layer chromatography after the choline bases had been extracted from the synaptosomes.

4.2.9.1. Extraction of ACh and Ch from synaptosomes

The method used was based on that described by Wonnacott & Marchbanks (1976). Fraction F4 (1ml) was loaded with [^{3}H]Ch (0.8µM), as described above in section 4.2.8.2., and after the 20 min incubation excess [^{3}H]Ch was removed by washing in Krebs buffer (1ml) and centrifugation in a microfuge at low speed (3,000g, 7 min). The pellet was resuspended in Krebs buffer (1ml) and samples (0.2ml) placed into four eppendorf tubes together with 3M perchloric acid (0.1ml). These were mixed and left at 4°C for 15 min.

A control sample (fraction F2) containing [^{3}H]ACh, synthesised as described in section 3.2.7., was set up to determine the percent hydrolysis of ACh that may occur during the extraction procedure. Fraction F2 (1ml) was incubated at 37°C for 30 min, washed with an equal vol of Krebs buffer with centrifugation in a microfuge, as above. The pellet was resuspended in Krebs buffer (1ml) and 0.2ml samples were placed into four eppendorf tubes together with 3M perchloric acid (0.1ml). These were mixed before [^{3}H]ACh (20µl; 1.0 x 10 ^{5}cpm) was added, mixed and left at 4°C for 15 min.

The following steps were applied to each of the test and control samples, at each step a sample (20µl) was taken to determine the amount of radioactivity present. All the solutions and samples were kept on ice, except during centrifugation, to keep ACh hydrolysis to a minimum.

After 15 min at 4°C the protein was sedimented by centrifugation in a microfuge, as before. A sample of the supernatant (0.25ml; step 1) was taken and mixed with Na_2HPO_4 (0.1ml; 1M) before 1ml of TPB/heptan2one (20mg/ml) was added. This was mixed for 15s before the two phases were separated by centrifugation, as above. TPB complexes with the choline bases and takes them into the organic solvent, heptan2one (see section 3.3.3.2.; Fonnum, 1969). A sample (0.8ml) of the organic phase (step 2) was mixed with 0.4M HCl (0.8ml) and the two phases were separated by centrifugation, as above. Strong acids are used to replace the choline esters by H^+ ions in the complex with TPB (Fonnum, 1969) so the bases pass into the aqueous phase. The upper organic phase was discarded and samples (0.65ml) of the aqueous phase (step 3) were frozen in liquid nitrogen before being freeze dried overnight.

4.2.9.2. Separation of the choline bases by thin layer chromatography

The separation of Ch and ACh by thin layer chromatography uses the method of Hemsworth & Morris (1964) as described by Marchbanks & Israel (1971).

The freeze dried samples were dissolved in a carrier solution (25µl; analar methanol containing 10mM Ch and 10mM ACh) and samples (10µl) were spotted onto thin layer chromatography plates coated with cellulose (MN300HR cellulose, 0.25mm thick). Samples of [^{3}H]Ch or [^{3}H]ACh (both 1:1 with the carrier solution) were also spotted on the plates. The [^{3}H]Ch spot would give an indication of the percent crossover of radioactivity from Ch to ACh on the plates and the [^{3}H]ACh spot would give the percent acetylation of the synthesised

[^{3}H]ACh standard which was used in the control samples.

The plates were then eluted with butanlol: 95% ethanol: glacial acetic acid: distilled water (8:2:1:3 by vol; Augustinsson & Grahn, 1953). Once the solvent front had ascended at least 12cm the solvent front was marked and the plates allowed to dry at room temperature. The choline bases were identified by spraying with iodoplatinate reagent (0.15% potassium chloroplatinate, 3% potassium iodide in HCl). ACh appeared as a purple spot with a Rf value of 5.6 and Ch appeared as a blue spot with a Rf value of 4.6 (see fig. 4.11). Rf values were determined by the distance the base had moved relative to the solvent front.

The spots were scraped off the plates into minivials, decolourised with 5% (w/v) Na_2SO_3 in ethanol (20µl) and 0.1M ethanolic ammonia solution (0.6ml). Radioactivity was counted in the presence of 3ml scintillant.

CALCULATIONS

The percent hydrolysis of ACh in the control samples was determined:

$$1 - \frac{ACh}{ACh + Ch} \times 100$$

where ACh = radioactivity in the ACh spot

Ch = radioactivity in the Ch spot

The percent acetylation of the test samples was determined:

$$\frac{ACh}{ACh + Ch} \times \frac{1}{1 - \text{fractional hydrolysis}} \times 100$$

where ACh = radioactivity in the ACh spot

Ch = radioactivity in the Ch spot

4.2.10. Superfusion of synaptosomes isolated on sucrose and Percoll gradients.

The effect of nicotine on ACh release from either the sucrose gradient synaptosome fraction or fraction F4 from the Percoll gradient was studied, in parallel, by superfusion (as described in section 3.2.5.).

The [^{3}H]Ch loaded synaptosomes (0.8μM, final concentration, 20 min at 37°C) were washed with an equal vol of Krebs buffer, to remove excess label. The pellets were gently resuspended in Krebs buffer (approximately 1mg/ml) and samples (150μl) were placed in the

superfusion chamber (see fig. 3.2). After a 40 min washout period, the synaptosomes were stimulated at 30 min intervals with a 20s pulse of drug (S1 & S2, 10μM nicotine; S3 Krebs buffer; S4, 20mM K^+). The agonist pulse was separated from the washing buffer by a 10s air bubble. The evoked release was quantified by summing the radioactivity in the fractions contributing to a peak of release, after subtraction of basal release, and expressed as fmoles ACh released/mg protein.

4.2.11. Electron microscopy

Each fraction from the Percoll gradient (S1, F1-F5, see fig. 4.1) and the sucrose gradient (PA, PB and PC, see fig. 3.1) was examined by electron microscopy.

Samples (0.2ml) of each fraction from both gradients (see section 3.2.1. for sucrose gradient; section 4.2.1. for Percoll gradient) were washed three times with 0.1M phosphate buffer (1ml; 0.5M Na_2HPO_4, 0.5M KH_2PO_4, pH 7.4) by centrifugation for 7 min in a bench microfuge, at low speed (3,000g). This removes bicarbonate from the samples which would otherwise cause granular precipitates with the osmium fix (see below). The proteins in the samples were then fixed in 1ml 2% (v/v) glutaraldehyde in 0.1M phosphate buffer at 4°C overnight.

The glutaraldehyde fixative was removed by washing the samples three times in 0.1M phosphate buffer (1ml) with centrifugation for 7 min in a bench microfuge, at low speed. The lipids in the samples were fixed with 1ml 1% osmium, in 0.1M phosphate, for 1 hr at room temperature. The osmium fixes the lipids by cross-linking with the

unsaturated bonds in the lipids. This cross-linking with osmium imparts some contrast as it is electron dense. Once the samples were fixed the excess osmium was removed by washing three times with distilled water with centrifugation, as above. The samples were 'en bloc' stained with 2% uranyl acetate for 30 min at room temperature in the dark, as uranyl acetate is light sensitive. The excess uranyl acetate was removed by washing three times with distilled water followed by centrifugation as before.

The samples were then dehydrated through a series of acetones, 50%, 70%, 90% and 100% (2 x 5 min at each concentration with centrifugation for 7 min at 3,000g). The acetone concentration was increased gradually to ensure complete dehydration of the samples. The samples were placed in Taab (medium hardness) Epoxy resin (50% v/v in 100% acetone) and left at room temperature overnight. The samples were infiltrated with 100% resin (twice, with centrifugation) and left in 100% resin for 4-6 hr at room temperature before adding 1ml 100% resin and curing the samples in an oven (70°C) for 48 hr. Once cured the samples were sectioned on a Reichert OMU3 ultramicrotome using a glass cutter. The colour of the section reflects its thickness and only sections which were silver/gold in colour (approximately 90nm) were taken and placed on copper grids.

The sections were stained, before viewing, by floating the grids on drops of 2% uranyl acetate for 7 min at room temperature, in the dark. Uranyl acetate was removed from the grids by washing four times on drops of distilled water before being placed on drops of Reynolds' lead citrate (Reynolds, 1963) for 7 min at room temperature. The lead citrate stain was applied in the presence of

0.1M NaOH which absorbs carbon dioxide from the air thus preventing the precipitation of lead carbonate. The lead acts as a general stain as it attaches to bound osmium in the membrane enhancing the contrast (Marinozzi, 1963). The excess lead citrate was removed by washing four times on drops of distilled water. The grids were then allowed to dry on filter paper and the sections were viewed and photographed on a 1200EX or 2000FX electron microscope.

Prints were made using Ilford multigrade paper and developed in Ilford multigrade developer for 2 min. The prints were then placed in a stopbath, water with a few drops of acetic acid, for 5-10s before the image was fixed in a solution of Ilford Ilfospeed fixer for 5-10 min. Excess reagents were washed away by a continual flow of water (for at least 15 min) before the prints were dried.

4.3. RESULTS AND DISCUSSION

4.3.1. Protein distribution across the Percoll gradient

When the S1 supernatant from the rat hippocampal homogenate was separated on Percoll gradients five major subcellular fractions were obtained (interfacial fractions F1-F4 and a pellet F5; see fig. 4.1). The protein concentration of each fraction was determined, see table 4.1.

35.5% of the S1 supernatent was recovered in the washed fractions (twice in Krebs buffer, see methods 4.2.1.) from the Percoll gradient. This low protein recovery probably reflects losses due to washing. Fraction F2 had two to five times more protein than any other fraction, which accounted for 44% of the recovered protein. A similar protein distribution was reported by Dunkley *et al* .(1988)

FRACTION	PROTEIN mg/g wet weight	RECOVERY (% S1)
S1	41.15 ± 2.7	(100)
F1	1.71 ± 0.4	4.2
F2	6.37 ± 0.4	15.5
F3	3.37 ± 0.2	8.2
F4	2.00 ± 0.3	4.9
F5	1.15 ± 0.1	2.8

Table 4.1. Protein distribution of the S1 supernatant on Percoll gradients. Values are the mean ± SEM of 6 experiments

for the separation of rat cortical S1 supernatant on Percoll gradients were 44.7% of the protein was recovered, the majority of which (42%) was present in fraction F2. This similarity with the work of Dunkley et al.,(1988) shows that the procedure has been reproduced for use with this discrete brain region.

4.3.2. Lactate dehydrogenase activity

Each fraction from the Percoll gradient was assayed for LDH activity (fig. 4.2), a high occluded LDH level indicates enrichment of synaptosomes in the fraction (Marchbanks, 1967).

As expected, the S1 supernatant had a high level of free LDH, only 20% of the total LDH activity was occluded, due to cytoplasmic LDH which was released during homogenisation. 81% of the S1 occluded LDH activity was recovered in the fractions from the gradient. Fraction F1, like the S1 fraction, had a high level of free LDH activity with only 20% of the total LDH activity occluded. Fraction F1 contains mainly myelin and membrane fragments, as shown by electron microscopy (Dunkley et al., 1988; section 4.3.6., fig. 4.8E) and is consistent with a low level of occluded LDH activity. A large amount of the free LDH from broken cells is present at the top of the gradient.

Fractions F2, F3 and F4 all had approximately 80% of the total LDH activity occluded, suggesting high concentrations of synaptosomes in these fractions. Electron microscopy (Dunkley et al., 1988; section 4.3.6., fig. 4.8F, G and H) shows a high synaptosomal content in these fractions. The synaptosome fraction, PB, from the sucrose gradient had a similarly high occluded LDH level (80%; section

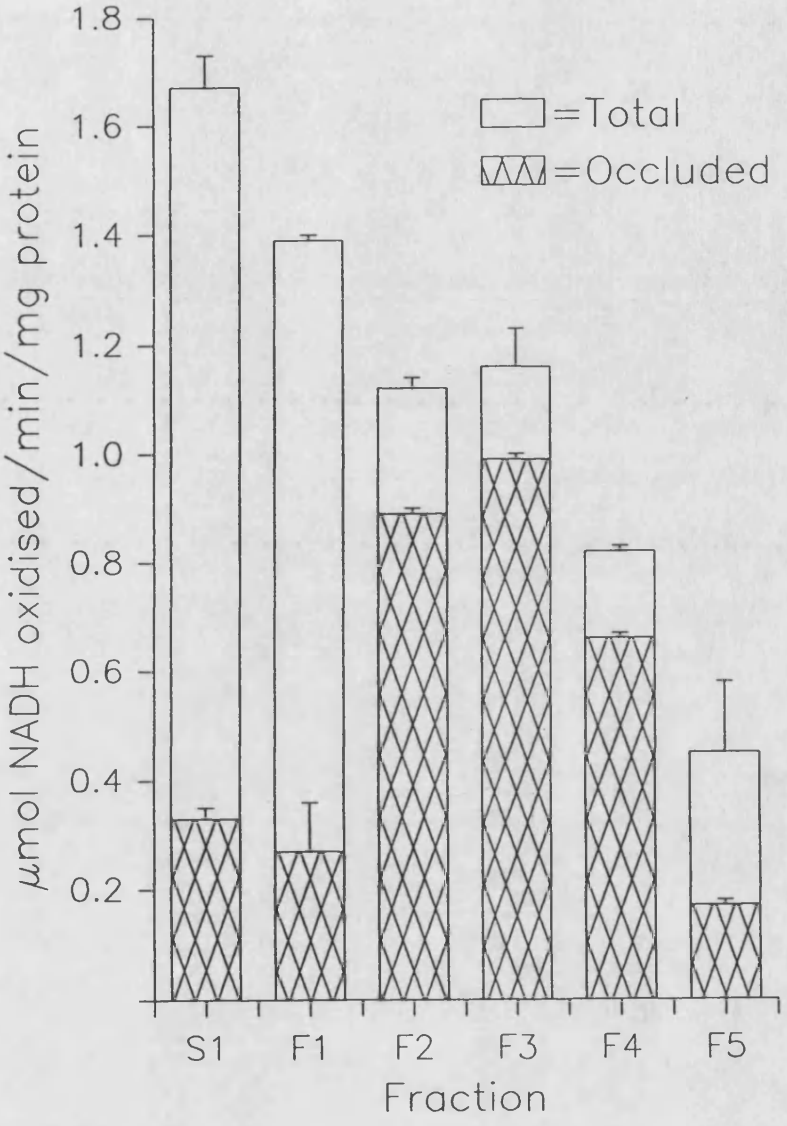

Fig. 4.2. LDH activity in fractions from the Percoll gradient.

Enzyme activity was assessed by measuring the oxidation of NADH at 340nm, with pyruvate as substrate, in the presence (total LDH) or absence (free LDH) of Triton X-100. Occluded levels were calculated as the difference between total and free LDH. Values are the mean ± SEM, n=8.

3.3.1.). The low LDH activity in fraction F5, 38% of which was occluded, suggests that the synaptosomal concentration in this fraction was small. The low level of occluded LDH in fraction F5 could indicate that the synaptosomes may not be as structurally intact, after washing, as those in the other fractions thus fraction F5 would have a relatively high level of free LDH. Electron microscopy showed (Dunkley et al., 1988; section 4.3.6., fig. 4.8I) that this fraction contained mainly extrasynaptosomal mitochondria.

This LDH distribution closely parallels that reported for the synaptosomal marker synapsin 1 (Dunkley et al., 1988). The high level of synapsin 1 activity in fraction F2 was due, in part, to fragments of synaptic plasma membrane present in the fraction as fraction F3 and F4 had higher functional synaptosomal activities. As shown in fig. 4.8F, fraction F2 contains empty membrane sacs which could entrap LDH before resealing thus giving an usually high LDH activity in this fraction.

4.3.3. Acetylcholinesterase activity

4.3.3.1. Activity across the Percoll gradient

Distribution of AChE activity across the Percoll gradient was used as a marker for cholinergic terminals in the fractions, fig. 4.3. Of the AChE activity in the S1 supernatant, 65% was recovered from the Percoll gradient in fractions F1-F5.

Although AChE activity was found in all gradient fractions, there was a significant enrichment in fractions F1-F4 relative to S1. The slightly higher activity in fraction F1 could be due to a greater abundance of membrane fragments, see fig. 4.8E. Fraction F5 appeared

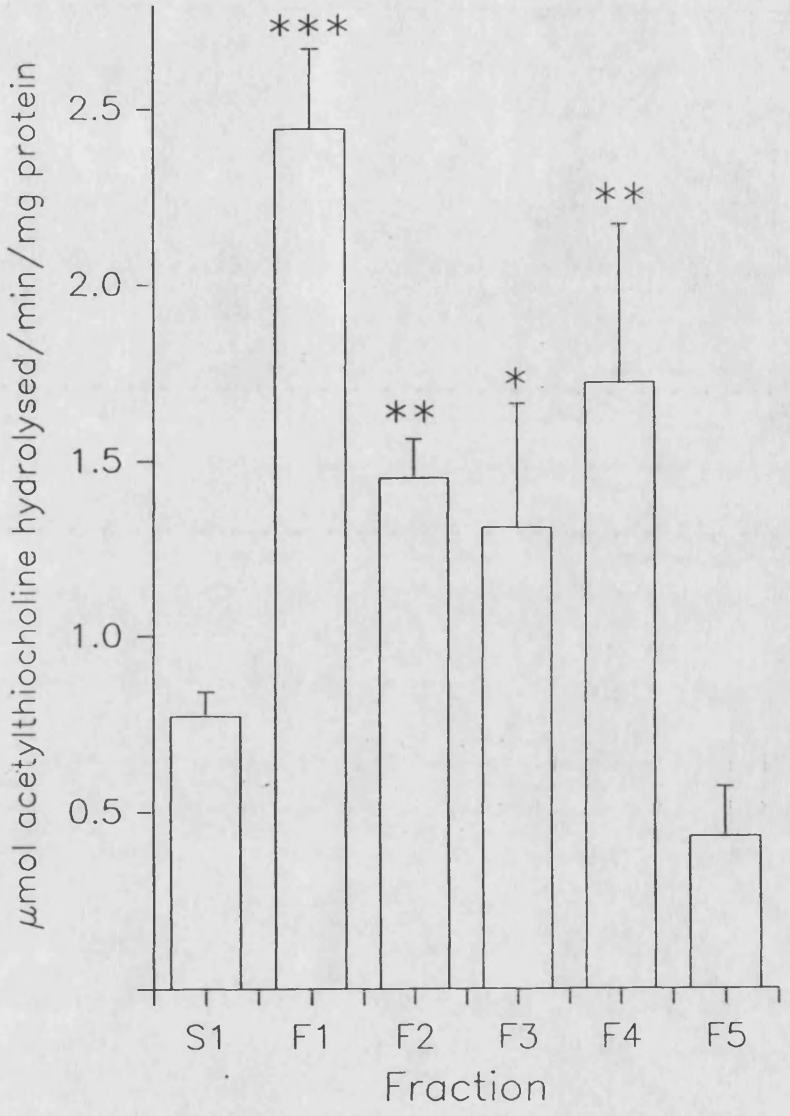

Fig. 4.3. AChE activity in fractions from the Percoll gradient. Enzyme activity was assessed by measuring the hydrolysis of acetyl thiocholine in the presence of DTNB at 412nm. Values are the mean ± SEM, n=4. Significantly different from the S1 supernatant, * $p<0.05$, ** $p<0.005$, *** $p<0.001$.

to have a lower AChE activity and probably reflects its high extrasynaptosomal mitochondrial and low plasma membrane content, see fig. 4.8I.

This ubiquitous distribution of AChE across the Percoll gradient shows that AChE activity is not a specific marker for cholinergic nerve terminals. Indeed, AChE activity has been reported in brain regions where there is little ACh (Eckenstein & Sofroniew, 1983) and in non-cholinergic and non neuronal cells; for example: erythrocytes, plasma, blood vessels and placenta (Small, 1989). Thus AChE activity alone is not a very specific indication of the cholinergic nature of the gradient fractions.

4.3.3.2. Acetylcholinesterase inhibition by BW284C51

When studying ACh release it is not advantageous to have AChE present, which breaks down ACh to Ch and acetate. In order to study nicotine-evoked ACh release from hippocampal slices, eletrophysiologically (see chapter 6), AChE activity was inhibited using the specific AChE inhibitor, BW284C51 (Mizobe & Livett, 1982). To determine what concentration of BW284C51 was needed to block AChE activity, the AChE assay was carried out in the presence of varying BW284C51 concentrations. The S1 supernatent was used as it gives a better representation of the enzyme activity in the hippocampus than any one of the fractions from the Percoll gradient.

From the inhibition curve, fig. 4.4a, maximal inhibition of AChE was approximately 90% and was achieved at an inhibitor concentration of 1μM or greater. Thus a BW284C51 concentration of 1μM or higher would be sufficient to achieve maximal enzyme inhibition. The IC50,

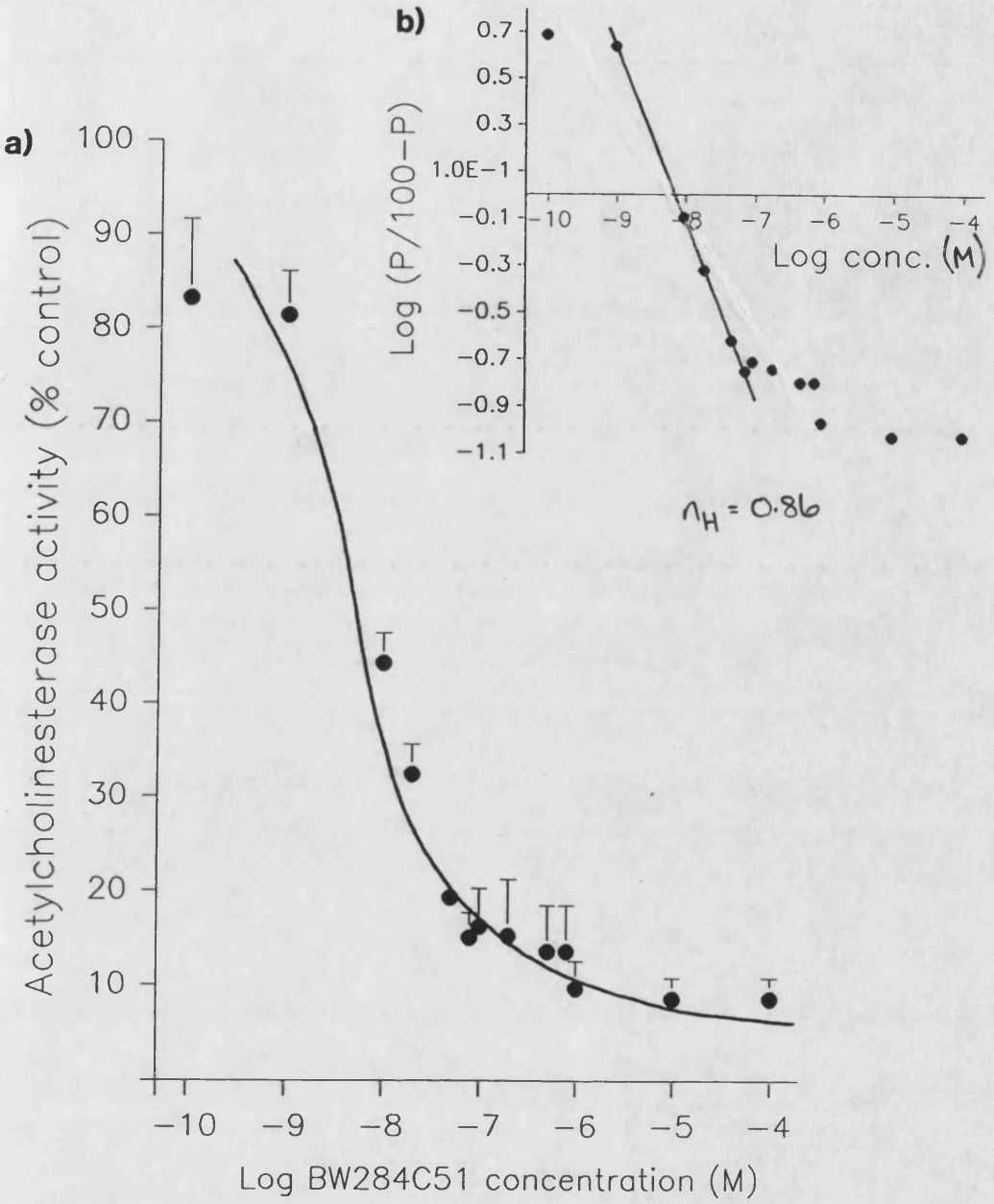

Fig. 4.4a). An inhibition curve of AChE activity by varying BW284C51 concentrations. The effect of BW284C51 concentration on the AChE activity of the S1 supernatent was measured by monitoring the hydrolysis of acetyl thiocholine in the presence of DTNB at 412nm. Values are the mean ± SEM, n=4.

Fig. 4.4 b). A Hill plot of AChE activity against BW284C51 concentration. P is the percent activity of the control (no BW284C51).

the concentration to achieve half maximal inhibition, was 7.4nM estimated from the inhibition curve, fig. 4.4a. A more accurate IC50 value of 5.6nM was obtained from a Hill Plot, fig. 4.4b, where P is the percent of AChE activity in the absence of BW284C51.

4.3.4. Choline acetyltransferase activity

The cholinergic nature of the Percoll gradient fractions was further investigated by assessing the ChAT activity across the gradient.

4.3.4.1. Concentration of bromoacetylcholine

As White & Wu (1973) reported that carnitine acetyltransferase will acetylate Ch to ACh, when carnitine levels are low, the contribution of this enzyme to the ACh level produced in the ChAT assay, see section 4.2.5., was determined. Morris & Grewaal (1971) reported that bromoacetylcholine (62.5μM) inhibited ChAT activity by 70%, but Kasa & Morris (1972) observed that 10mM bromoacetylcholine caused a 77% ChAT inhibition. Roskoski et al..(1974) stated that 0.1mM bromoacetylcholine inhibited 61% of the ChAT activity and that this inhibitor had no effect on carnitine acetyltransferase activity. Thus bromoacetylcholine appears to be a specific inhibitor of ChAT activity. The concentration of bromoacetylcholine to use was determined by assaying for ChAT activity in the presence of varying concentrations (0.01-10mM) of the inhibitor, see fig. 4.5. The S1 supernatant was used, as the ChAT activity would be greater in this fraction than any one from the gradient and so a bromoacetylcholine concentration sufficient to block all ChAT activity could be obtained.

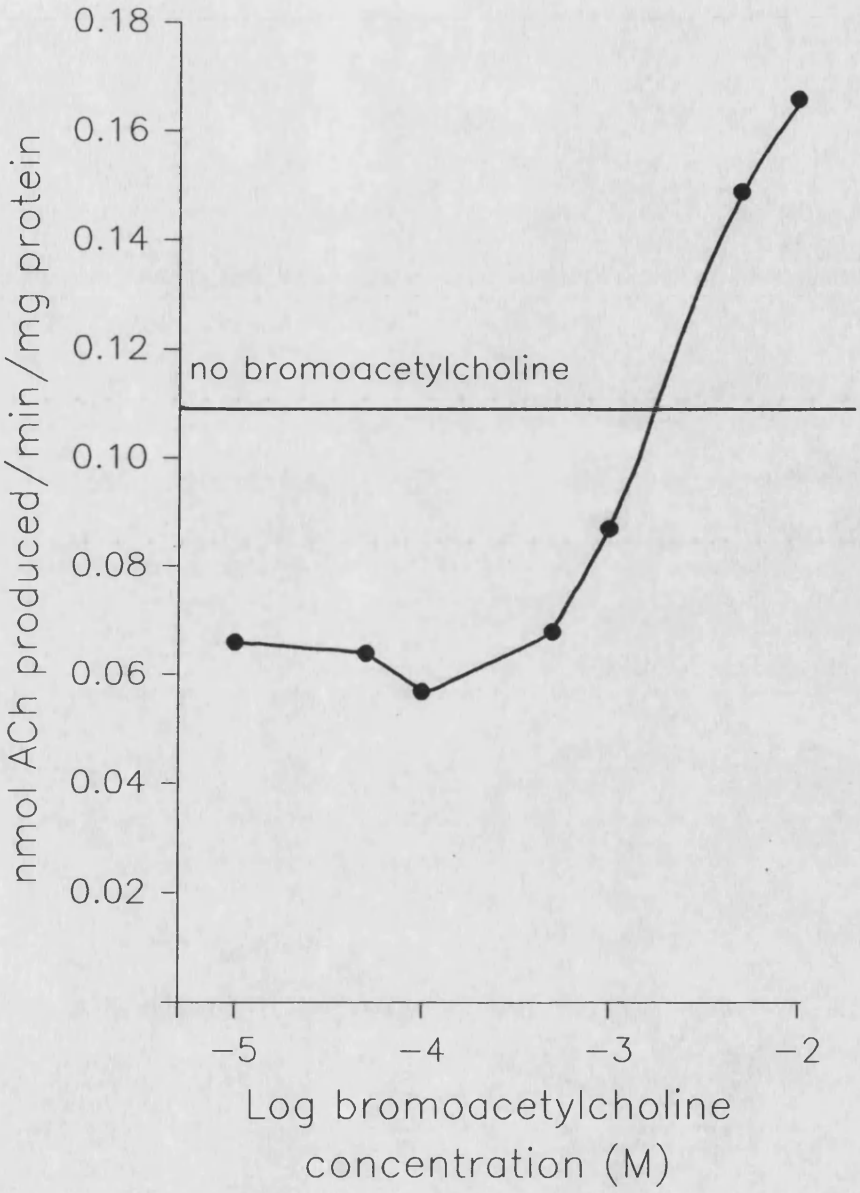

Fig. 4.5. The effect of bromoacetylcholine concentration on ChAT activity. The level of ACh produced by the S1 supernatent in the presence of varying bromoacetylcholine concentrations (0.01-10mM) was measured as described in the methods section 4.2.5.

From fig. 4.5, the maximum inhibition of ChAT activity in the S1 supernatant (48% of the control, no bromoacetylcholine) was achieved with 0.1mM bromoacetylcholine. It was this concentration that was used to determine non-specific acetyltransferase activity in the fractions from the Percoll gradient. At bromoacetylcholine concentrations of 1.75mM and greater the inhibitor appears to act as a substrate in the assay as levels of radiolabelled product increase above those of the control, that has no bromoacetylcholine.

4.3.4.2. Choline acetyltransferase activity across the Percoll gradient

ChAT activity in the gradient fractions was determined as described in section 4.2.5, non-specific acetyltransferase activity was determined in the presence of 0.1mM bromoacetylcholine, see fig. 4.6.

Approximately 62% of the S1 ChAT activity was recovered in the gradient fractions, with fractions F4 and F5 having the highest ChAT activity/mg of protein. The high mitochondrial and low synaptosomal content (shown by low occluded LDH activity, fig. 4.2, and electron microscopy, fig. 4.8I) of fraction F5 suggests that some of the ACh produced could be as a result of non-specific acetyltransferase activity. In the presence of bromoacetylcholine, non-specific acetyltransferase activity accounted for 30% of the ACh produced in fraction F5 which was approximately twice that of fraction F4. ChAT has been reported to bind to membranes (Rylett, 1989) under certain conditions of pH and ionic strength (Fonnum, 1967) which could account for high residual ChAT activity in fraction F5, considering the low synaptosomal content.

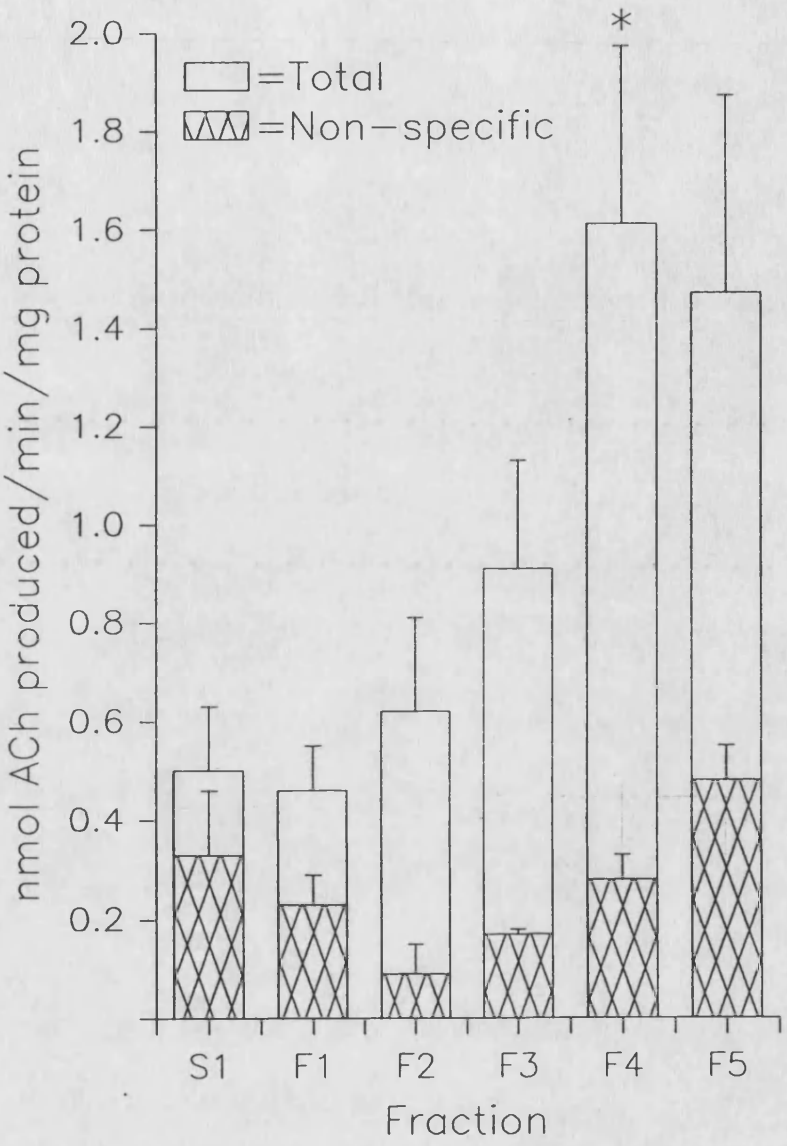

Fig. 4.6. ChAT activity in fractions from the Percoll gradient. The level of ACh produced was determined as described in the methods (section 4.2.5). Non-specific acetyltransferase activity was determined in the presence of 0.1mM bromoacetylcholine. Values are the mean ± SEM, n=6. Significantly different from the total activity in the S1 supernatant, * $p<0.001$.

Fraction F1 has a low synaptosomal content (low occluded LDH, fig. 4.2; electron microscopy, fig. 4.8E) and so as expected had a low ChAT activity. The lower ChAT activity in fractions F2 and F3, compared to fraction F4, indicates that although there is a high synaptosomal content, as shown by high occluded LDH levels (fig. 4.2) and electron microscopy, fig. 4.8F and G, only a small proportion of these synaptosomes are cholinergic in nature. AChE activity in the presence of ChAT is specific for cholinergic terminals but, as shown by the ubiquitous AChE distribution across the gradient (fig. 4.3), AChE activity alone has a low cholinergic specificity.

The high synaptosomal content but low level of ChAT activity in fractions F2 and F3 lends to the possibility of isolating subpopulations of synaptosomes, based on transmitter type, in different fractions from the Percoll gradient. However, studies with five different transmitters have shown that such subdivision of synaptosomes does not occur. Dopamine (Robinson & Lovenberg, 1986), noradrenaline (Dunkley et al., 1987, 1988), GABA (Thorne et al., 1988) and ACh (this report) markers all have highest activity in fraction F4. Only 5HT (Robinson & Lovenberg, 1986) had a higher specific activity in another fraction, fraction F3.

4.3.5. Choline uptake across the gradient

In order for ChAT to produce ACh there needs to be a supply of Ch, and [^{3}H]Ch uptake was used as a functional assessment of cholinergic synaptosomes, see fig. 4.7.

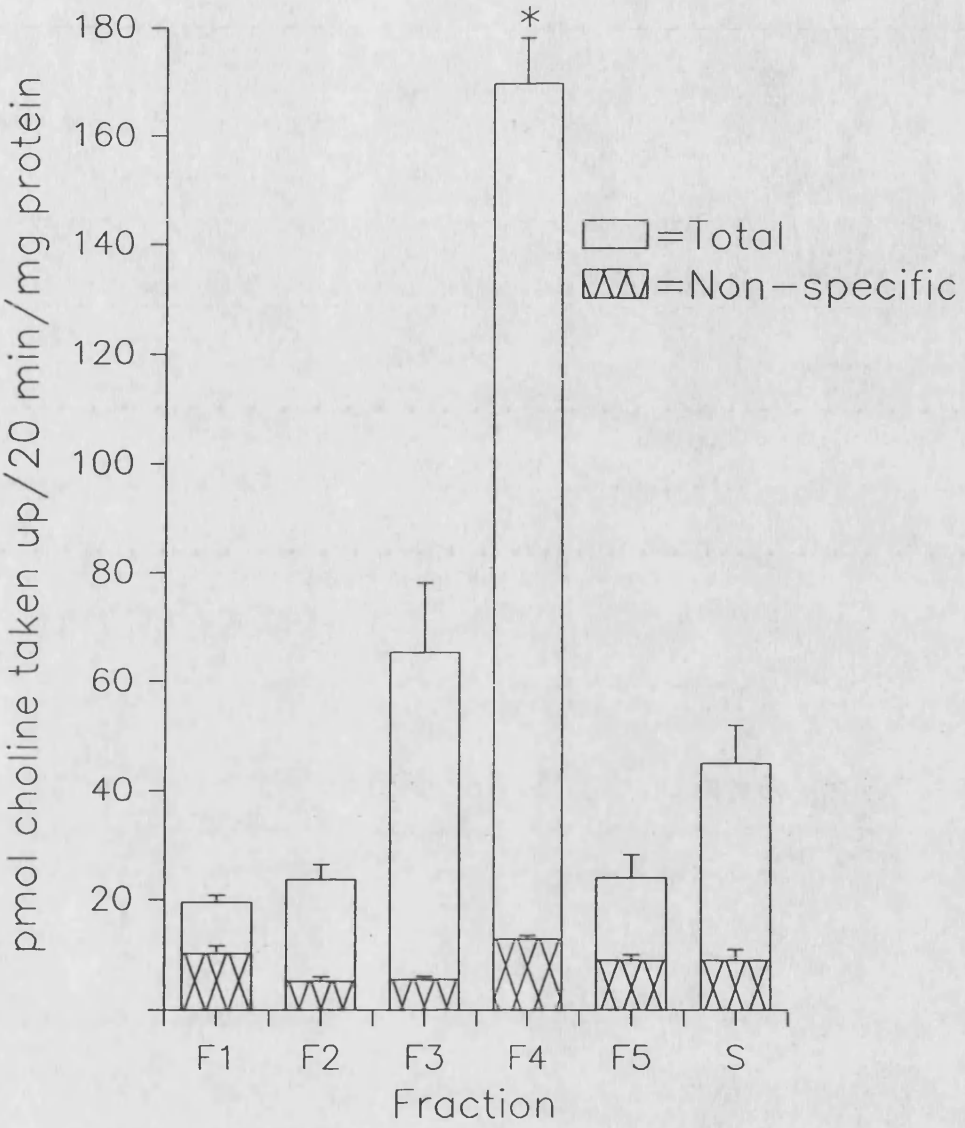

Fig. 4.7. [^{3}H]Ch uptake by fractions from the Percoll gradient.

After incubation with 0.8μM [^{3}H]Ch for 20min at 37°C, samples (100μl) were withdrawn, filtered and washed. Non-specific uptake was determined in the presence of HC-3 (1μM). Values are the mean ± SEM, n=4. S was the uptake into the sucrose synaptosome fraction, under the same conditions.

Fraction F1 had little specific Ch uptake (10 pmol/20 min/mg protein) corresponding to a low synaptosome content, as shown by low occluded LDH levels (fig. 4.2) and electron microscopy (fig. 4.8E). Ch uptake into fraction F2 (19 pmol/20 min/mg protein) was low considering the ChAT activity in this fraction (fig. 4.6), as Ch uptake has been reported to be associated with ChAT activity (Yamamura & Snyder, 1973). This adds support to the suggestion that the cholinergic nature of these fraction F2 synaptosomes is low. Fraction F3 had a significant amount of Ch uptake (59 pmol/20 min/mg protein) which corresponds with the ChAT activity in this fraction (fig. 4.6). The Ch uptake into fraction F3 was approximately three times higher than that into fraction F2 even though the ChAT activity was almost equivalent. The high ChAT activity in fraction F2 could be due to the enzyme being bound to membranes (Fonnum, 1967) in this fraction. The highest Ch uptake (157 pmol/20 min/mg protein) was found in fraction F4, which correlates with the high ChAT activity in this fraction. This Ch uptake into fraction F4 was almost three times that taken into fraction F3. Specific Ch uptake into fraction F5 was low (15 pmol/20 min/mg protein) adding to the suggestion that the ACh produced in this fraction (fig. 4.6) was from non-specific acetyltransferases, for example carnitine acetyltransferase, or from membrane bound ChAT activity.

From these markers fraction F4 is more enriched in cholinergic terminals than any other fraction from the gradient. Fraction F4 has high occluded LDH levels showing a large synaptosomal content which has the greatest ChAT activity and Ch uptake as well as having AChE activity. There was low occluded LDH, ChAT activity and Ch uptake in fraction F1 indicating a small number of cholinergic synaptosomes.

The high AChE levels in this F1 fraction are probably due to enzyme bound to membrane fragments. Although fractions F2 and F3 have a high synaptosomal content, from LDH activity, few are cholinergic in nature. Fraction F3 had slightly greater ChAT activity and Ch uptake than fraction F2. The low occluded LDH levels in fraction F5 indicated a small synaptosomal content which exhibited low levels of AChE activity and Ch uptake indicating a small number of cholinergic terminals. Although ChAT activity in fraction F5 was relatively high this could be as a result of enzyme binding to membranes or non-specific acetyltransferases giving an incorrect value for ChAT activity.

After a 20 min incubation, at 37°C, with 0.8μM [^{3}H]Ch specific uptake into fraction F4 (157 pmol/20 min/mg protein) was four to five times greater than that into sucrose isolated synaptosomes (35 pmol/20 min/mg protein), see fig. 4.7. This suggests that fraction F4 from the Percoll gradient is a purer synaptosome preparation for studying cholinergic function than the sucrose synaptosome fraction, even though both had a similar occluded LDH level (80% of total LDH).

Non-specific uptake was approximately equivalent in both fraction F4 and the sucrose isolated synaptosomes.

4.3.6. Electron microscopy

Having characterised the fractions from the Percoll gradient biochemically they were further studied morphologically by electron microscopy along with the fractions from the sucrose gradient. Prints from each fraction are shown in fig. 4.8A-I.

Fig. 4.8. Electron micrographs of fractions from the sucrose and Percoll gradients.

A1. The sucrose PA fraction. Myelin (MY), resealed vesicles (RV) and some synaptosomes (SY) can be seen. Bar = 1μm.

A2. A high magnification of fraction PA. This high power depicts the lamellae (L) of the myelin. Bar = 100nm.

A1

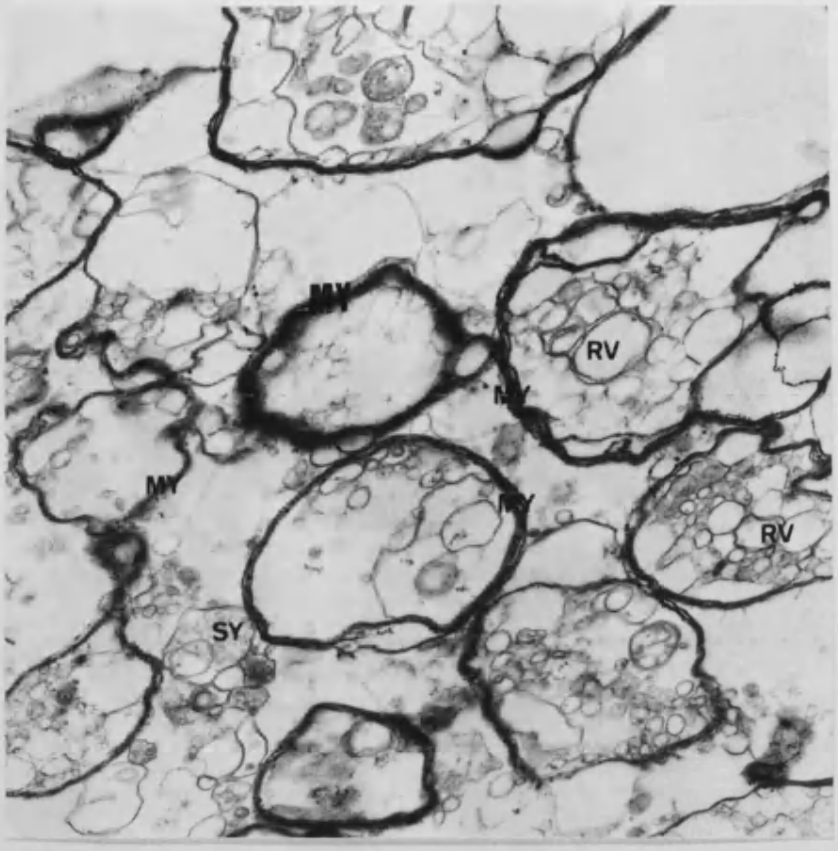

A2

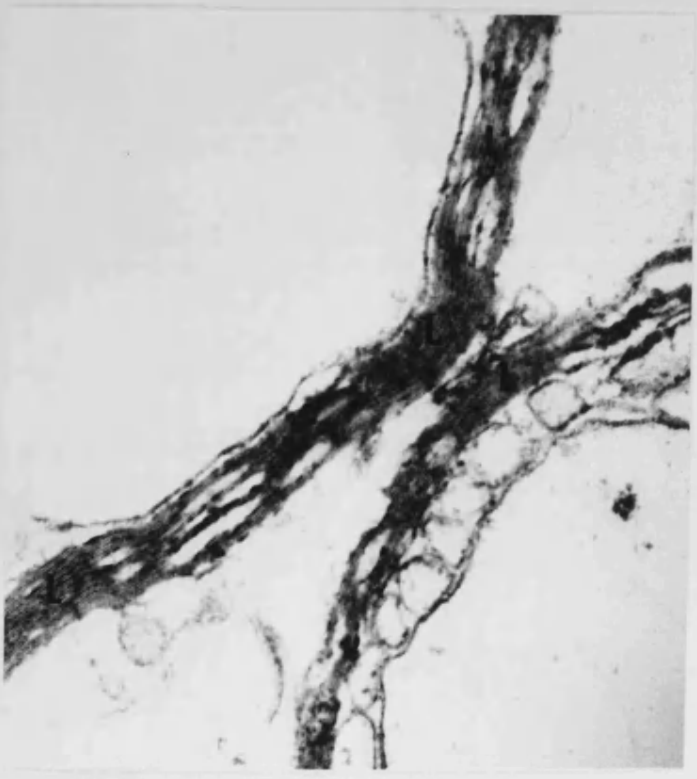

B1. The sucrose PB fraction. This fraction contains synaptosomes (SY) with synaptic vesicles (V) and mitochondria (M), also extrasynaptosomal mitochondria (EM) and resealed vesicles (RV). Bar = 200nm.

B2. A high magnification of a PB fraction synaptosome. At this power synaptic vesicles (V) and mitochondria (M) are seen. Bar = 100nm.

B1

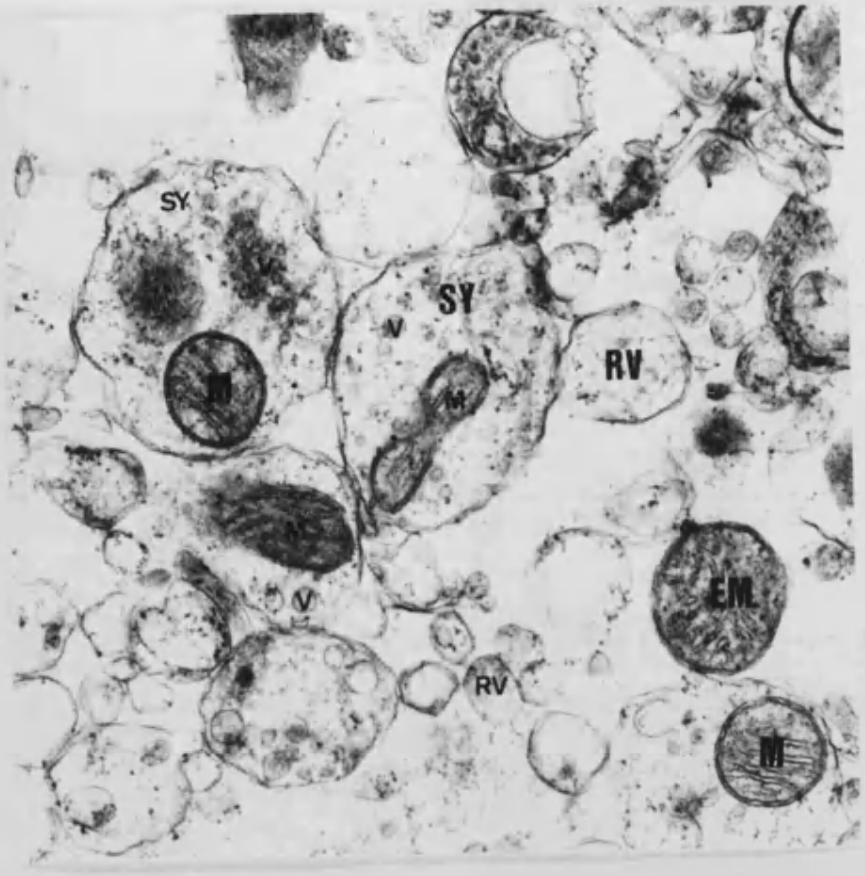

B2

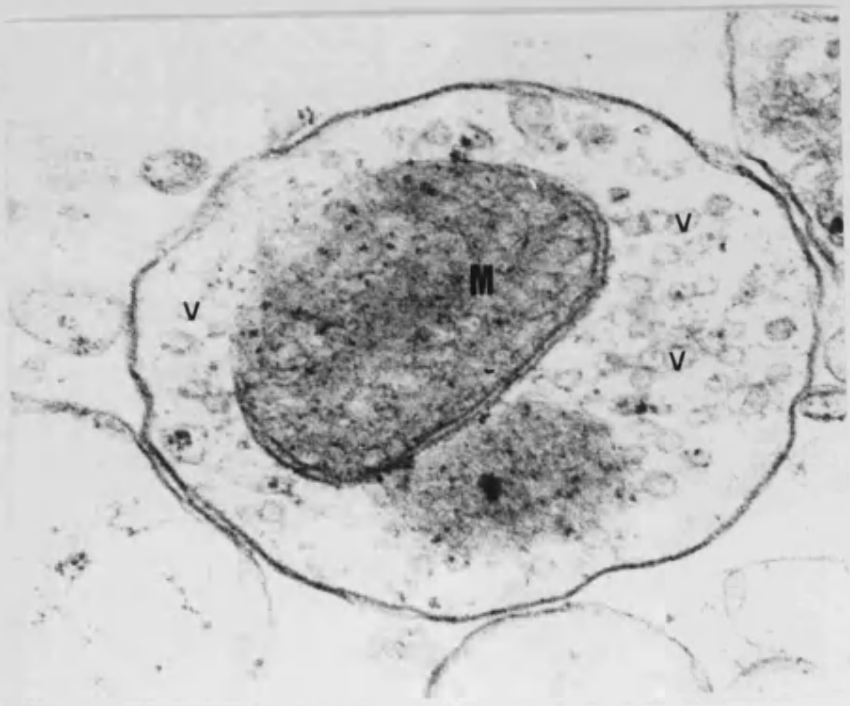

C1. The sucrose PC fraction. At this low magnification a nucleus (N), extrasynaptosomal mitochondria (EM) and membrane fragments (MF) can be seen. Bar = 1µm.

C2. A high magnification of the PC fraction. Many resealed vesicles (RV) are present though few contain vesicles (V) and/or mitochondria (M). Bar = 200nm.

C1

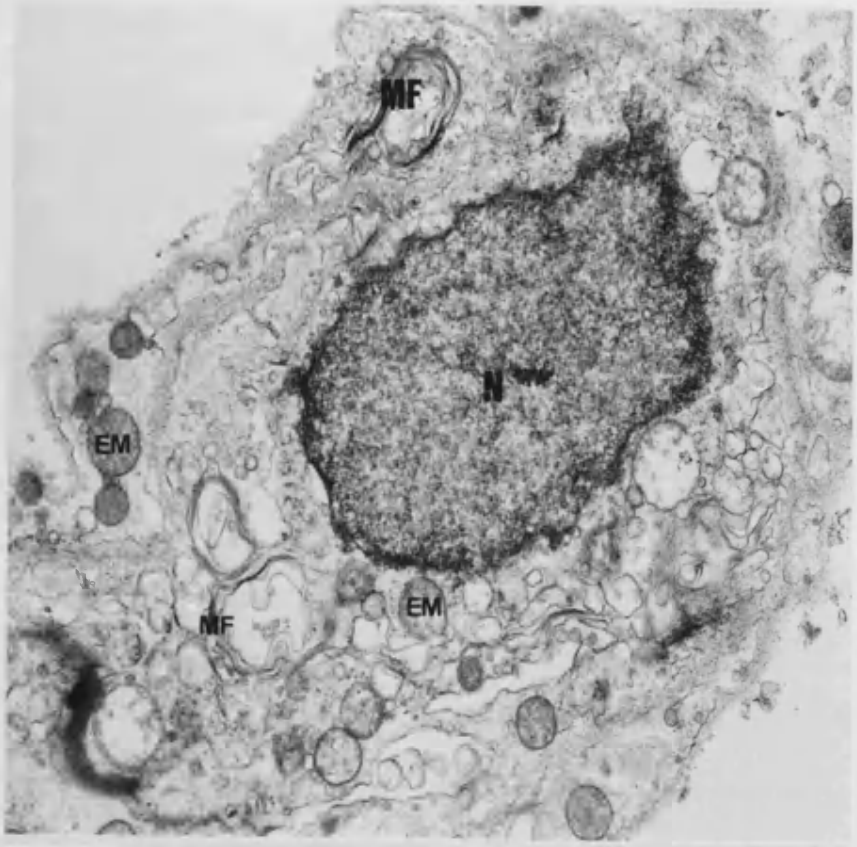

C2

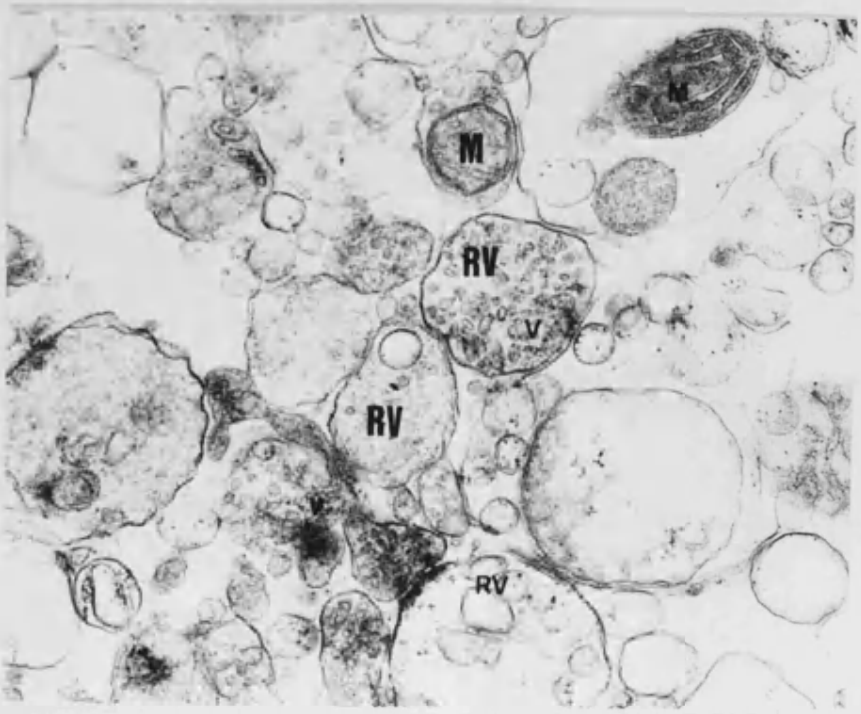

D. The Percoll S1 supernatant. Synaptosomes (SY), containing vesicles (V) and mitochondria (M), and many resealed vesicles (RV) are present. Bar = 200nm.

E. The Percoll F1 fraction. This fraction has myelin (MY) and many resealed vesicles (RV). Bar = 200nm.

D

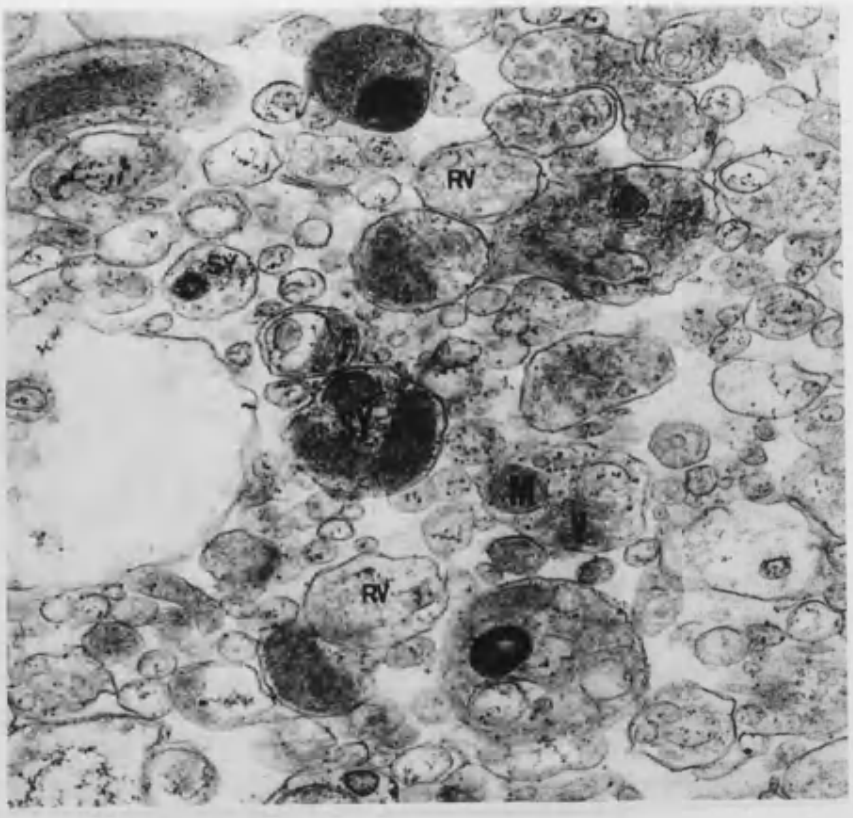

E

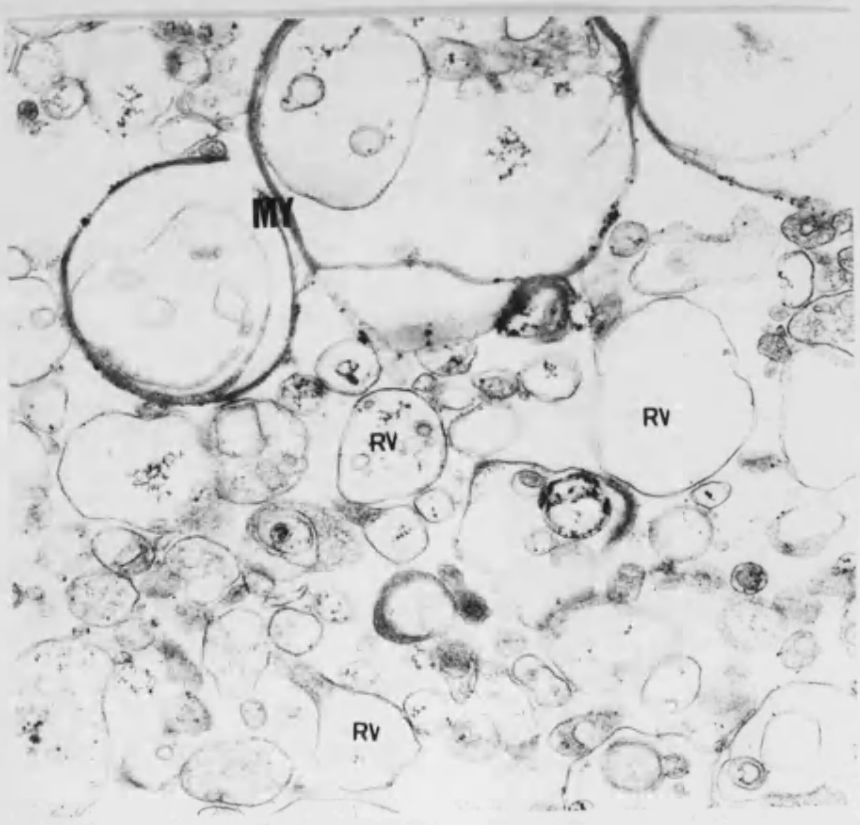

F. The Percoll F2 fraction. Depicted are synaptosomes (SY), containing both synaptic vesicles (V) and mitochondria (M), and also empty resealed vesicles (RV). Bar = 200nm.

G. The Percoll F3 fraction. Contents include synaptosomes (SY) with synaptic vesicles (V) and mitochondria (M), also present are resealed vesicles (RV). Bar = 200nm.

F

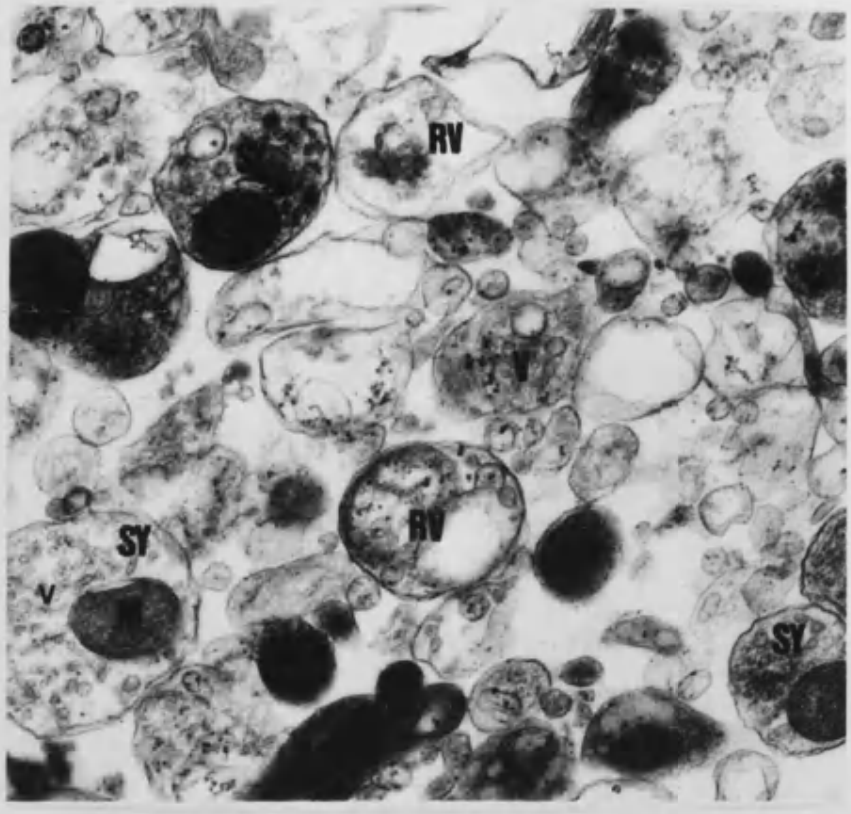

G

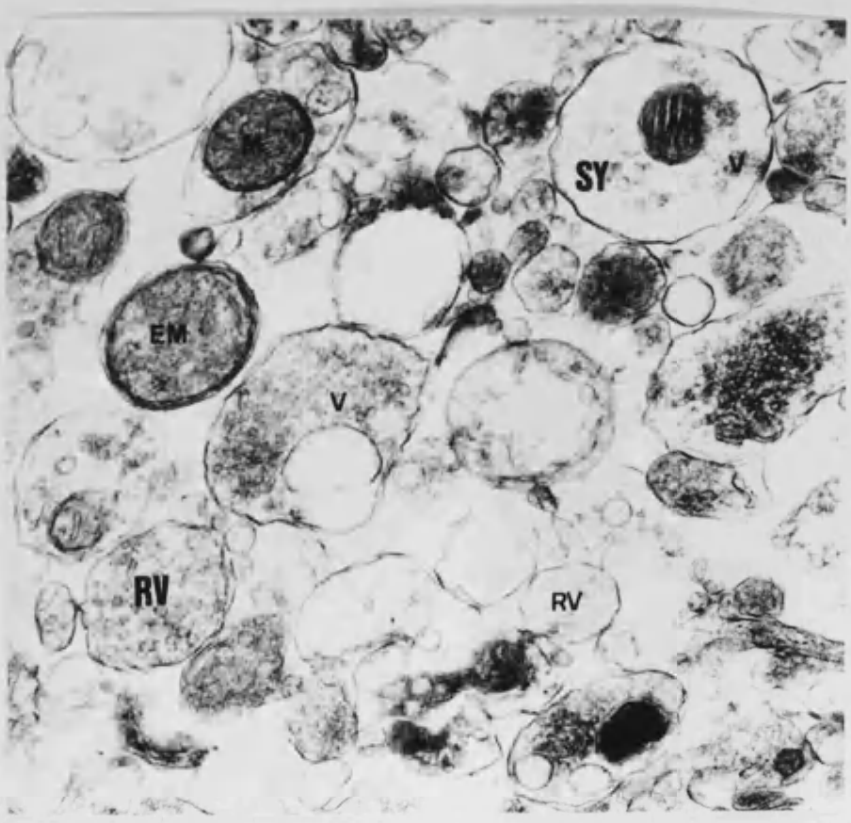

H1. The Percoll F4 fraction. Present in this fraction are synaptosomes (SY), containing vesicles (V) and mitochondria (M), and also extrasynaptosomal mitochondria (EM). Bar = 200nm.

H2. A higher magnification of a fraction F4 synaptosome. Within the synaptosome (SY), both synaptic vesicles (V) and mitochondria (M) can be seen. Bar = 100nm.

H1

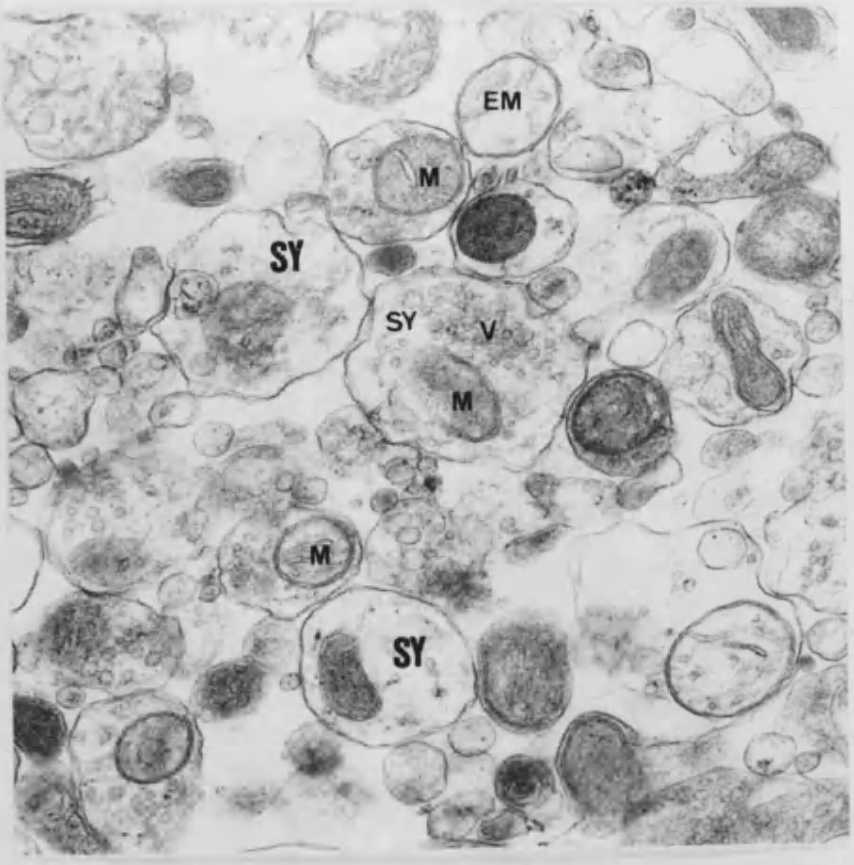

H2

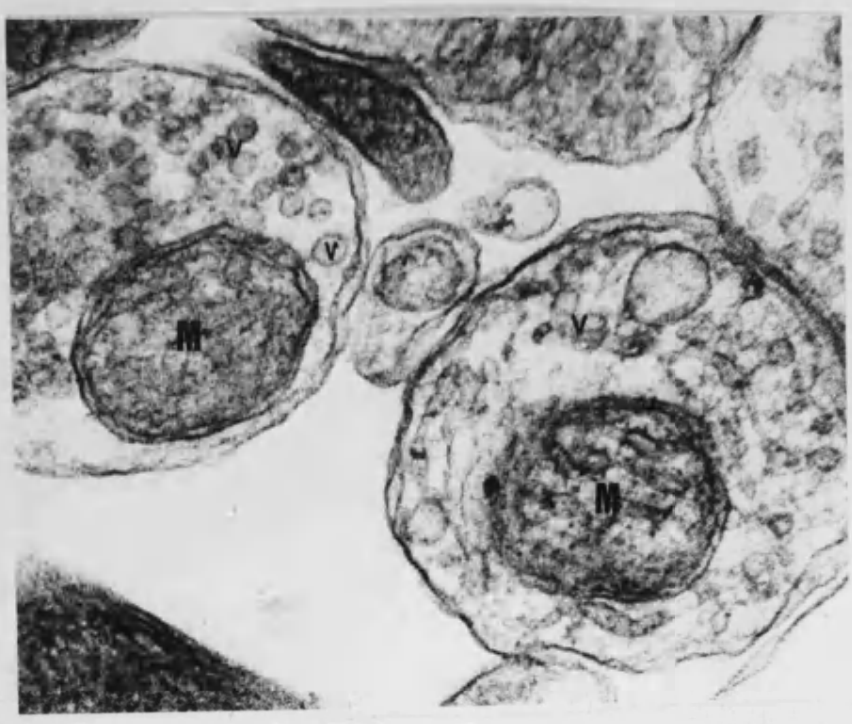

I. The Percoll F5 fraction. This fraction has a high extrasynaptosomal mitochondrial (EM) content. Bar = 200nm.

I

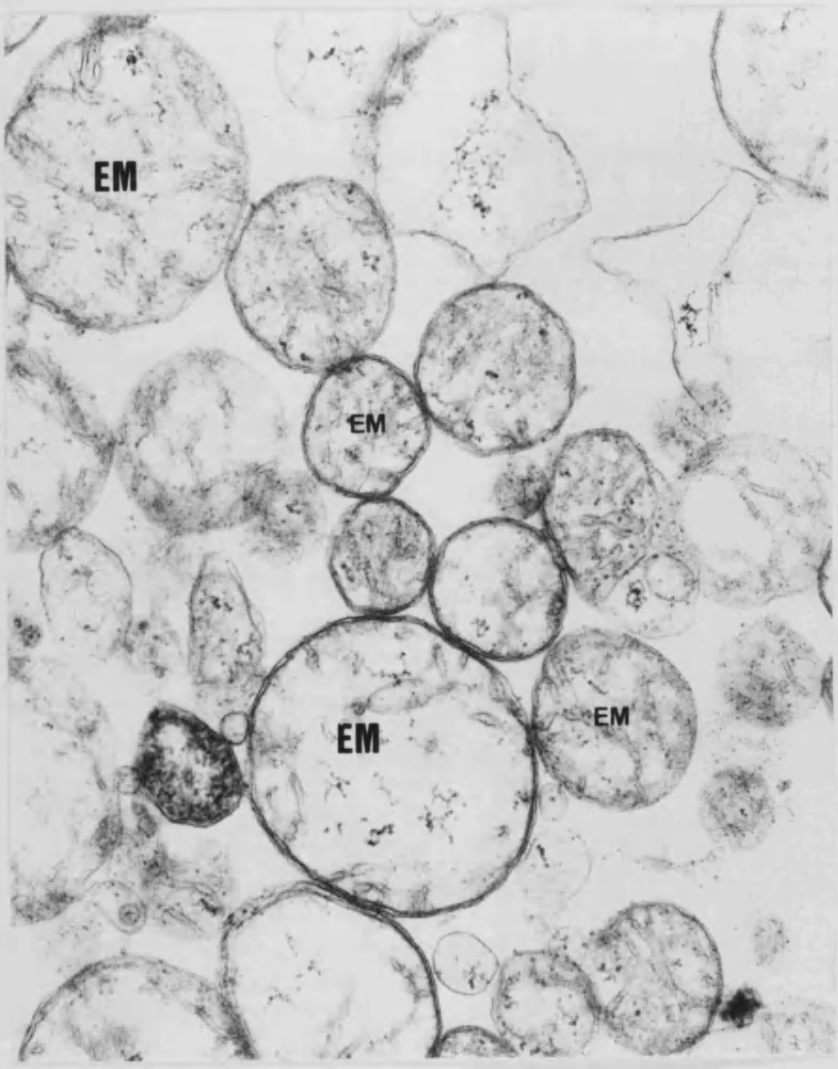

4.3.6.1. The sucrose gradient

The electron micrographs of the fractions from the sucrose gradient (see fig. 3.1) are shown in fig. 4.8A-C. In fig. 4.8A1 it can be seen that the PA fraction contains a large amount of myelin (MY) which as expected would be at the top of the gradient. The high power electron micrograph, fig. 4.8A2, shows the distinctive lamellae (L) of the myelin. Abundant within this PA fraction are small empty resealed vesicles (RV). A few of these structures contained smalled synaptic vesicles and so were thought to be synaptosomes (SY). The low occluded LDH levels (fig. 3.3) in this fraction was as a result of a low synaptosomal content. The high free LDH levels in this fraction was due to cytoplasm at the top of the gradient.

The PB fraction, fig. 4.8B1, contained a higher proportion of synaptosomes (SY) containing synaptic vesicles (V) and mitochondria (M). This high synaptosome content would give the high occluded LDH activity seen in fig. 3.3. There were also many empty resealed vesicles (RV) and extrasynaptosomal mitochondria (EM) indicating a crude synaptosome preparation. Fig. 4.8B1 is a "dirtier" print due to specks of lead carbonate which precipitated during staining of the sections, see section 4.2.11. A high power view of a synaptosome was depicted in fig. 4.8B2 showing synaptic vesicles (V) and a mitochondrion (M).

Fig. 4.8C1 shows the contents of the PC fraction which are many extrasynaptosomal mitochondria (EM), large membrane fragments (MF) and a nucleus (N). A higher magnification of this fraction, fig. 4.8C2, showed many resealed vesicles (RV) though few contained synaptic vesicles (V) and/or mitochondria (M). As there is a low

synaptosome content in this fraction the occluded LDH levels were low, see fig. 3.3.

This distribution of subcellular organelles on the sucrose gradient is similar to that described by Gray & Whittaker (1962) in that the PA fraction contained mainly myelin and the PB fraction mostly synaptosomes. However, in the method of Gray & Whittaker the nuclei were first pelleted and discarded before layering the P2 pellet on a sucrose gradient, and so the PC fraction in this procedure has a slightly different composition.

4.3.6.2. The Percoll gradient

The S1 supernatant, fig. 4.8D, contained many resealed vesicles containing synaptic vesicles (V) and/or mitochondria (M) and were probably synaptosomes. There were also smaller empty resealed vesicles (RV) and some myelin, not shown in the print. The F1 fraction (fig. 4.8E) contained mainly myelin (MY) and empty resealed vesicles (RV). The high free LDH activity in this fraction (see fig. 4.2) is probably due to cytoplasm remaining at the top of the gradient. With a low synaptosomal content the occluded LDH, ChAT activity and Ch uptake was small. The high AChE activity in this fraction is probably as a result of membrane bound enzyme, possibly on postsynaptic membrane fragments.

Fractions F2 (fig. 4.8F) and F3 (fig. 4.8G), contained many synaptosomes (SY) with synaptic vesicles (V) and mitochondria (M). Unidentified resealed vesicles (RV) were also present in both fractions. Fraction F4, fig. 4.8H1, contained a higher proportion of synaptosomes (SY) than resealed vesicles (RV) than fractions F2 and

F3 though it had more extrasynaptosomal mitochondria (EM). Fig. 4.8H2 shows a higher magnification of a fraction F4 synaptosome. Fraction F5, fig. 4.8I contained mostly extrasynaptosomal mitochondria (EM) which could explain the unexpected high levels of ACh produced in the ChAT assay (fig. 4.6) being due to non-specific acetyltransferase activities of the mitochondria, for example carnitine acetyltransferase.

As reported by Dunkley et al. (1988) fraction F1 was richer in myelin whereas fraction F5 had the highest extrasynaptosomal mitochondrial content than any other fraction. Synaptosomal content of the fractions increased across the gradient, fractions F1-F4, with enrichment in fraction F4.

4.3.7. Choline uptake into fraction F4

Having established that fraction F4 from the Percoll gradient was enriched in cholinergic synaptosomes the parameters for [^{3}H]Ch uptake into this fraction were optimised.

4.3.7.1. The effect of incubation time

The effect of incubation time on [^{3}H]Ch uptake (0.8μM) was studied over a period of 0-60 min at 37°C, see fig. 4.9.

Non-specific uptake, at 4°C, was essentially linear with time and accounted for only 2% of the total Ch taken up. Non-specific uptake at 4°C (2 pmol/20 min/mg protein) was lower than in the presence of HC-3 (1μM; 13 pmol/20 min/mg protein) as non-selective transport systems as well as HAChT are probably blocked at 4°C. Specific uptake (the difference between total and non-specific

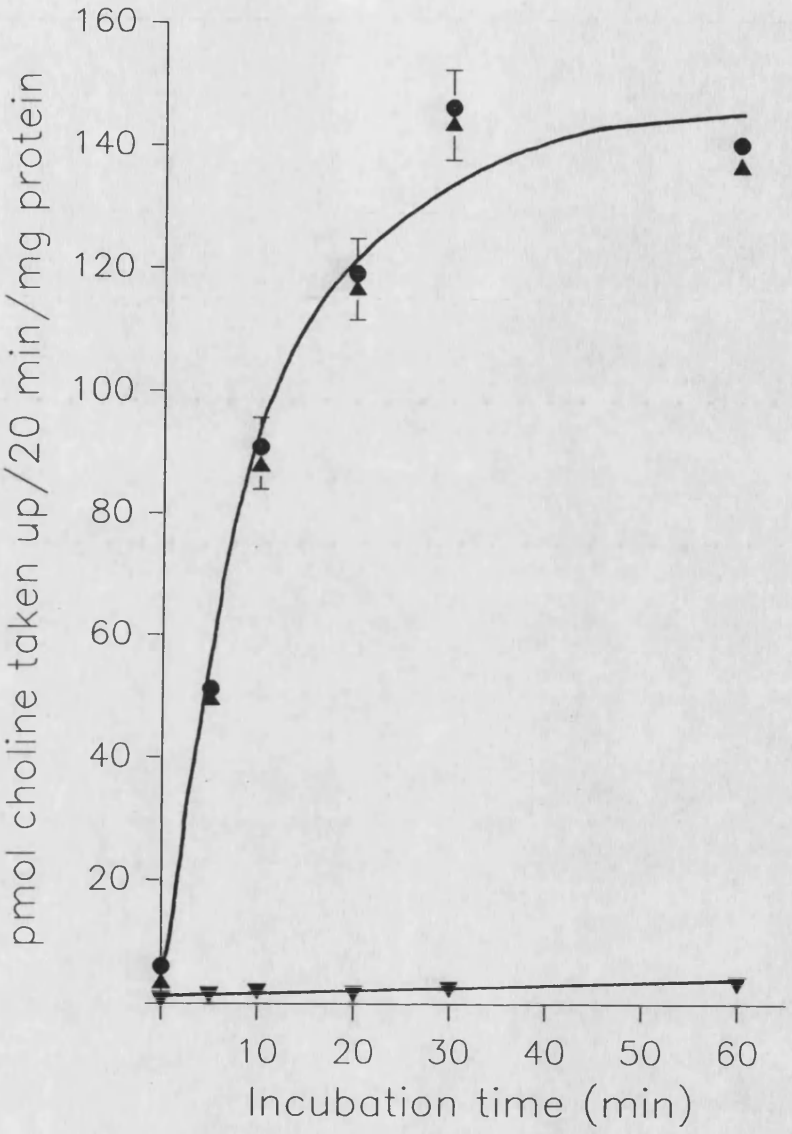

Fig. 4.9. The time course of [^{3}H]Ch uptake by Percoll fraction F4. After the addition of [^{3}H]Ch (0.8μM), samples were incubated at 37°C and at time intervals (0-60min) 100μl were taken, filtered and washed. Non-specific uptake was determined at 4°C. The values for total (●), specific (▲) and non-specific (▼) uptake are the mean ± SEM, n=4.

uptake) approached maximal at 30 min. Thus sufficient labelling of synaptosomes could be achieved by a 20 min incubation and this was used in future experiments.

4.3.7.2. The effect of choline concentration

The dependence of [^{3}H]Ch uptake on Ch concentration was studied over the range 0.1-2.0μM, see fig. 4.10.

Non-specific uptake, at 4°C, was essentially linear with time and again accounted for about 2% of the total Ch taken up. Specific uptake approached saturation at 1μM and so sufficient labelling of the synaptosomes could be achieved at a Ch concentration of 0.8μM and this was used in future experiments. Examination of the time course (fig. 3.4 and fig. 4.9) and Ch concentration dependence (fig. 3.5 and fig. 4.10) of [^{3}H]Ch uptake confirmed that a 20 min incubation, at 37°C, with 0.8μM Ch was optimal for labelling synaptosomes from both the sucrose and Percoll gradients.

Using a direct linear plot, not shown, a Kt value of 0.51μM (the concentration for half maximal transport) and a Vmax of 173.8 pmol/20 min/mg protein were obtained for uptake into fraction F4. The Kt value was equivalent to that obtained for uptake into sucrose isolated synaptosomes, see section 3.3.2.2., which was as expected as there is no change in the transport system with a different isolating medium and within the range reported for specific HAChT into hippocampal synaptosomes: 0.43-0.90μM (Sorimachi & Kataoka, 1974; Atweh et al., 1975; Murrin & Kuhar, 1976; Simon & Kuhar, 1976; Simon et al., 1976). The F4 fraction Vmax value (173.8 pmol/20 min/mg protein) was five times greater than the Vmax for Ch uptake into

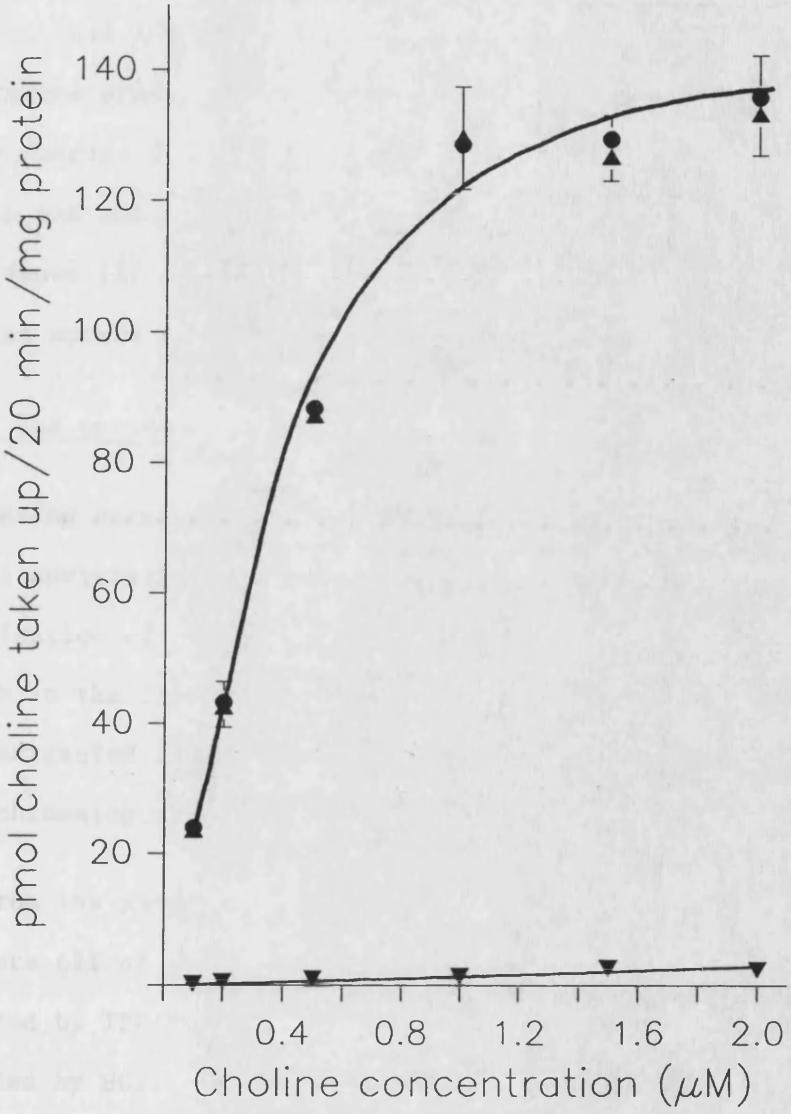

Fig. 4.10. The effect of Ch concentration on [^{3}H]Ch uptake by Percoll fraction F4. Samples were incubated with varying [^{3}H]Ch concentrations (0.1-2.0μM) and after 20 min at 37°C, 100μl were taken, filtered and washed. Non-specific uptake was determined at 4°C. The values for total (●), specific (▲) and non-specific (▼) uptake are the mean ± SEM, n=4.

sucrose isolated synaptosomes (34.5 pmol/20 min/mg protein). This suggests that the Percoll method produces an enriched functional synaptosome preparation for studying cholinergic terminals compared to the sucrose procedure. From fig. 4.9 a Vmax of 42.5 pmol/4min/mg protein was obtained which is within the range reported by those named above (16-56.4 pmol/4 min/mg protein). The Vmax at 4 min was used, as uptake at this time interval was still linear.

4.3.8. The percent acetylation of [^{3}H]Ch in fraction F4

Having obtained the optimum [^{3}H]Ch uptake conditions, the percent acetylation of this accumulated [^{3}H]Ch was determined to give an indication of the proportions of radioactivity associated with Ch and ACh in the fraction F4 synaptosomes. The choline bases were first extracted from the synaptosomes and then separated by thin layer chromatography.

From the samples taken at steps (1-3) throughout the extraction procedure 62% of the radioactivity in the perchloric acid was extracted by TPB/heptan2one. Of this radioactivity, 85% was extracted by HCl. These values are similar to those reported by Fonnum (1969).

The choline bases, Ch and ACh, could be separated by thin layer chromatography as shown in fig. 4.11. The standard Ch and ACh spots had Rf values of 0.37 and 0.49, respectively, see table 4.2, which correlates well with those reported by Augustinsson & Grahn (1953) of 0.37/0.38 for Ch and 0.46/0.47 for ACh. The choline bases of the extracted samples (F4: [^{3}H]Ch loaded fraction F4 synaptosomes; F2: control, fraction F2 synaptosomes with added [^{3}H]ACh) had higher Rf

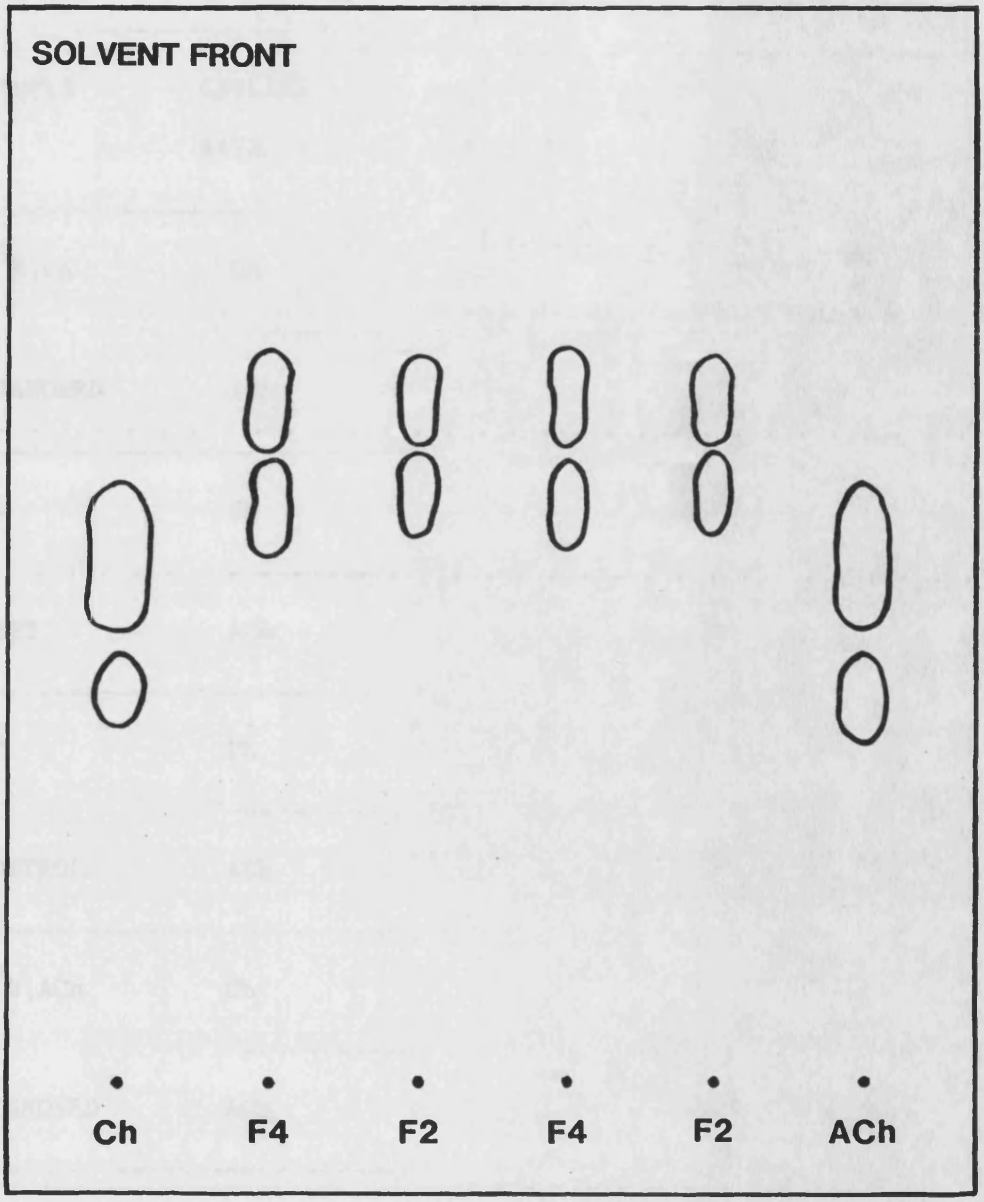

Fig. 4.11. A schematic diagram of an eluted thin layer chromatography plate. Samples, in a carrier solution, were eluted in butan-1-ol:ethanol:glacial acetic acid:distilled water (8:2:1:3 by vol). Ch was [^{3}H]Ch, F4 were the extracted test samples, F2 were the extracted control samples, ACh was [^{3}H]ACh.

SAMPLE	CHOLINE BASE	Rf VALUE	%RADIOACTIVITY IN ACh SPOT
[^{3}H]Ch	Ch	0.39 ± 0.04	
			2.4 ± 0.8
STANDARD	ACh	0.51 ± 0.03	
F4	Ch	0.55 ± 0.01	
			101.0 ± 1.6
TEST	ACh	0.63 ± 0.01	
F2	Ch	0.55 ± 0.01	
			69.2 ± 1.0
CONTROL	ACh	0.63 ± 0.01	
[^{3}H]ACh	Ch	0.36 ± 0.02	
			96.6 ± 0.2
STANDARD	ACh	0.48 ± 0.02	

Table 4.2. Separation of Ch and ACh on thin layer chromatography plates. This was used to determine the percent radioactivity associated with ACh in each of the test (F4) and control (F2) samples (in quadruplicate, n=2 independent extractions), also in [^{3}H]ACh and [^{3}H]Ch standards (in duplicate, n=2 experiments). Values are the mean ± SEM.

values than the standards, see table 4.2, probably due to the presence of some residual solvent, from the extraction procedure.

From table 4.2, the [^{3}H]ACh used as the standard and in the F2 control samples was shown to be 96.6% ACh suggesting that Ch acetylation with acetic anhydride (see section 3.2.7., for synthesis of [^{3}H]ACh) was almost 100% efficient. During the extraction process this ACh was hydrolysed by 30% as only 70% of the radioactivity in the F2 control samples was associated with the ACh spot. Taking into account this hydrolysis, the acetylation of Ch in the F4 test samples was 98%, once the percent crossover of radioactivity (2.4%, see [^{3}H]Ch standard) had been considered. This high acetylation is in agreement with the suggestion of Barker & Mittag (1975) and Benishun & Carroll (1981) that ChAT activity and HAChT are coupled in the nerve terminal. Similarly high acetylations of Ch to ACh have been reported: 69% (Wonnacott & Marchbanks, 1976); 75% (Moss & Wonnacott, 1985); 87% (Rowell & Winkler, 1984); 91% (Wong & Prince, 1978). Thus with such a high acetylation most if not all of the radioactivity collected from the superfusion system would be expected to be [^{3}H]ACh and this was shown to be so in section 3.3.3.1.4., where [^{3}H]ACh was separated from [^{3}H]Ch by an enzymic extraction procedure.

4.3.9. Superfusion of synaptosomes isolated on sucrose and Percoll gradients

The functional responsiveness of synaptosomes isolated on sucrose (PB fraction) or Percoll (fraction F4) gradients were compared by superfusion. ACh release from synaptosomes, derived from the same homogenate by either method, was monitored after loading with [^{3}H]Ch under identical conditions. Excess [^{3}H]Ch was removed by

centrifugation with an equal volume of Krebs buffer before equal amounts of protein (approximately 150µg) were loaded into the superfusion chambers, see fig. 3.2, two chambers contained Percoll fraction F4 and two chambers contained sucrose synaptosomes. The synaptosomes were continually perfused with Krebs buffer and subjected to 20s pulses of drug (10µM nicotine, S1, S2; Krebs buffer, S3; 20mM K^+, S4) at 30 min intervals after an initial washout period of 40 min. The collected fractions were than counted in the presence of scintillant, see fig. 4.12 and table 4.3.

From fig. 4.12 it is clear that release from Percoll fraction F4 was greater than that from sucrose synaptosomes. Fraction F4 has a higher basal release than the sucrose synaptosomes which is proportional to the higher [^{3}H]Ch uptake in this fraction (157 pmol/20 min/mg protein in fraction F4, 35 pmol/20 min/mg protein in sucrose synaptosomes, see section 4.3.5. and fig. 4.7). Nicotine evoked ACh release was four to five times greater from fraction F4 than from sucrose synaptosomes showing that the Percoll method produces a purer synaptosome preparation for studying cholinergic function. The response to air bubble in the sucrose synaptosome was approximately 44% of the S1 nicotine response whereas in fraction F4 the response was 32% of the S1 (determined by S3/S1 ratios). This reduction in air bubble effect probably reflects the increase in response of the purer synaptosome population in fraction F4. A similar decrease in air bubble effect with increase in response was seen in section 3.3.3.4.3. where 10µM nicotine evoked a greater ACh release than 50µM nicotine.

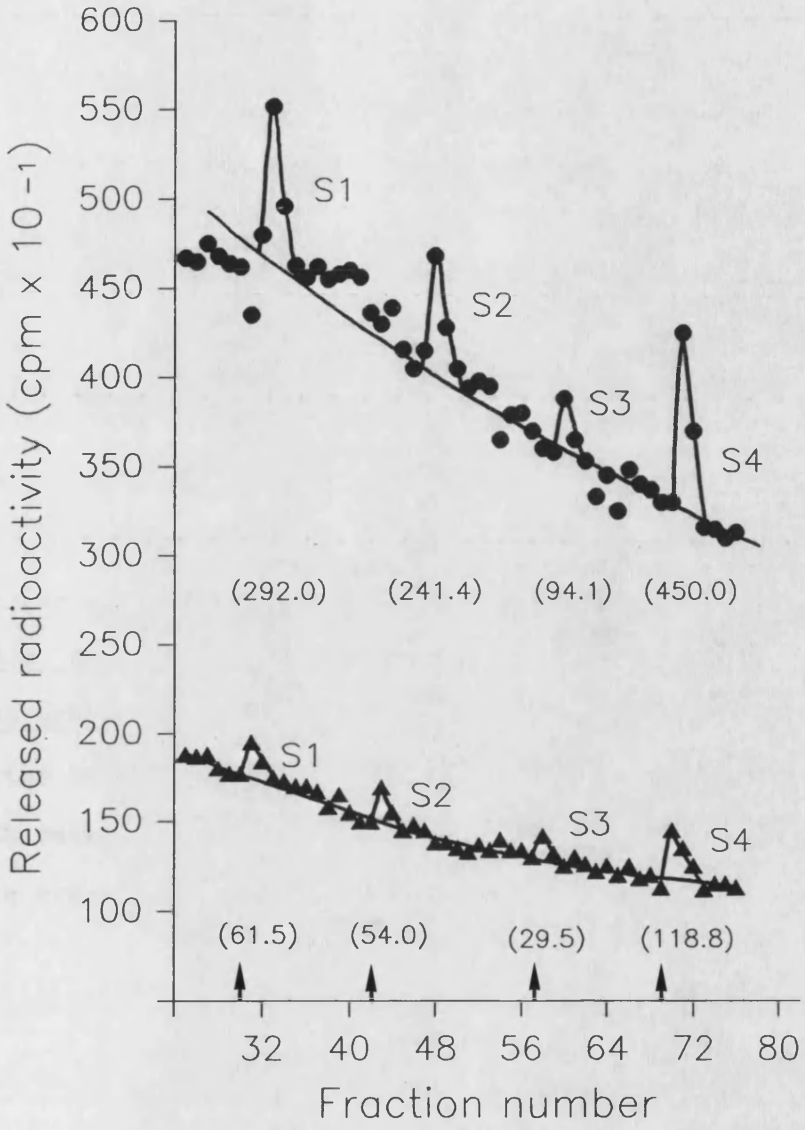

Fig. 4.12. Superfusion profiles of ACh release from (●) Percoll fraction F4 and (▲) sucrose isolated synaptosomes. After a 40 min washout period the synaptosomes were subjected to successive stimulations with: nicotine (10μM; S1, S2), Krebs buffer (S3) and K^+ (20mM, S4) at 30 min intervals. ↑ Indicates pulse arriving at the synaptosomes. Numbers in brackets are fmol ACh released/mg protein.

	S1 NICOTINE 10μM	S2 NICOTINE 10μM	S3 KREBS BUFFER	S4 K^+ 20mM
SUCROSE	62.0 ± 2.5	53.8 ± 3.3	27.5 ± 2.4	117.4 ± 1.4
PERCOLL	290.0 ± 4.7	240.4 ± 4.4	93.1 ± 3.2	450.0 ± 4.2

Table 4.3. Evoked ACh release from sucrose or Percoll isolated synaptosomes. Release was provoked by nicotine (10μM; S1, S2), Krebs buffer (S3) or K^+ (20mM; S4) and values are expressed as fmol ACh released/mg protein ± SEM. The values are the mean of 3 separate experiments.

The greater response to stimulation in fraction F4 will make differences in drug evoked ACh release easier to determine than using sucrose synaptosomes, where the response is much smaller. Thus fraction F4 provides a pure, highly functional cholinergic synaptosome preparation for studying nicotine evoked ACh release and so this synaptosome fraction from the Percoll gradient was used in future experiments.

4.4. SUMMARY

Due to the low nicotine evoked ACh release from sucrose isolated synaptosomes, the use of Percoll for synaptosome isolation was investigated to determine if a purer cholinergic synaptosome population could be obtained. The method used was that described by Dunkley et al., (1987, 1988) for the preparation of cortical synaptosomes and this was applied for use with the hippocampus. A similar protein distribution (table 4.1) and subcellular organelle content of fractions across the gradient showed that the procedure had been faithfully reproduced for this discrete brain region.

Five fractions were obtained from the Percoll gradient and the cholinergic nature of these were examined. Fraction F1 had a low synaptosomal content (from LDH, fig. 4.2 , and electron microscopy, fig. 4.8E) and so had low levels of the cholinergic markers ChAT and Ch uptake. The high AChE activity in this fraction was probably as a result of postsynaptic membrane fragments, with bound enzyme, being present in the F1 fraction. Although fractions F2 and F3 exhibited high levels of synaptosomes (from LDH and electron microscopy) cholinergic markers were relatively low (ChAT and Ch uptake; activities were higher in fraction F3 than F2) and so there was no

apparent cholinergic enrichment in these fractions. The highest cholinergic synaptosome content was in fraction F4, the activities of which were at least two to threefold greater than any other fraction.

Fraction F5 had a low synaptosome content (from LDH and electron microscopy) with a correspondingly low functional cholinergic activity ([^{3}H]Ch uptake). The apparently high ChAT activity of this fraction is probably due, in part, to non-specific acetyltransferase activity like carnitine acetyltransferase.

The response of Percoll fraction F4 to nicotine stimulation was compared with that of sucrose synaptosomes, by superfusion. The evoked ACh release was four times greater from fraction F4 than from sucrose synaptosomes. Thus the Percoll method produces an enriched cholinergic population of synaptosomes for the study of nicotine evoked ACh release.

CHAPTER 5. NICOTINE-EVOKED ACETYLCHOLINE RELEASE FROM SYNAPTOSOMES ISOLATED ON PERCOLL GRADIENTS

5.1. INTRODUCTION

The Percoll gradient method produces a highly purified synaptosome preparation for studying cholinergic function (see chapter 4). Nicotine evoked ACh release, from these synaptosomes, was studied using a modified version of the superfusion system of Rapier et al., (1988) as outlined in section 3.3.4.

The effect of nicotine concentration on ACh release was examined and the nicotinic nature of this response was studied using DHβE. The dependency of this evoked release on the presence of Ca^{++} ions was also ascertained.

As mentioned in section 1.2.4., the AChE inhibitors THA and physostigmine have both been used therapeutically, in SDAT, to increase ACh levels. Although there have been reports of moderate (THA; Summers et al., 1986) or transient (physostigmine; Christie et al., 1981) improvements in memory-related tasks in SDAT, the mode of action of these drugs may not be limited to enzyme inhibition. As it has been observed that both THA (Perry et al., 1988) and physostigmine (Shaw et al., 1985) interact directly with the nAChR. Thus the effects of these AChE inhibitors on nicotine-evoked ACh release was studied, by superfusion, to determine whether the mode of action was via the receptor.

5.2. METHODS

Hippocampal synaptosomes were prepared and isolated on four step Percoll gradients, as described in section 4.2.1. The F4 fraction was removed and washed twice with Krebs buffer (10ml; 15 min at 15,000g) to remove the Percoll. The pellet was resuspended in 1ml

Krebs buffer and then loaded with [^{3}H]Ch (0.8μM; 20min at 37°C). Excess [^{3}H]Ch was removed by washing with Krebs buffer (1ml) followed by centrifugation (7 min at 3,000g) before resuspension in Krebs buffer (1ml) and samples (150μl) placed in superfusion chambers (see section 3.2.5.; fig. 3.2).

The synaptosmes were superfused with Krebs buffer and subjected to an inital nicotine pulse (10μM; S1), to standardise the chambers, after a 40 min washout period. The effect of nicotine concentration on ACh release was studied by varying the concentration (1-100μM) in the S2 pulse. The nicotinic nature of this response was studied by introducing buffer, containing the nicotinic agonist DHβE (10μM) 15 min after the S1 pulse. The subsequent S2 (nicotine, 10μM), S3 (buffer) and S4 (K^+, 20mM) pulses were with drugs made up in the DHβE buffer.

The effect of the AChE inhibitors on ACh release was studied, where the drug was either administered as a discrete pulse (S2) or continuously in the buffer, introduced 15 min after the S1 pulse. BW284C51 was used at a concentration of 1μM which was the maximum inhibition of AChE activity (see section 4.3.3.2.) and was the concentration used in the electrophysiological studies (see section 6.3.2.). Physostigmine (1μM) was used as a direct comparison with BW284C51. THA was used at 20μM as this was the reported IC50 at the nAChR (Perry et al., 1988).

Ca^{++} dependence was studied as described above, except the synaptosomes from the gradient were washed and superfused with Ca^{++}-free buffer (where the $CaCl_2$ in the Krebs buffer had been replaced with NaCl). Pulses of drug (either nicotine (10μM), K^+

(20mM) or buffer, made in Ca^{++}-free buffer) were administered at 30 min intervals after the 40 min washout period. Ca^{++} was introduced 15 min after S2 and subsequent stimulations were with drugs made in Krebs buffer.

5.3. RESULTS AND DISCUSSION

5.3.1. Calcium dependency

In the absence of Ca^{++} both basal and evoked ACh release were reduced compared to that in the presence of Ca^{++}, see fig. 5.1 and table 5.1. The slight increase in basal release with time, in the absence of Ca^{++} (fig. 5.1) could be due to mobilisation of internal Ca^{++} stores as suggested by Rowell & Winkler (1984). In the presence of Ca^{++}, basal release returns to 'normal', see fig. 4.12.

Table 5.1 shows that the air bubble effect was not Ca^{++} dependent, as Ca^{++} had no effect on the level of tritium released by a pulse of Krebs buffer, adding to the suggestion that this response was a result of a mechanical and not a physiological process.

After the air bubble effect had been deducted, the ratio of $-Ca^{++}$ (nicotine)/$+Ca^{++}$ (nicotine) was approximately 36% indicating that nicotine evoked ACh release was 64% dependent on exogenous Ca^{++}. A similar ratio of K^{+} evoked release showed that response was 65% dependent on Ca^{++}.

This Ca^{++} dependency of nicotine- and K^{+}-evoked ACh release indicates that the superfusion system is monitoring a physiological response and is consistent with other reports. Rowell & Winkler (1984) observed that nicotine stimulated ACh release was 58%

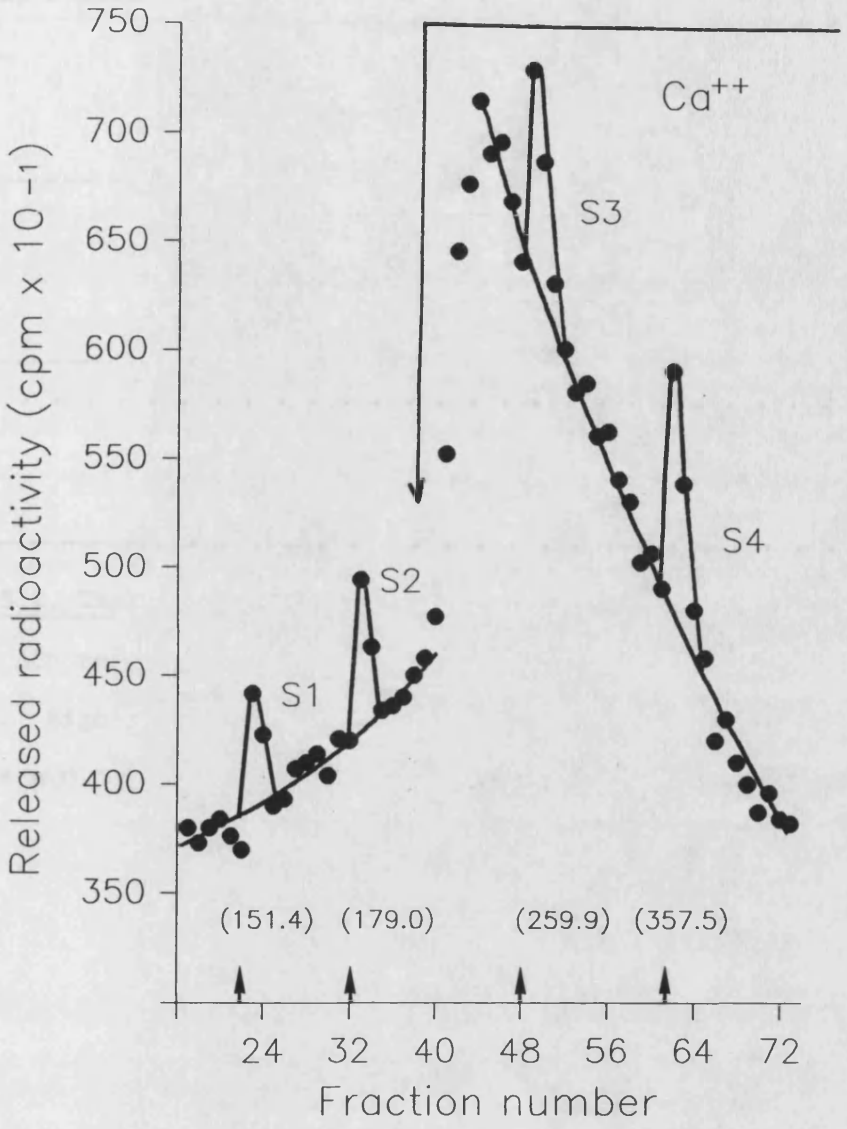

Fig. 5.1. A superfusion profile showing the effect of Ca^{++} on evoked ACh release. The synaptosomes were subjected to successive stimulations with nicotine (10μM; S1, S3) and K^{+} (20mM; S2, S4). Ca^{++} was introduced into the system 15 min after the S2 pulse. ↑ Indicates pulse arriving at the synaptosomes. Numbers in brackets are fmol ACh released/mg protein.

PULSE	NICOTINE 10μM	K^+ 20mM	KREBS BUFFER
$-Ca^{++}$	157.1* ± 2.5	188.0* ± 2.3	102.2 ± 1.7
$+Ca^{++}$	255.1 ± 2.7	348.5 ± 2.7	101.4 ± 1.7

Table 5.1. The effect of Ca^{++} on evoked ACh release. Values are fmoles ACh released/mg protein, n=8, before subtraction of air bubble effect. Significantly different from the response in the presence of Ca^{++}, * $p<0.001$.

dependent on the anion. Nicotine- and K^+-evoked dopamine release from striatal synaptosomes was approximately 62% dependent on exogenous Ca^{++} (Rapier et al., 1988).

5.3.2. Nicotine-evoked acetylcholine release

5.3.2.1. Nicotine concentration

To check for variation between chambers and experiments a S1 pulse of 10μM nicotine was consistently given. However, a tendency for variation between chambers was minimal in the system used as the response to 10μM nicotine (S1) was constant throughout these experiments and with those in sections 4.3.9., 5.3.3. and 5.3.4.

The effect of nicotine concentration on ACh release was studied by varying the concentration in the S2 pulse, see table 5.2. The effect due to air bubble was routinely determined in a S3 pulse of Krebs buffer, which was then deducted from the S2 value to obtain the response to drug. To ensure that the air bubble effect did not vary throughout the experiment buffer pulses were given as S2, S3 and S4 (see table 5.2, 0μM nicotine). The response to air bubble was constant (37% of the S1), indicating a mechanical process, confirming the validity of using the S3 buffer value to correct the S2 drug response.

As seen in table 5.2, there is a decrease in response with repetitive stimulation with 10μM nicotine such that S2/S1 (after deduction of the air bubble effect) = 85.5%. This suggests a reduction in synaptosome responsiveness with time and similar decreases with repetitive stimulations of drug was seen in section 3.3.3.2. with 50μM nicotine (S2/S1 = 84%) and section 3.3.3.3.1.

S2 NICOTINE (μM)	S1 NICOTINE (10μM)	S2	S3 KREBS BUFFER	S4 K^+ (20mM)	S2/S1
0 (n=4)	284.5 ± 2.3	107.1 ± 1.8	105.0 ± 2.0	106.0 ± 1.5 (Krebs buffer)	-
1 (n=6)	280.6 ± 1.9	120.7 ± 2.2	105.8 ± 1.8	345.0 ± 3.1	8.5%
3 (n=3)	276.1 ± 2.7	203.0 ± 1.5	104.9 ± 1.5	340.8 ± 3.0	57.3%
10 (n=6)	284.1 ± 3.8	259.2 ± 2.1	108.8 ± 1.9	340.1 ± 2.6	85.8%
30 (n=4)	278.1 ± 1.4	282.1 ± 2.9	107.9 ± 1.6	340.0 ± 3.5	102.4%
100 (n=5)	282.3 ± 2.1	220.2 ± 2.4	108.7 ± 1.5	341.6 ± 3.3	64.2%

Table 5.2. The effect of nicotine concentration on ACh release. Nicotine concentration was varied (1-100μM) in the S2 pulse. Values are fmoles ACh released/mg protein ± SEM. The S2/S1 ratio was calculated after deduction of the S3 buffer pulse.

with 10μM ANTX (S2/S1 = 90%).

Nicotine-evoked ACh release increased in a dose-dependent manner reaching a maximum response at 30μM, see fig. 5.2. The decrease in release at higher (100μM) concentrations is unusual and difficult to interpret. If at this higher concentration the receptor had become desensitized, ACh release would be expected to reach a maximum and then plateau. A similar dose related effect on transmitter release, from brain slices, was seen by Lapchak et al., (1989) using a nicotinic agonist, methylcarbamylcholine.

A direct linear plot of ACh release (after deduction of the air bubble effect) against nicotine concentration, not shown, gave an EC50 (concentration to give half maximal effect) of 5μM and a Vmax (maximum effect) of 136.3±7.1 fmol ACh released/20s/mg protein. In section 3.3.3.3.2B, ANTX evoked ACh release, from sucrose isolated synaptosomes, had an EC50 of 7.5μM similar to that of nicotine reported here. However, the Vmax of the ANTX evoked response was 23.9±3 fmol ACh released/40s/mg protein which was approximately six fold lower than that reported here. This increase in Vmax suggests that the Percoll method of isolating synaptosomes produces a purer and more responsive preparation for studying transmitter release than the sucrose method and is consistent with the six fold higher levels of [^{3}H]Ch uptake (see fig. 4.7).

5.3.2.2. The effect of DHβE

The nicotinic nature of this evoked release was studied in the presence of the antagonist DHβE (10μM), see table 5.3.

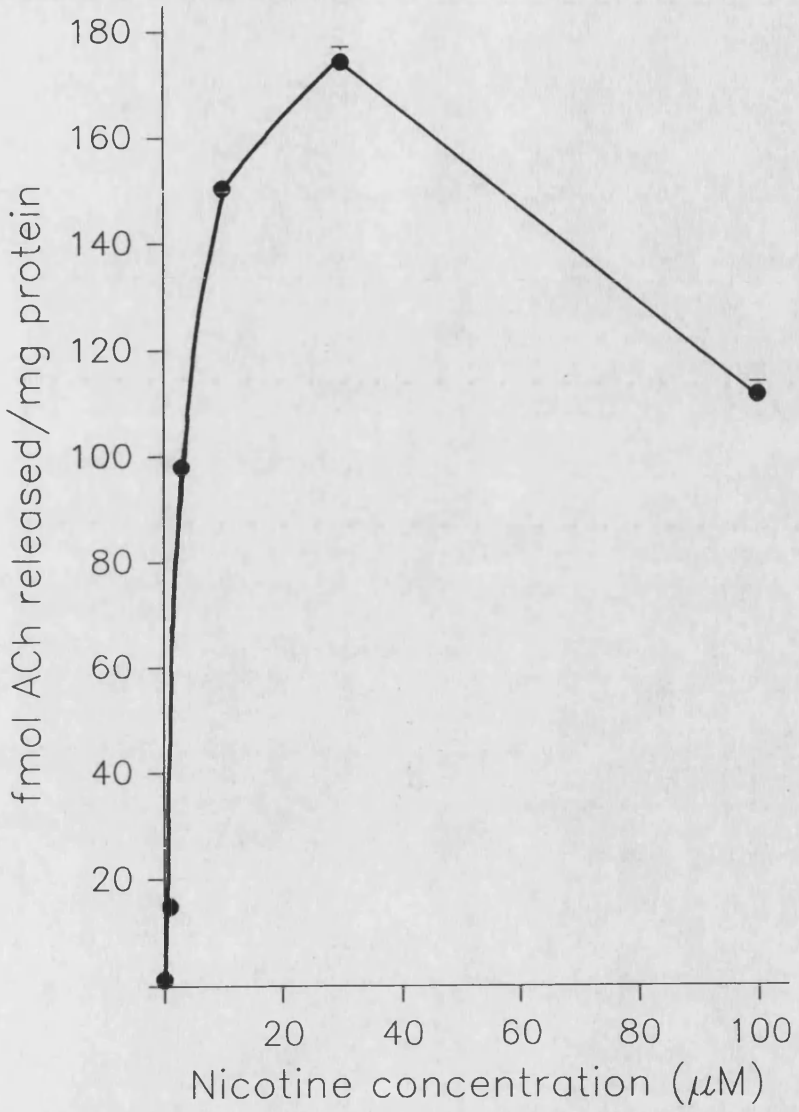

Fig. 5.2. The effect of nicotine concentration on ACh release.

The nicotine concentration was varied in the S2 pulse.

DHβE 10μM	S1 NICOTINE 10μM	S2 NICOTINE 10μM	S3 KREBS BUFFER	S4 K^+ 20mM	S2/S1
-	281.1 ± 2.2	248.4 ± 2.7	103.8 ± 1.2	346.5 ± 2.2	81.6%
+	285.0 ± 2.0	174.3* ± 3.1	108.8 ± 1.5	342.0 ± 2.1	37.2%

Table 5.3. The effect of DHβE on nicotine evoked ACh release. DHβE (10μM) was introduced 15 min after S1. Values are expressed as fmol ACh released/mg protein ± SEM of 10 chambers. S2/S1 ratio was determined after subtraction of the buffer pulse. Significantly different from control (no DHβE) * $p<0.001$.

Nicotine-evoked ACh release, in the presence of DHβE, was 45% of the control (no DHβE). This reduction (55%) in ACh release by DHβE suggests that the response was via a nAChR. A similar inhibition of nicotine evoked transmitter release by DHβE was reported by Wonnacott et al., (1988) for both ACh and GABA release from hippocampal synaptosomes. DHβE inhibited ANTX induced ACh release by a similar amount, 50%, see section 3.3.3.3.1. As expected DHβE had no effect on K^+ evoked ACh as this depolarisation is not via the nAChR. The air bubble effect was not affected by DHβE which was as expected as this is a mechanical response.

5.3.3. Effect of acetylcholinesterase inhibitors on release

5.3.3.1. AChE inhibitors as stimulators of ACh release

Any stimulatory effects of the AChE inhibitors: BW284C51, physostigmine and THA, on ACh release were examined by administering the drugs as a S2 pulse, see table 5.4.

Responses to THA were comparable to those produced by Krebs buffer alone. Thus THA had little or no effect on ACh release. Perry et al., (1988) reported that 20μM was the IC50 for THA binding to the nicotinic receptor. However, at this concentration THA may bind to the receptor but have no stimulatory effect on ACh release, for example by binding to the β subunit of the receptor and not the agonist binding α subunit (see section 1.3.2.3.).

Both BW284C51 and physostigmine elicited substantial ACh release. Although the response to BW284C51 was lower than that produced by nicotine, physostigmine effects were the same. The enzymic extraction procedure, described in section 3.3.3.1.4., showed that most, if not all, the released radioactivity collected in the

S2 PULSE	S1 NICOTINE 10μM	S2	S3 KREBS BUFFER	S4 K^+ 20mM	S2/S1	% CONTROL
NICOTINE 10μM (n=6)	308.6 ±4.0	277.1 ±4.1	108.3 ±2.0	379.4 ±4.4	84.3%	(100)
BW284C51 1μM (n=4)	288.3 ±4.7	240.4* ±2.7	102.1 ±2.5	338.5 ±1.4	74.3%	81.9
PHYSOSTIGMINE 1μM (n=5)	287.3 ±3.8	271.6 ±2.7	97.4 ±3.7	335.6 ±3.0	91.7%	103.2
THA 20μM (n=4)	298.3 ±3.4	107.9* ±2.6	101.7 ±2.4	359.1 ±4.0	3.2%	3.7

Table 5.4. The effect of AChE inhibitors as stimulators of ACh release. BW284C51 (1μM), physostigmine (1μM) or THA (20μM) were introduced as a S2 pulse. Values are fmol ACh released/mg protein ± SEM. S2/S1 ratios were determined after the deduction of the buffer pulse. Significantly different from the control (10μM nicotine), * $p<0.001$.

superfusion samples was ACh and so there was little, or no, ACh hydrolysis. Thus the increase in ACh levels, above basal, in the presence of these AChE inhibitors was not as a result of preventing ACh hydrolysis.

BW284C51 stimulated release was 82% of the response to nicotine. This suggests that BW284C51 could be interacting with the nAChR by acting as a nicotinic agonist. However, Mizobe & Livett (1982) reported that 1μM BW284C51 exhibited only AChE inhibitory action but at higher concentrations BW284C51 did appear to interact with the nAChR of chromaffin cell cultures. Thus 1μM BW284C51 may be eliciting ACh release not through the nAChR but via some other mechanism perhaps by interacting with ion channels causing depolarisation.

Physostigmine-evoked ACh release was 103% of that produced by nicotine, suggesting there was interaction with the nAChR. This finding is contrary to that of Mizobe & Livett (1982) who reported that physostigmine (at concentrations of 1μM or less) had only AChE inhibitory actions in chromaffin cell cultures. However, the suggestion that physostigmine interacts with the nAChR is consistent with the findings of Shaw et al., (1985) who observed that physostigmine acted as a nicotinic agonist at the frog muscle nAChR at concentrations as low as 0.5μM.

5.3.3.2. AChE inhibitor's effect on basal and evoked ACh release

The effect of the prolonged presence of the AChE inhibitors in the washing buffer, introduced 15 min after S1, on basal release of ACh was shown in fig. 5.3 and the effect of AChE inhibitors on evoked

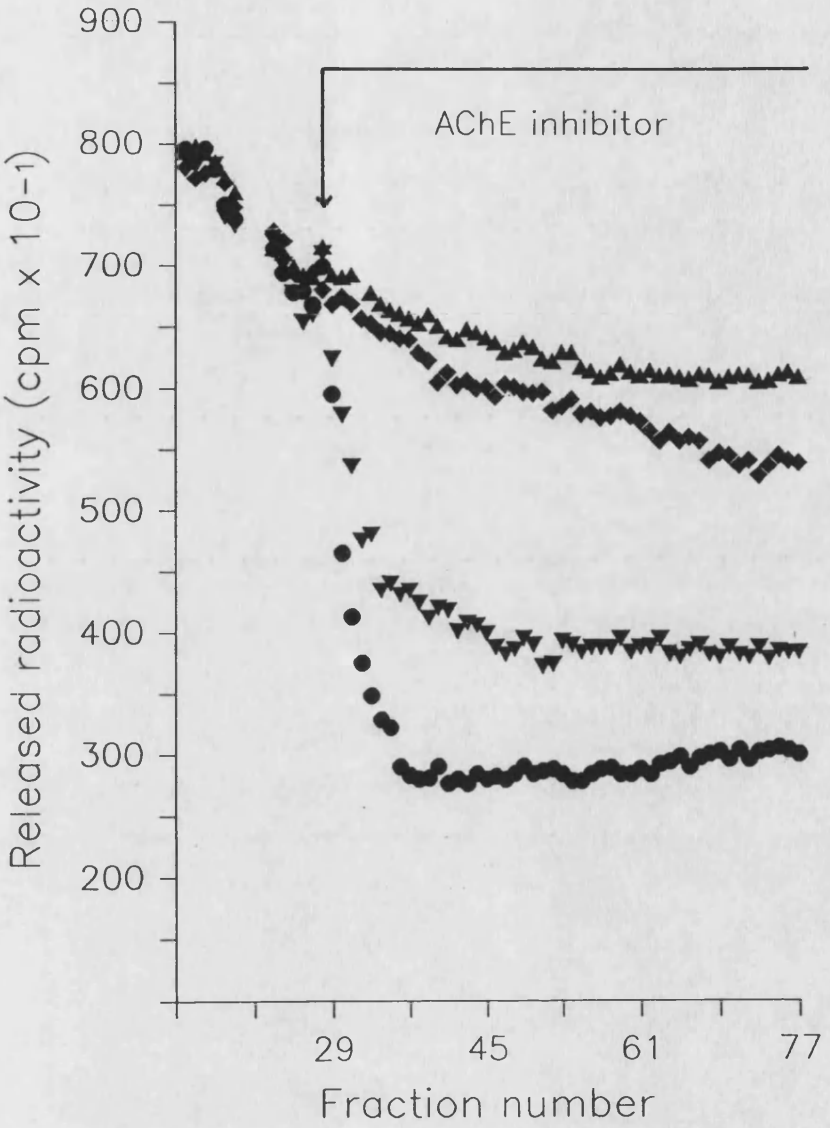

Fig. 5.3. Superfusion profiles of the effect of Krebs buffer, containing AChE inhibitors, on basal release. AChE inhibitor was introduced into the washing Krebs buffer 15 min after the S1 pulse. Physostigmine (1μM,▲); Krebs buffer (◆); BW284C51 (1μM,▼); THA (20μM,●).

ACh release was shown in table 5.5. Physostigmine (1μM) appeared to slightly increase basal ACh release compared to the normal Krebs washing buffer whereas the baseline with BW284C51 (1μM) was approximately 70% of that of Krebs buffer. However, THA (20μM) dramatically dropped the baseline to 50% of that of the control (Krebs buffer alone).

BW284C51 appeared to have little or no effect on nicotine or K^+-evoked ACh release, despite the 30% drop in basal release, indicating that BW284C51 (1μM) does not interfere with either the nicotine binding site nor K^+ depolarisation. The mode of action of this AChE inhibitor is unclear but the reduction in basal release could be due to interaction with ion channels other than those involved in K^+ depolarisation.

Physostigmine enhanced the nicotine response by about 30%, which is consistent with its own ability to release transmitter as shown by the increase in basal release (fig. 5.3) and by administration of a pulse of 1μM physostigmine (see table 5.4 and 5.5). Both nicotine and K^+ responses were increased in the presence of 1μM physostigmine which is consistent with the findings of Shaw et al., (1985) who reported that low μM concentrations of physostigmine interact with the nAChR evoking ACh release. Sadoshima et al., (1988) observed that at physostigmine concentrations of 10μM or greater this enhancement of ACh release was reduced in a dose dependent manner.

THA had a dramatic effect on basal release with a corresponding reduction in nicotine- and K^+-evoked ACh release. Stevens & Cotman (1987) and Rogawski (1987) reported that THA blocked specific K^+ (I_A) currents and also voltage dependent Na^+ channels (Rogawski, 1987) and

BUFFER	S1 NICOTINE 10μM	S2 NICOTINE 10μM	S3 BUFFER	S4 K^+ 20mM	S2/S1	S4/S1
KREBS (CONTROL) (n=6)	308.6 ±4.0	277.1 ±4.1	108.3 ±2.0	379.4 ±4.4	86.5%	122.9%
BW284C51 1μM (n=4)	299.8 ±4.2	245.5 ±2.3	102.9 ±3.5	364.3 ±4.6	81.9%	121.5%
PHYSOSTIGMINE 1μM (n=5)	316.4 ±5.6	351.3* ±3.7	283.3 ±4.4	423.6* ±3.5	111%	133.9%
THA 20μM (n=3)	291.3 ±4.4	113.4* ±3.1	105.3 ±3.7	138.1* ±2.9	38.9%	47.4%

Table 5.5. The effect of AChE inhibitors on evoked ACh release. The AChE inhibitors were introduced into the washing buffer 15 min after S1. Subsequent pulses (S2-S4) were with drug made up in buffer containing AChE inhibitor. Values are expressed in fmol ACh released/mg protein and are the mean ± SEM. The S2/S1 and S4/S1 ratios were determined before deduction of the buffer pulse. Significantly different from the control (Krebs buffer), * $p<0.001$.

this could explain the reduction in basal release. The effect of THA on evoked ACh release is difficult to interpret as the contribution of the action of THA on the ion channels to the reduction in nicotine stimulated ACh release needs to be determined. Perry et al., (1988) reported that 20μM was the IC50 for THA binding to the nAChR but when THA (20μM) was given as a discrete pulse (table 5.4) there was little or no enhanced ACh release, above the air bubble effect. Until the mode of action of THA has been determined then the effect of THA on evoked ACh release can not be elucidated.

5.4 SUMMARY

The Percoll fraction F4 is enriched in synaptosomes which are cholinergic in nature, as shown by the markers ChAT and [^{3}H]Ch uptake (section 4.3.4.2. and 4.3.5., respectively). Nicotine stimulated ACh release from these synaptosomes, in a dose dependent manner, which was blocked by the antagonist DHβE, suggesting that evoked release was via a nAChR. This nicotine induced ACh release was dependent on exogenous Ca^{++}, indicating that the response to the drug was a physiological process.

The nAChR needs to be fully characterised (using agonists: DMPP, ANTX and antagonists: d-tubocurarine, hexamethonium, mecamylamine) before the mAChR can be studied (using agonists: muscarine, oxotremorine and antagonists: atropine and scopolamine). Having determined how each receptor contributes to ACh release, under known conditions, the effect of ACh on its own release could be examined. Thus the self regulation of ACh at the hippocampal nerve terminal could be determined.

From these experiments, section 5.3.3, it is clear that the drugs BW284C51, physostigmine and THA not only have AChE inhibitory action but also effect ACh release from hippocampal synaptosomes. BW284C51 (1μM) has a stimulatory effect on ACh release when administered as a discrete pulse. However, prolonged application of BW284C51 decreases the basal release by 30%, see section 5.3.3.2., but has little or no effect on nicotine-evoked ACh release, suggesting that BW284C51 does not bind to the nAChR. The reduction in basal release and the stimulatory response of BW284C51 suggests that this AChE inhibitor may interact with other ion channels.

Physostigmine increases both basal and nicotine-evoked ACh release, which is consistent with physostigmine interacting with the nAChR. To examine if physostigmine stimulated ACh release is via the nAChR, experiments should be repeated in the presence of the antagonist DHβE.

The AChE inhibitor THA had little or no stimulatory effect on ACh release, when given as a discrete pulse, but reduced the basal release by 50% when administered for a prolonged period, see section 5.3.3. and fig. 5.3. The decrease in baseline is consistent with reports that THA interacts with ion channels, the profile looks similar to that obtained in Ca^{++} free buffer (fig. 5.1), and so the effects, if any, of THA on the nicotine-evoked ACh release, via the nAChR, was masked. However, 20μM THA is much higher than the plasma levels obtained from patients treated for SDAT with this drug, thus the therapeutic relevance of this ion channel effect is unclear. Experiments at lower THA levels (0.02-1μM in plasma, Park et al., 1986) are needed to ascertain whether these effects are present at

therapeutic levels. If so then the ion channels involved in this phenomenon can be determined using channel blockers, for example: mM concentrations of tetraethylammonium, 4-aminopyridine and barium block Ca^{++} independent K^{+} currents. To examine if the THA action involves the blockade of Ca^{++} ions the Ca^{++} ionophore A23187 could be used to circumvent endogenous Ca^{++} channels. Having determined the THA effects in the synaptosome then the response in more complex models may be easier to interpret and so the therapeutic benefits of this drug, in the treatment of SDAT, can be better evaluated.

CHAPTER 6. AN ELECTROPHYSIOLOGICAL STUDY OF THE NICOTINIC ACETYLCHOLINE RECEPTOR IN RAT HIPPOCAMPAL SLICES.

6.1. INTRODUCTION

Having studied the nAChR in the synaptosome preparation, the presence of functional nAChRs in a more complex model, the hippocampal slice, was assessed in preliminary electrophysiological studies using evoked field potentials.

6.1.1. The hippocampus as a model for studying long term potentiation

Electrophysiological recordings from brain slices was first developed by Yamamoto & McIlwain (1966) who showed that isolated slices of prepyriform cortex could be maintained *in vitro* and still exhibit electrical activity comparable to that obtained from the intact brain. Skrede & Westgaard (1971) were instrumental in establishing the hippocampus as a candidate for brain slice studies. The hippocampus is ideally suited for such studies because of its laminated geometry allowing the consistent positioning of electrodes into the area of interest, see fig. 6.1.

The observation that a change in synaptic efficacy can be seen at the hippocampal synapse, both *in vivo* and *in vitro*, provided a strong impetus for the continued use of this brain slice preparation to study the memory-related phenomenon, long term potentiation (LTP). LTP is characterised by a stable, relatively long lasting increase in the magnitude of the postsynaptic response to a constant afferent volley, following a brief tetanic (high frequency) stimulation (Teyler, 1987).

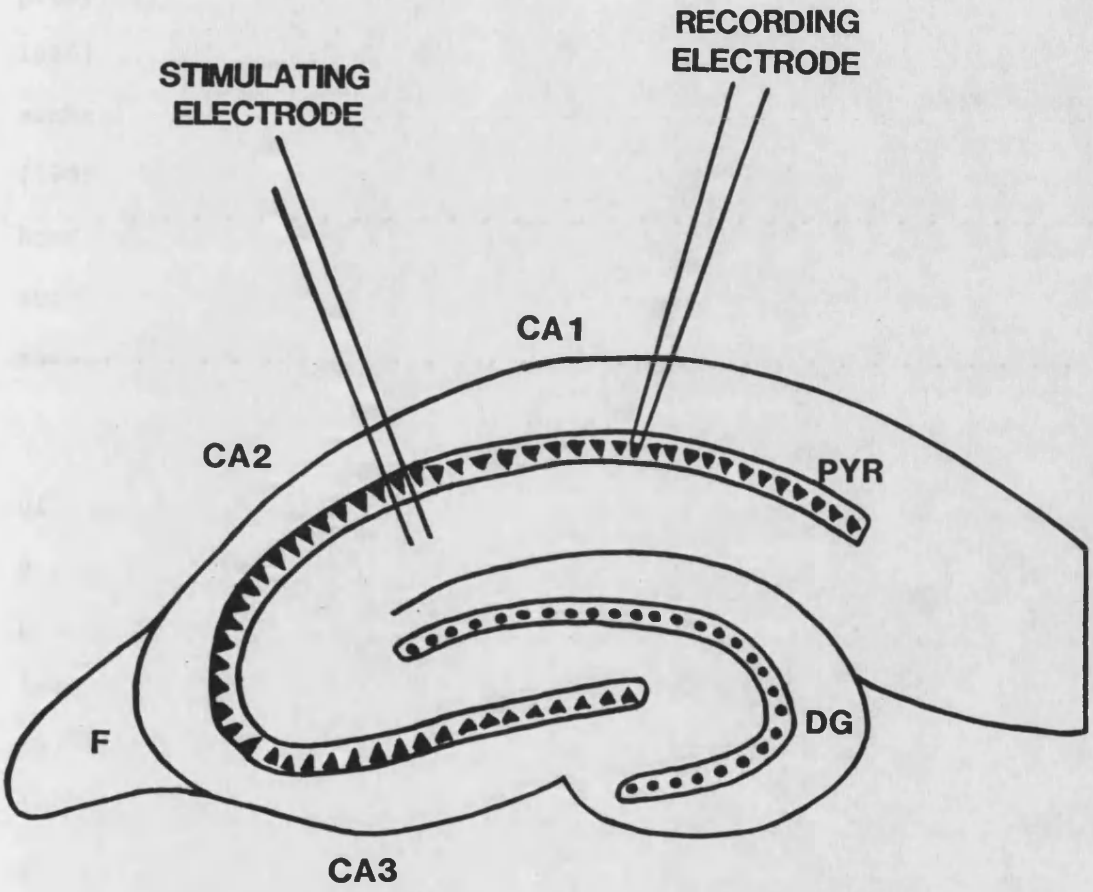

Fig. 6.1. A schematic diagram of a hippocampal slice. This depicts the laminar pyramidal cells (CA1, CA2, CA3) of the pyramidal layer (PYR) and the positions of the stimulating and recording electrodes. F, fimbria; DG, dentate gyrus.

LTP is dependent on synaptic transmission and the density of innervation to a given neurone or neuronal population. There is, however, some controversy as to whether LTP is maintained by a presynaptic (more transmitter release; Sastry, 1982; Bliss et al., 1986) or a postsynaptic mechanism (greater sensitivity of the target membrane; Lynch & Baudry, 1984; Muller et al., 1988). Davies et al. (1989) found that the mechanism is presynaptic for the first half hour and gradually the postsynaptic membrane becomes more sensitive, such that with time an increased sensitivity of the postsynaptic membrane grows so that LTP is maintained by a postsynaptic mechanism.

This complicated mechanism fits with other recent observations of Kauer et al., (1988) who showed that LTP had two temporal phases: a transient phase which lasted for 30 min (the same as the presynaptic response of Davies et al., 1989) which could be evoked in isolation by applying transmitter directly into the synapses. Malinow et al., (1988) showed that in the presence of kinase inhibitors the transient phase of LTP was still evoked but the maintained phase failed to develop, thus suggesting that the maintained component of LTP results from an increased sensitivity of postsynaptic receptors to neurotransmitter resulting from some kinase activity (for review see Stevens, 1989).

LTP in the hippocampus is widely studied as the mechanisms involved in its induction and maintenance are believed to underlie fundamental properties of learning and memory in vertebrates (Bliss & Lynch, 1988).

6.1.2. The nicotinic acetylcholine receptor in the hippocampus

The electrophysiological evidence for a functional nAChR, in the hippocampus, has been much debated. Bird & Aghajanian (1976) reported that muscarine and other muscarinic agonists caused postsynaptic excitation at concentrations lower than those needed for ACh to elicit a response. This excitation was blocked by both scopolamine (a mAChR antagonist) and DHβE (a nAChR antagonist). From this they deduced that there was a single receptor type exhibiting both nicotinic and muscarinic effects and not two independent receptor types due to the crossover effect of DHβE on muscarinic excitation.

Haas (1982) and Cole & Nicoll (1984a) reported that carbachol (which acts differentially at both the nAChR and mAChR) caused excitation similar to that of ACh and that this response was blocked by the muscarinic antagonist atropine. Haas made no conclusion on whether the effect was purely muscarinic, even though the response was blocked by atropine. Cole & Nicoll suggested that only mAChR and not nAChR or a nicotinic/muscarinic receptor was involved in the depolarisation as DHβE had no effect on the carbachol excitation. The conclusion of Cole & Nicoll was in support of the findings of Segal (1978) who also reported the existence of only mAChR actions.

Rovira et al., (1983) did detect a nicotinic input associated with the CA1 pyramidal cells of the hippocampus (see fig. 6.1) and observed a clear cut distinction between mAChR and nAChR actions. Muscarine depressed the amplitude of the evoked negative field whereas nicotine increased the potential (especially its duration) and is consistent with presynaptic nAChR facilitating transmitter

release. There have been several reports to support the existence of distinct nicotinic and muscarinic receptors where the actions of nicotine are blocked by nicotinic antagonists and not muscarinic antagonists, and nicotinic antagonists are ineffective against muscarinic agonists (McLennan & Hicks, 1978; Bradley & Lucy, 1983; Takagi, 1984).

cDNA cloning techniques have revealed at least three subtypes of neuronal nAChR in the brain which are functionally expressed and structurally related, but different, to that found in muscle (for a review see Steinbach & Ifune, 1989; this report section 1.3.2.).

6.1.3. Practical aspects of electrophysiology

In order to study the nAChR in the hippocampal slice the following practical aspects of electrophysiology have to be considered.

6.1.3.1. Types of recordings

There are three types of electrophysiological recordings from which data can be obtained to determine functional receptor activity:

1. Extracellular recordings are the least specific as they monitor the transmitter effects of a field of neurones (Bird & Aghajanian, 1976; Vidal & Changeux, 1989; this report).
2. Intracellular recordings monitor the excitatory or inhibitory effects of a transmitter or drug on a single neurone (Haas, 1982; Cole & Nicoll, 1983, 1984a, b; Egan & North, 1986).
3. Patch clamp recordings which monitor the transmitter

effects at a single receptor channel (Aracava et al., 1987).

6.1.3.2. The tissue chamber

The tissue chamber provides the necessary environment for bathing the slice in medium. The medium contains a balanced salt content and substrate source, usually glucose, also the appropriate oxygen and carbon dioxide levels for slice survival. The chamber acts as a mechanical support for the slice and has illumination for placing the electrodes. The chamber is temperature controlled to provide optimum conditions for electrical activity. It also has provisions for changing the chemical composition of the medium, if required.

There are numerous designs for the tissue chamber but four of the most common are depicted in fig. 6.2 and are as follows:

1. Superfused chambers (fig. 6.2a) where the tissue rests at the medium/gas interface. The medium is continually flowing through the system.
2. Plate chambers (fig. 6.2b) which are like the superfused chamber except that there is no pool of medium. This has one advantage over the superfused model in that there is reduced dead volume when changing the medium.
3. Static chambers (fig. 6.2c) where the tissue is at the medium/gas interface but has a static pool of medium that could be changed by a push-pull pump. The advantage of this model is that it maintains the ultrastructure of the tissue which may become disturbed by flowing medium.
4. Submerged chambers (fig. 6.2d) where the tissue is

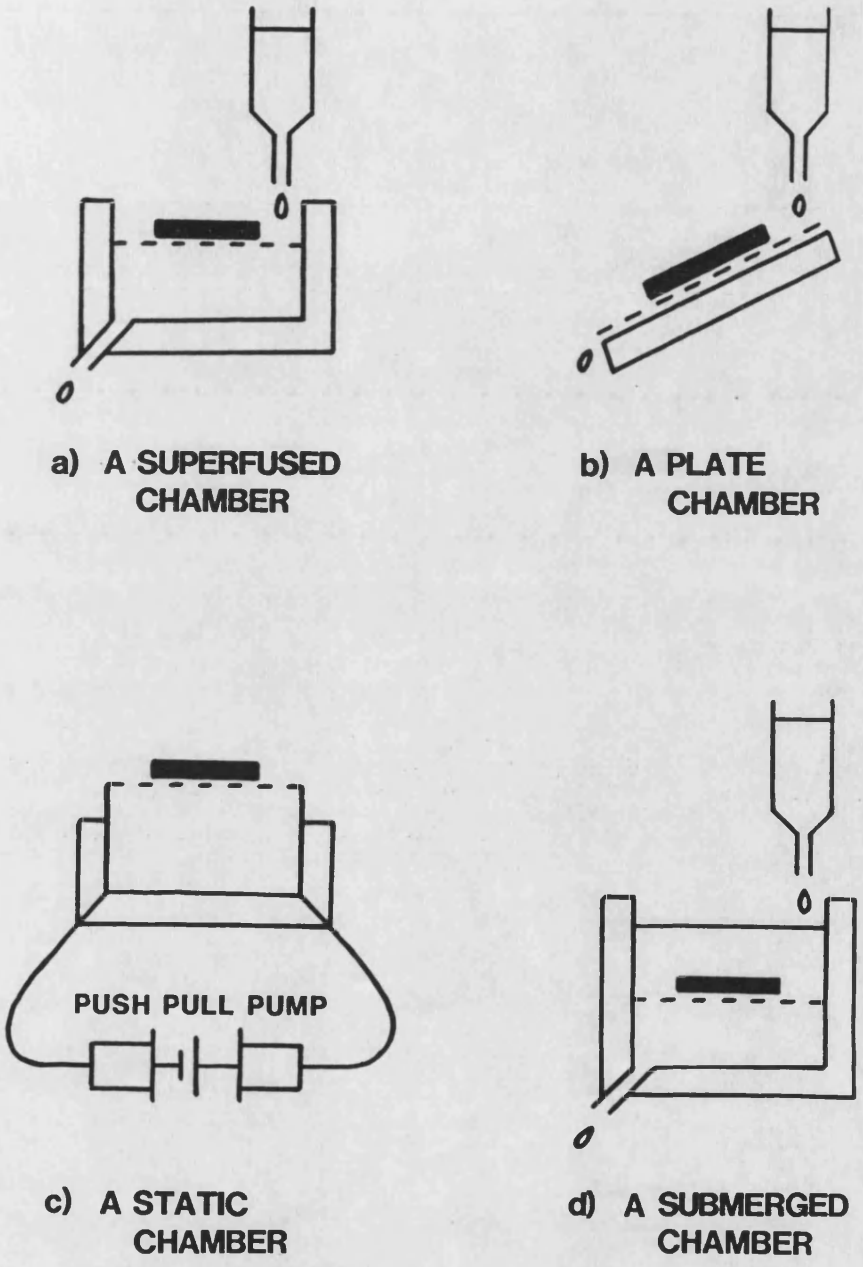

Fig. 6.2. Schematic diagrams of four of the most commonly used tissue chambers.

submerged in the medium. This needs moderate flow rates of well oxygenated medium to maintain optimal physiological conditions of the tissue. Submerged chambers are used when studying alterations in medium composition or when delivering drugs as it has two surfaces for diffusion into the tissue. A submerged chamber was used in the experiments reported in this thesis.

6.1.3.3. Electrodes

A variety of recording and stimulating electrodes have been successfully used in brain slice experiments.

6.1.3.3.1. Recording electrodes

Metal or glass micropipettes are adequate for recording extracellular field potentials or intracellular readings. Electrolyte filled micropipettes, used in this study, are commonly used for recording field potentials. The disadvantage of finely drawn micropipettes is the difficulty of seeing them while manipulating them relative to the slice. The addition of dye (such as Fast Green) into the electrolyte aids visualisation and marks the location of the recording electrode but may be associated with a certain amount of toxicity to the tissue. Thus it is important to ensure that any contrast enhancing medium is without effect on the system under study.

6.1.3.3.2. Stimulating electrodes

The small distance between the stimulating and recording electrodes compound the problem of stimulus artefact (fig. 6.3) when monopolar stimulating leads are employed. Use of a twisted pair stimulating electrodes, used in this study, or concentric bipolar electrodes reduce the stimulus artefact.

6.1.4. Factors to consider for reproducibility

In order to produce consistent slices and responses a number of factors have to be considered:

6.1.4.1. Presacrifice condition of the animal

The state of the animal just prior to sacrifice can affect slice experiments. Harris & Teyler (1983) showed that the time of sacrifice relative to the animal's circadian rhythm, affects the induction of LTP in the slice. Therefore animals of the same species, sex and age and the time of sacrifice should be consistent.

Presacrifice stressors might also confound the experiments as Foy et al., (1985) reported, LTP could not be elicited in hippocampal CA1 pyramidal cells from rats that were given a series of tail pinches 30 min prior to sacrifice. This effect was significantly correlated to corticosterone levels.

6.1.4.2. Slice preparation

The slice preparation time is an important factor in maintaining consistent results. Speed of preparation must be counterbalanced by a gentle dissection.

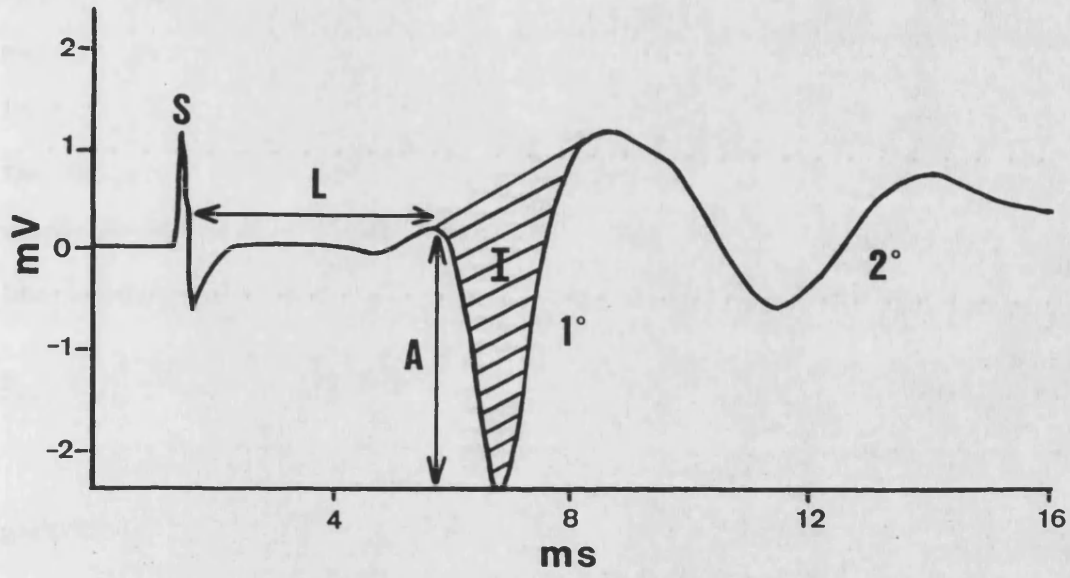

Fig. 6.3. A typical waveform. This waveform was produced by nicotine (100μM) in the presence of BW284C51 (1μM) showing the primary (1°) and secondary (2°) potential. A: amplitude, I: integral, L: latency, S: stimulus artefact.

The older the animal the harder the skull becomes which often breaks in pieces rather than along the suture lines. The meninges also appear tougher thus increasing the handling and time needed to remove the brain. The tissue should be removed with minimal handling without applying obvious physical stress and keeping the tissue moist. Extended preparation time and excessive handling often result in multiple population spikes following single pulse stimulation in the CA1 area (DiScenna, 1987). The average time of slicing for this work was 10 min from the time of sacrifice to slices being placed in the recovery bath (see section 6.2.1.).

6.1.4.3. Slice orientation

Slices at an angle perpendicular to the septo-temporal axis are generally used producing hippocampal slices like the one depicted in fig. 6.1. This angle can shift along the length of the hippocampus probably due to differences in the distribution pattern of intrinsic hippocampal fibres (Swanson et al., 1978).

It is best to take slices from the same septo-temporal segment since differences in the excitability of dorsal and ventral regions of the hippocampus have been noted (Mizuno et al., 1984).

6.1.4.4. Slice thickness

The slice has a zone 50-100μm at the cut edge in which cells are badly damaged (Misgeld & Froetscher, 1982). Thus this outer region should be considered dead tissue and it is not possible to obtain good electrophysiological responses from the top 50μm+ of the slice (Bak et al., 1980).

On the other hand, excessively thick slices are unable to maintain adequate oxygenation and substrate supply which occurs at approximately 500µm. The isolated hippocampal slice is devoid of a functional vascular network and so is dependent upon the superfusing oxygenated buffer for delivery of nutrients and gases, as well as the removal of waste products. Oxygen diffuses into slices at the medium/gas interface in chambers other than the submerged model. A thickness of 400µm, used in this study, represents a suitable distance through which waste products and nutrients can diffuse to preserve function (Tseng et al., 1987).

Slices with nicks, torn or frayed edges, smeared or widened cell fields, or swollen, thick or uneven appearance should be avoided. Though these slices may initially provide acceptable responses, they seldom demonstrate adequate stability resulting in wasted effort (DiScenna, 1987). Slices with smooth edges, a clear translucent appearance with even thickness and crisp well-defined cell fields should be used.

6.1.4.5. Electrode placement

One advantage of slice preparations, over intact structures, is the ability to visualise cell body and afferent fibre zones. Therefore electrode location can be optimised to produce consistent responses and response range. The optimum recording site is half way through the slice.

Many hippocampal afferents terminate in a laminar pattern in the dendritic fields of the pyramidal and granule cells (Steward, 1976; see fig. 6.1). This laminar pattern can be used for consistent

placement of the electrodes thus increasing the probability of studying homogenous afferent populations.

6.2. EXPERIMENTAL METHODS AND APPARATUS

A 2% agar solution was made and allowed to cool before use. A bicarbonate buffer (composed of, mM: NaCl, 124; $NaHCO_3$, 26; KCl, 5; $MgSO_4$, 2; KH_2PO_4, 1.25; $CaCl_2$, 2; glucose, 10) was continuously gassed with 95% oxygen/5% carbon dioxide.

6.2.1. Preparation of hippocampal slices

A male Hooded Listar rat was anaesthetised with diethyl ether and then decapitated. The brain was rapidy removed and placed on a petri dish containing some bicarbonate buffer. The cerebellum was removed and the brain cut sagittally along the longitudinal fasiculus. The neocortex, overlaying the hippocampus, was removed before the tissue was placed on the stage of the vibratome and stuck to an agar block such that the dorsal surface of hippocampus faced the blade and the medial aspect was uppermost. The stage was placed in the vibratome reservoir containing continuously gassed bicarbonate buffer. Slices, 400µm thick, were cut from the dorsal hippocampus which were then separated from the underlying thalamus before being transferred to a recovery bath. The recovery bath contained continuously gassed bicarbonate buffer and the slices remained here for 2 hr to recover electrical activity and overcame the effects of hypoxia (Reid et al., 1984).

6.2.2. Preparation of the apparatus

Meanwhile, the tissue chamber was prepared by continual superfusion with distilled water with the temperature controller set at 32°C. The temperature of 32°C is a compromise between being too high, causing greater metabolic demands on the slice and generating spontaneous activity, and being too low thus reducing metabolic activity (Schiff & Somjen, 1985). The tissue slice is easier to keep alive below 37°C. Once the chamber was at 32°C the distilled water was replaced with continuously gassed bicarbonate buffer at a flow rate of 2ml/min.

The Neurolog equipment, through which the electrical stimulus was administered and the response captured, amplified and displayed on a cathode ray oscilloscope, was switched on to warm up.

A glass micropipette recording electrode was made using a microelectrode puller and filled with 4M NaCl. Only micropipettes with an electrical resistance of 5-10 Ohm were used.

After the 2 hr recovery period a hippocampal slice was placed in the submerged tissue chamber. Using micromanipulators, the recording electrode was placed in the CA1 area and the stimulating electrode (SNEX-200, Clark Electomedical) was placed in the CA2 area (see fig. 6.1).

Stimulation of the CA2 area with square waves of 200-400μA, 0.1-0.2ms produce population potentials of 1-4mV amplitude. It is important not to stimulate the pathway at too high a frequency, otherwise short term potentiation may occur (Schurr et al., 1986). Thus a stimulation frequency of 0.1-0.2Hz was used.

The threshold and maximum stimulus parameters for the production of a population potential were determined and a stimulus current which produced 85-95% of the maximum observed potential was selected.

This waveform was averaged, 8 sweeps per average, every 15 min for 3/4-1 hr to ensure the stability of the recording. Only pyramidal cells with an amplitude of 2-4mV were used in this study. A typical waveform is shown in fig. 6.3, when only bicarbonate buffer was present there was no secondary potential.

6.2.3. Preparation of test drugs

Nicotine (1-100μM) or the AChE inhibitor BW284C51 (1-30μM) were made up in gassed bicarbonate buffer and substituted for the buffer superfusing the tissue slice. The effect of these drugs on the development of a secondary potential was monitored on the oscilloscope and averages were taken every 15 min. Successive concentrations of nicotine or BW284C51 were tested in an accumulative manner by increasing the concentration of the drug in the superfusing buffer, changes in the medium were made after the 15 min averaging. After the drug effects had been determined the response could be returned to normal by replacing the superfusing medium with bicarbonate buffer or the effect of antagonist (DHβE, 10μM; scopolamine, 1μM) could be studied.

6.2.4. Types of measurements obtained

The measurements that can be obtained from a waveform are depicted in fig. 6.3 and are as follows:

1. LATENCY - the time delay between the stimulus and recording the potential, which is determined by the

conduction velocity of the stimulated fibres and the synaptic delay at the pyramidal cells.

2. AMPLITUDE - a function of both the number and the time period over which neurones are activated.
3. INTEGRAL - a more accurate measure of the number of neurones activated since this represents the algebraic sum of the individual cell potentials. It was this measurement that was used to assess the effect of nicotine and other drugs on the hippocampal slice.

6.3. RESULTS AND DISCUSSION

Nicotine (1-100μM) had little or no effect on the amplitude or integral of the primary potential. In only one out of five experiments did 100μM nicotine elicit a slight secondary potential, indicating that nicotine may be effective at higher concentrations. This was supported by Freund et al., (1988) who reported that nicotine elicited a secondary potential at a concentration of 800μM. However, such high concentrations are not thought to be physiologically relevant.

Cole & Nicoll (1983, 1984a, b) and Egan & North (1986) reported that ACh needed the presence of an AChE inhibitor (physostigmine, 1-10μM or neostigmine, 0.1-10μM) to elicit a potential response at concentrations of 1-100μM. If there was no AChE inhibitor present then a 10-100 fold higher ACh concentration was required to achieve the same response.

If the nicotinic effect is presynaptic, enhancing ACh release, as suggested by the superfusion data in this report then ACh hydrolysis by AChE would reduce the nicotine response recorded. Vidal & Changeux (1989) reported that the nicotinic effect of ACh was observed only in the presence of physostigmine (1-10μM). This suggests that an AChE inhibitor is needed in order to study the functional response of drugs at the nAChR. In this study the AChE inhibitor BW284C51 was used.

6.3.1. The effect of BW284C51

Fig. 6.4 shows that the development of a secondary potential increased with BW284C51 concentration. This suggests that BW284C51 is blocking AChE activity resulting in an increase in ACh levels that elicit a secondary potential. At a concentration of 5μM or greater the secondary potential began to decrease and this could be due to a build up of ACh causing a negative feedback on its release via the presynaptic mAChR (see fig. 1.1). Thus ACh is no longer released and so the secondary potential decreases. Alternatively, the reduction in response could be due to receptor desensitisation where the receptor is no longer responsive to the stimulus.

The cholinergic nature of this secondary potential was examined by studying the effect of DHβE (the nAChR antagonist, 10μM) and scopolamine (the mAChR antagonist, 1μM) on the response elicited in the presence of 3μM BW284C51, see fig. 6.4. DHβE (10μM) had little or no effect on the response elicited by 3μM BW284C51. Scopolamine (1μM) completely blocked the production of a secondary potential, suggesting that the postsynaptic effect, recorded in the potential, was purely muscarinic.

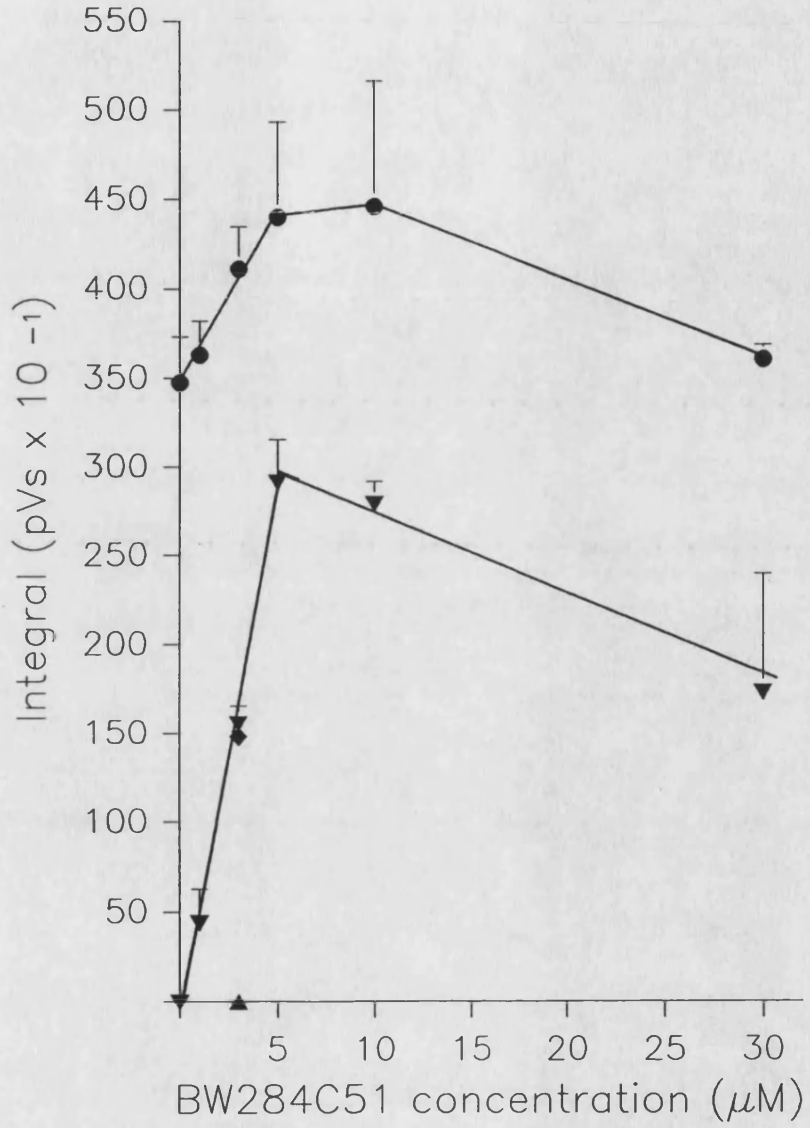

Fig. 6.4. The effect of BW284C51 concentration on the development of a secondary potential. BW284C51 concentration in the superfusing buffer was increased after the 15 min averaging and the integral of the secondary potential was recorded (▼). The effect of DHβE (10μM,◆) and scopolamine (1μM,▲) on this secondary potential was also examined. (●) is the integral of the primary potential. Values are the means ± SEM, n=4.

6.3.2. The effect of nicotine

A BW284C51 concentration of 1μM was used to study the effect of nicotine on ACh release. At this concentration a small secondary potential had developed (fig. 6.4 and 6.5) suggesting the AChE activity had been blocked, increasing ACh levels, but the BW284C51 effects were not too great as to mask the response elicited by nicotine. Section 4.3.3.2. (fig. 4.4a) showed that 1μM BW284C51 was sufficient to block 90% of the AChE activity in the S1 supernatant of the hippocampal homogenate. The S1 supernatant was used as it was more representative of the enzyme activity in the slice than any one of the fractions from the Percoll gradient. Mizobe & Livett (1982), in their study on the effect of AChE inhibitors on the nicotinic response to acetylcholine in cultured adrenal chromaffin cells, showed that 1μM BW284C51 inhibited 85% of AChE activity. Thus the effect of nicotine concentration (1-100μM) on eliciting a secondary potential was studied in the presence of 1μM BW284C51, assuming up to 90% inhibition of AChE activity.

Nicotine, in the presence of BW284C51, showed a dose dependent increase in the secondary potential (fig. 6.5). The effect was approaching maximal at a nicotine concentration of 100μM. DHβE (10μM) completely abolished the nicotine effect indicating that the response was via a nAChR. However, scopolamine (1μM) only reduced the secondary potential by 60%. This was less than expected because if the recorded postsynaptic effect is purely muscarinic then scopolamine should completely block the response elicited by nicotine and BW284C51. Nicotine has been reported to elicit the release of other transmitters: dopamine (Rapier et al., 1988) and GABA

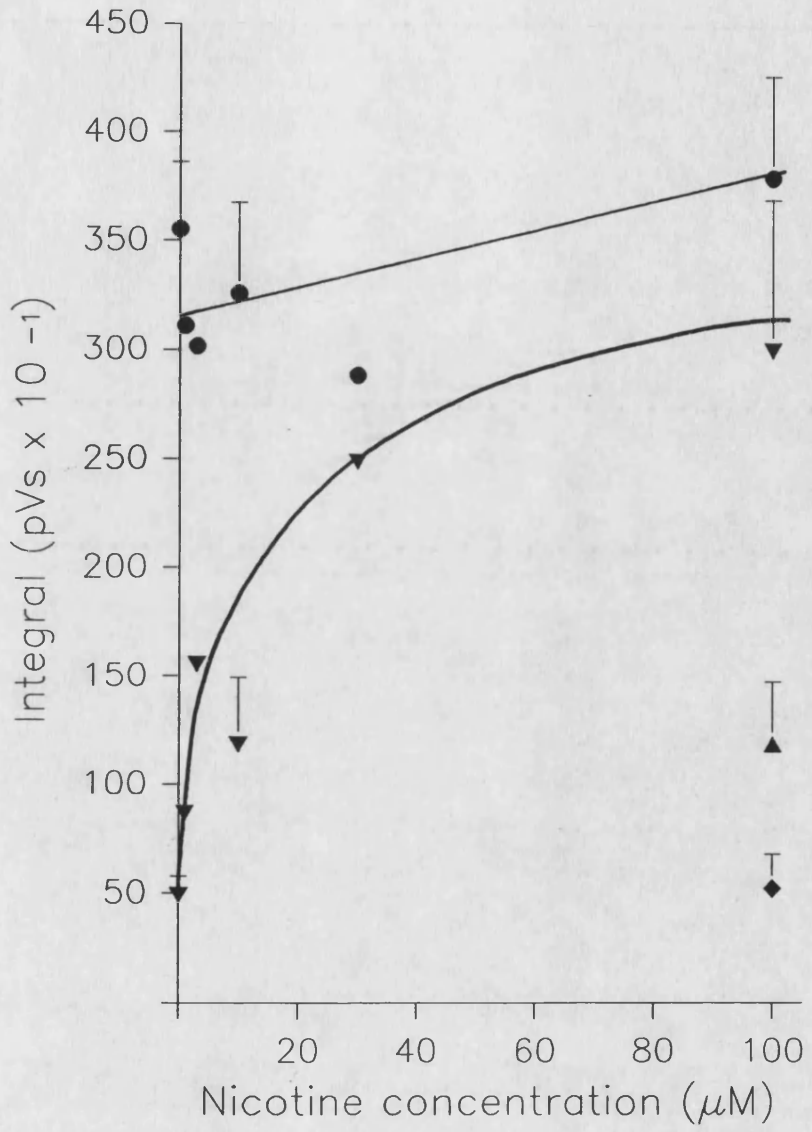

Fig. 6.5. The effect of nicotine concentration on the development of a secondary potential. Nicotine concentration, in the presence of 1μM BW284C51, was increased after the 15 min averaging and the integral of the secondary potential was recorded (▼). The effect of DHβE (10μM,◆) and scopolamine (1μM,▲) on this secondary potential was also examined. (●) is the integral of the primary potential. Values are the mean ± SEM, n=3.

(Wonnacott et al., 1988) and this could account for 40% of the nicotine evoked secondary potential not being blocked by the anticholinergic scopolamine.

6.4. SUMMARY

This preliminary work shows that there is a functionally active nAChR in the hippocampus. Experiments with the AChE inhibitor BW284C51 and the cholinergic antagonists DHβE (nicotinic) and scopolamine (muscarinic) suggest a presynaptic nAChR and a postsynaptic mAChR localisation. The secondary potential measures the postsynaptic changes and the secondary potential produced by BW284C51 was blocked by scopolamine but DHβE had little or no effect, see fig. 6.4. Nicotine enhanced the secondary potential, this enhancement was blocked by DHβE whereas scopolamine had less effect, see fig. 6.5. However, prolonged nicotine stimulation, used in these experiments to construct the concentration curve, has been reported to cause desensitisation of the nAChR in intracellular recordings from rat locus coerulus (Egan & North, 1986) and this could explain the lack of a postsynaptic nAChR effect.

Extended nicotine stimulation, in the superfusion buffer, of the electrophysiological work was necessary to ensure complete diffusion of the drug through the slice. Long washout periods are also required (1-2 hr) to ensure that all the drug has been removed and so repetitive stimulations, returning to baseline between each drug administration, are not easily achieved. Superfusion experiments with synaptosomes need only short drug stimulations, 20s, as the preparation is considered to be a monolayer in the chamber. Repetitive stimulations are easier to administer to synaptosomes as

response returns to baseline 10-20 min after the drug pulse. However, synaptosomes have no neuronal interconnections which are present in the slice and so are less representative of in vivo responses.

Further experiments to fully characterise this nicotinic response are needed and the use of agonists and antagonists for other transmitters would ascertain whether the development of the secondary potential is only via cholinergic receptors.

APPENDIX: CHEMICAL STRUCTURES

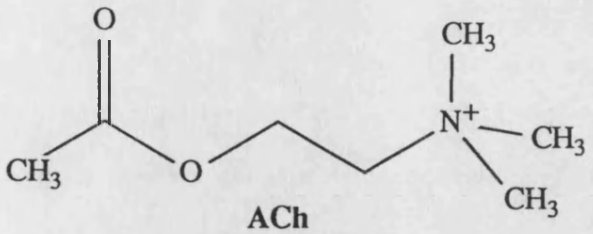

ACh
ACETYLCHOLINE

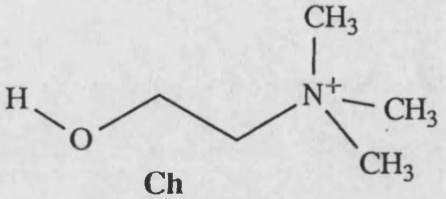

Ch
CHOLINE

AGONISTS

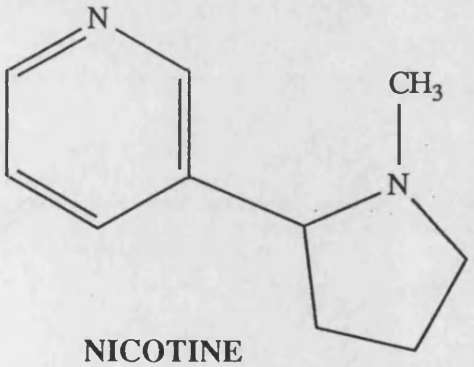

NICOTINE

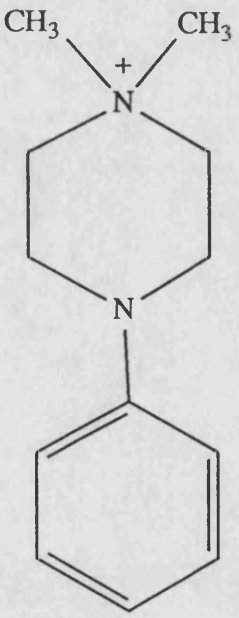

DMPP
1,1-DIMETHYL-4-PHENYL-PIPERAZINIUM

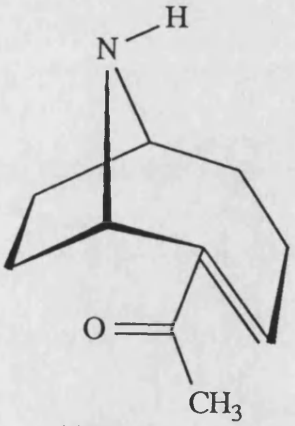

ANTX
ANATOXIN-A

ANTAGONISTS

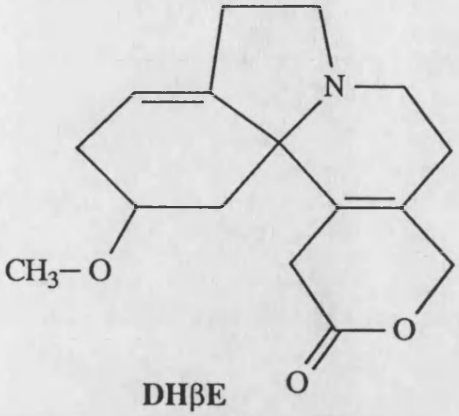

DHβE
DIHYDROβERYTHROIDINE
(NICOTINIC)

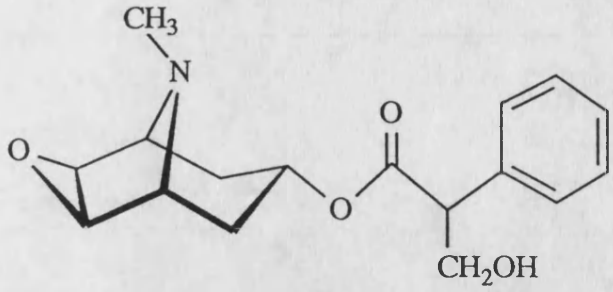

SCOPOLAMINE
(MUSCARINIC)

ACETYLCHOLINESTERASE INHIBITORS

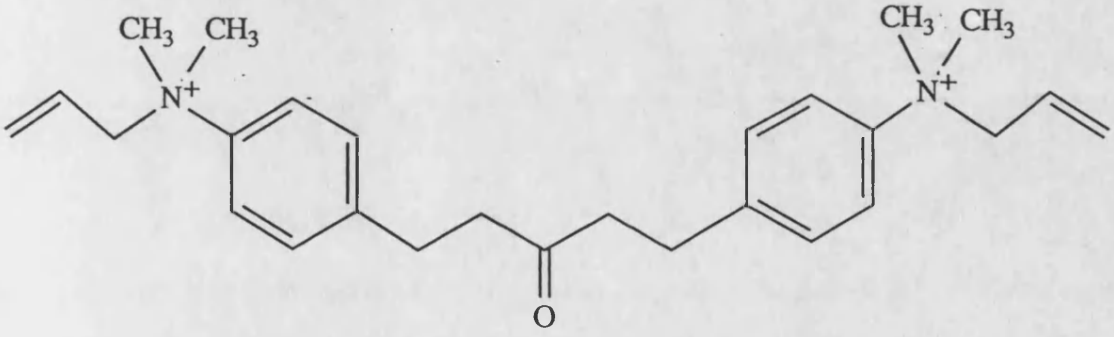

BW284C51
1,5-BIS (4-ALLYLDIMETHYLAMMONIUM PHENYL) PENTAN-3-ONE

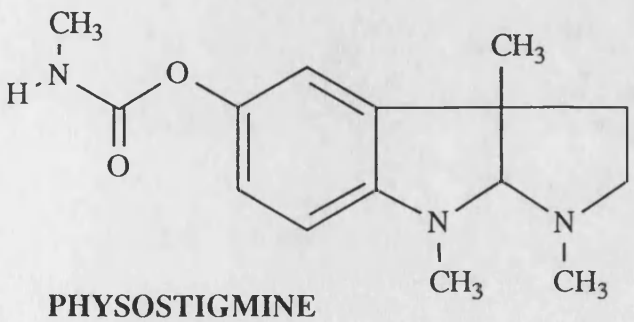

PHYSOSTIGMINE
(ESERINE)

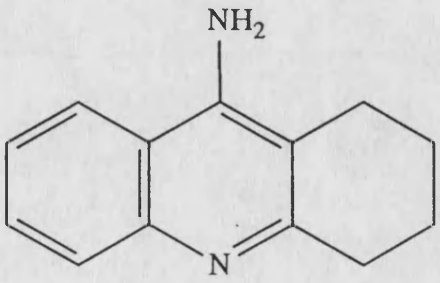

THA
9-AMINO-1,2,3,4-
TETRAHYDROACRIDINE

CHOLINE ACETYLTRANSFERASE INHIBITOR

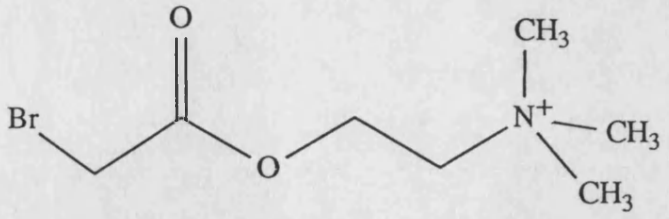

BrACh
BROMOACETYLCHOLINE

CHOLINE UPTAKE INHIBITOR

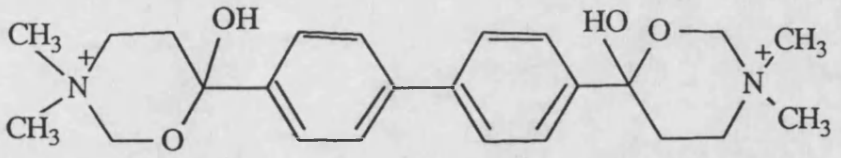

HC-3
HEMICHOLINIUM-3

PUBLICATIONS

Lunt, G., Wonnacott, S., Thorne, B., Rapoport, H., Aracava, Y. & Albuquerque, E.X. (1987). Anatoxin-a acts at central nicotinic acetylcholine receptors. SOC. NEUROSCI., 13, 260.13.

Thorne, B., Irons, J., Lunt, G.G., Wonnacott, S. & Dunkley, P.R. (1988). Comparison of methods for rapid isolation of synaptosomes from brain regions for uptake and release studies. BIOCHEM. SOC. TRANS., 16, 309-310.

Wonnacott, S., Irons, J., Rapier, C., Thorne, B. & Lunt, G.G. (1989). Presynaptic modulation of transmitter release by nicotinic receptors. In: Nicotinic receptors in the CNS - their role in synaptic transmission. PROG. BRAIN RES., 79, (Nordberg, A., Fuxe, K., Holmstedt, B. & Sundwall, A., eds). Elsevier, Amsterdam. pp 157-163.

REFERENCES

Abdel-Latif, A.A. (1966). A simple method for isolation of nerve ending particles from rat brain. BIOCHIM. BIOPHYS. ACTA, 121, 403-406.

Adolfsson, R., Gottfries, C.G., Roos, B.E. & Winblad, B. (1979). Changes in the brain catecholamines in patients with dementia of Alzheimer type. BRIT. J. PSYCHIAT., 135, 216-223.

Alzheimer, A. (1907). Uber eine eigenartige Erkrankung der Hirnrinde. ALLG. Z. PSYCHIATR. PSYCH. GERICHTL. MED., 64, 146-148.

Anonymous (1987). Cholinergic treatment in Alzheimer's disease: encouraging results. LANCET, 1, 139-141.

Aracava, Y., Deshpande, S.S., Swanson, K.L., Rapoport, H., Wonnacott, S., Lunt, G. & Albuquerque, E.X. (1987). Nicotinic acetylcholine receptors in cultured neurons from the hippocampus and brain stem of the rat characterised by single channel recording. FEBS Lett., 22, 63-70.

Arantius, J.C. (1587). De humano foetu .... Ejusdem anatomicorum observationum liber, Venetiis, pp 44-45. (As translated by Meaker, S.R., Department of Anatomy, Harvard Medical School, USA).

Atweh, S., Simon, J.R. & Kuhar, M.J. (1975). Utilisation of sodium-dependent high affinity choline uptake in vitro as a measure of the activity of cholinergic neurons in vivo. LIFE SCI., 17, 1535-1544.

Augustinsson, K.-B. & Grahn, M. (1953). The separation of choline esters by paper chromatography. ACTA CHEM. SCAND., 7, 906-912.

Autilo, L.A., Appel, S.H., Pettis, P. & Gambetti, P.L. (1968). Biochemical studies of synaptosomes in vitro. 1. Protein synthesis. BIOCHEM., 7, 2615-2622.

Bak, I.J., Misgeld, U., Weiler, M. & Morgan, E. (1980). The preservation of nerve cells in rat neostriatal slices maintained in vitro: a morphological study. BRAIN RES., 197, 341-353.

Barker, L.A. & Mittag, T.W. (1975). Comparative studies of substrates and inhibitors of choline transport and choline acetyltransferase. J. PHARMACOL. EXP. THER., 192, 86-94.

Barnard, E.A. & Dolly, J.O. (1982). Peripheral and central nicotinic acetylcholine receptors - how similar are they? TRENDS NEUROSCI., 5, 325-327.

Bartus, R., Dean, R., Beer, B. & Lippa, A. (1982). The cholinergic hypothesis of geriatric memory dysfunction. SCI. (USA), 17, 408-417.

Benishun, C.G. & Carroll, P.T. (1981). Acetylation of choline and homocholine by membrane-bound choline-o-acetyltransferase in mouse forebrain nerve endings. J. NEUROCHEM., 36, 732-740.

Benjamin, A.M. & Quastel, J.H. (1981). Acetylcholine synthesis in synaptosomes: mode of transfer of mitochondrial acetyl coenzyme A. SCI. (USA), 213, 1495-1497.

Berridge, M.J. & Irvine, R.F. (1984). Inositol triphosphate, a novel second messenger in cellular signal transduction. NATURE (LOND.), 312, 315-321.

Bird, S.J. & Aghajanian, G.K. (1976). The cholinergic pharmacology of hippocampal pyramidal cells: a microiontophoretic study. NEUROPHARMACOL., 15, 273-282.

Birdsall, N.J.M. & Hulme, E.C. (1987). Characterisation of muscarinic acetylcholine receptors and their subtypes. ISI ATLAS OF SCIENCE PHARMACOL., pp 98-100.

Birdsall, N.J.M., Burgen, A.S.V. & Hulme, E.C. (1979). A study of the muscarinic receptor by gel electrophoresis. BR. J. PHARMAC., 66, 337-342.

Bliss, T.V.P. & Lynch, M.A. (1988). Long-term potentiation of synaptic transmission in the hippocampus: properties and mechanisms. NEUROL. NEUROBIOL., 35, 3-72.

Bliss, T.V.P., Douglas, R.M., Errington, M.L. & Lynch, M.A. (1986). Correlation between long-term potentiation and release of endogenous amino acids from dentate gyrus of anaesthetised rats. J. PHYSIOL. (LOND.), 377, 391-408.

Bogdanski, D.F., Blaszkowski, T.P. & Tissari, A.H. (1970). Mechanisms of biogenic amine transport and storage IV. Relationship between K^+ and the Na^+ requirement for transport and storage of 5-hydroxytryptamine and norepinephrine in synaptosomes. BIOCHIM. BIOPHYS. ACTA, 11, 521-532.

Bondareff, W., Mountjoy, C.Q. & Roth, M. (1981). Selective loss of neurones of origin of adrenergic projection to cerebral cortex (nucleus coerulus) in senile dementia. LANCET, 1, 783-784.

Boulter, J., Evans, K., Goldman, D., Martin, G., Treco, D., Heinemann, S. & Patrick, J. (1986). Isolation of a cDNA clone coding for a possible neural nicotinic acetylcholine receptor α-subunit. NATURE (LOND.), 319, 368-374.

Bourne, H.R. (1986). One molecular machine can translate diverse signals. NATURE (LOND.), 321, 814-816.

Bowen, D.M. & Davison, A.N. (1986). Biochemical studies of nerve cells and energy metabolism in Alzheimer's disease. BRIT. MED. BULL., 42, 75-80.

Bowen, D.M. & Marek, K.L. (1982). Evidence for the pharmacological similarity between the presynaptic muscarinic autoreceptor and postsynaptic muscarinic receptors. BR. J. PHARMAC., 75, 367-372.

Bradley, P.B. & Lucy, A.P. (1983). Cholinoceptive properties of respiratory neurones in the rat medulla. NEUROPHARMACOL., 22, 853-858.

Breitweiser, G.E. & Szabo, G. (1985). Uncoupling of cardiac muscarinic and β adrenergic receptors from ion channels by guanine nucleotide analogue. NATURE (LOND.), 317, 538-540.

Briggs, C.A. & Cooper, J.R. (1982). Cholinergic modulation of the release of [^{3}H]acetylcholine from synaptosomes of the myenteric plexus. J. NEUROCHEM., 38, 501-508.

Burgess, E.J. & Prince, A.K. (1977). Effect of reserpine on choline acetyltransferase and high affinity choline uptake in the rat brain. BR. J. PHARMAC., 60, 301P-302P.

Candy, J.M., Klinowski, J., Perry, R.H., Perry, E.K., Fairbairn, A., Oakley, A.E., Carpenter, T.A., Atack, J.R., Blessed, G. & Edwardson, J.A. (1986). Aluminosilicates and senile plaque formation in Alzheimer's disease. LANCET, 1, 354-357.

Carmichael, W.W., Biggs, D.F. & Gorham, P.R. (1975). Toxicology and pharmacological action of Anabaena flos-aquae toxin. SCI. (USA), 187, 542-544.

Changeux, J.-P., Devillers-Thiery, A. & Chemouilli, P. (1984). Acetylcholine receptor: an allosteric protein. SCI. (USA), 225, 1335-1345.

Changeux, J.-P., Giraudat, J. & Dennis, M. (1987). The nicotinic acetylcholine receptor: molecular architecture of a ligand-regulated ion channel. TRENDS PHARMACOL. SCI., 8, 459-465.

Chiou, C.-Y. & Sastry, B.V.R. (1968). Acetylcholinesterase hydrolysis of halogen substituted acetylcholines. BIOCHEM. PHARMACOL., 17, 805-815.

Christie, J.E., Shering, A., Ferguson, J. & Glen, A.I.M. (1981). Physostigmine and arecholine: effects of intravenous infusions in Alzheimer presenile dementia. BRIT. J. PSYCHIAT., 138, 46-50.

Christie, M.J. & North, R.A. (1988). Control of ion conductances by muscarinic receptors. TRENDS PHARMACOL. SCI., 9 (Suppl), 30-34.

Chronister, R.B. & Whyte, L.E. Jr. (1975). Fiberarchitecture of the hippocampal formation: anatomy projections and structural significance. In: The Hippocampus (Isaacson, R.L. & Pribham, K.H., eds.) Plenum Press, New York, pp 9-39.

Clarke, P.B.S., Pert, C.B. & Pert, A. (1984). Autoradiographic distribution of nicotine receptors in rat brain. BRAIN RES., 323, 390-395.

Clarke, P.B.S., Schwartz, R.D., Paul, S.M., Pert, C.B. & Pert, A. (1985). Nicotine binding in rat brain: autoradiographic comparison of [^{3}H]acetylcholine, [^{3}H]nicotine and [^{125}I]αbungarotoxin. J. NEUROSCI., 5, 1307-1315.

Cole, A.E. & Nicoll, R.A. (1983). Acetylcholine mediates a slow synaptic potential in hippocampal pyramid cells. SCI. (USA), 221, 1299-1301.

Cole, A.E. & Nicoll, R.A. (1984a). The pharmacology of cholinergic excitatory responses in hippocampal pyramidal cells. BRAIN RES., 305, 283-290.

Cole, A.E. & Nicoll, R.A. (1984b). Characterisation of a slow cholinergic postsynaptic potential recorded in vitro from rat hippocampal pyramidal cells. J. PHYSIOL. (LOND.), 352, 173-188.

Consolo, S., Wang, J.-X., Fusi, R., Vinci, R., Forloni, G. & Ladinsky, H. (1984). In vitro and in vivo evidence for the existence of presynaptic muscarinic cholinergic receptors in the rat hippocampus. BRAIN RES., 309, 147-151.

Conti-Tronconi, B.M. & Raftery, M.A. (1982). The nicotinic cholinergic receptor: correlation of molecular structure with functional properties. ANN. REV. BIOCHEM., 51, 491-530.

Conti-Tronconi, B.M., Dunn, S.M.J., Barnard, E.A., Dolly, J.O., Lai, F.A., Ray, N. & Raftery, M.A. (1985). Brain and muscle nicotinic acetylcholine receptors are different but homologous proteins. PROC. NAT. ACAD. SCI. (USA), 82, 5208-5212.

Corkin, S. (1981). Acetylcholine, aging and Alzheimer's disease: implications for treatment. TRENDS NEUROSCI., 4, 287-290.

Cotman, C.W. & Matthews, D.A. (1971). Synaptic plasma membranes from rat brain synaptosomes: isolation and partial characterisation. BIOCHIM. BIOPHYS. ACTA, 249, 380-394.

Coyle, J.T., Price, D.L. & DeLong, M.R. (1983). Alzheimer's disease: a disorder of cortical cholinergic innervation. SCI. (USA), 219, 1184-1190.

Coyle, J.T., Price, D. & DeLong, M. (1984). Anatomy of cholinergic projections to cerebral cortex: implications for the pathophysiology of senile dementia of the Alzheimer's type. TRENDS PHARMACOL. SCI., 5 (Suppl.), 90-93.

Crosland, R.D., Martin, J.V. & McClure, W.O. (1983). Effect of liposomes containing various divalent cations on the release of acetylcholine from synaptosomes. J. NEUROCHEM., 40, 681-687.

Cross, A.J., Crow, T.I., Perry, E.K., Perry, R.H., Blessed, G. & Tomlinson, B.E. (1981). Reduced dopamine-beta-hydroxylase activity in Alzheimer's disease. BRIT. MED. J., 282, 93-94.

Cross, A.J., Crow, T.J., Johnson, J.A., Joseph, M.H., Perry, E.K., Perry R.H., Blessed, G. & Tomlinson, B.E. (1983). Monoamine metabolism in senile dementia of Alzheimer type. J. NEUROL. SCI., 60, 383-392.

Cunnane, T.C. (1984). The mechanism of neurotransmitter release from sympathetic nerves. TRENDS NEUROSCI., 7, 248-253.

Dale, H.H. (1914). The action of certain esters and ethers of choline and their relation to muscarine. J. PHARMACOL. EXP. THER., 6, 147-190.

Dani, J.A. (1989). Site-directed mutagenesis and single-channel currents define the ionic channel of the nicotinic acetylcholine receptor. TRENDS NEUROSCI., 12, 125-128.

Davies, K.L. & Mohs, R.C. (1982). Enhancement of memory processes in Alzheimer's disease with multiple-dose intravenous physostigmine. AM. J. PSYCHIATRY, 139, 1421-1424.

Davies, P. & Verth, A.H. (1978). Regional distribution of muscarinic acetylcholine receptor in normal and Alzheimer's-type dementia brains. BRAIN RES., 138, 385-392.

Davies, K.L., Mohs, R.C., Tinklenberg, J.R., Pfefferbaum, A., Hollister, L.E. & Kopell, B.S. (1978). Physostigmine: improvement of long-term memory processes in normal humans. SCI. (USA), 201, 272-274.

Davies, P., Katzman, R. & Terry, R.D. (1980). Reduced somatostatin-like immunoreactivity in cerebral cortex from cases of Alzheimer disease and Alzheimer senile dementia. NATURE (LOND.), 288, 279-280.

Davies, S.N., Lester, R.A.J., Reymann. K.G. & Collingridge, G.L. (1989). Temporally distinct pre- and post-synaptic mechanisms maintain long term potentiation. NATURE (LOND.), 338, 500-503.

Day, E.D., McMillen, P.N., Mickey, D.D. & Appel, S.H. (1971). Zonal centrifuge profiles of rat brain homogenates: instability in sucrose, stability in isoosmotic Ficoll/sucrose. ANAL. BIOCHEM., 39, 29-45.

DeBelleroche, J.S. & Bradford, H.F. (1973). The synaptosome: an isolated working, neuronal compartment. PROG. NEUROBIOL. 1, 275-305

DeBelleroche, J.S. & Bradford, H.F. (1980). Presynaptic control of the synthesis and release of dopamine from striatal synaptosomes: a comparison between the effects of 5-hydroxytryptamine, acetylcholine and glutamate. J. NEUROCHEM., 35, 1227-1234.

Deneris, E.S., Connolly, J., Boulter, J., Wada, E., Wada, K., Swanson, L.W., Patrick, J. & Heinemann, S. (1988). Primary structure and expression of β_2: a novel subunit of neuronal nicotinic acetylcholine receptors. NEURON, 1, 45-54.

DeRobertis, E., Pellegrino de Iraldi, A., Rodriguez de Lores Arnaiz, G. & Salganicoff, L. (1962). Cholinergic and non-cholinergic nerve endings in rat brain. Isolation and subcellular distribution of acetylcholine and acetylcholinesterase. J. NEUROCHEM., 9, 23-35.

DiScenna, P. (1987). Method and myth in maintaining brain slices. In: Brain slices: fundamentals, applications and implications. (Schurr, A., Teyler, T.J. & Tseng, M.T., eds.) Karger, Basel, pp 10-21.

Dowdall, M.J. & Simon, E.J. (1973). Comparative studies on synaptosomes: uptake of [N-Me-^{3}H]choline by synaptosomes from squid optic lobes. J. NEUROCHEM., 21, 969-982.

Dunant, Y. (1986). On the mechanism of acetylcholine release. PROG. NEUROBIOL., 26, 55-92.

Dunkley, P.R., Rostas, J.A.P., Heath, J.W. & Powis, D.A. (1987). The preparation and use of synaptosomes for studying secretion of catecholamines. In: The Secretory Process, 3, In vitro methods for studying secretion. (Poisner, A. & Trifaro, J.M., eds.) Elsevier, Amsterdam, pp 315-334.

Dunkley, P.R., Heath, J.W., Harrison, S.M., Jarvie, P.E., Glenfield, P.J. & Rostas, J.A.P. (1988). A rapid Percoll gradient procedure for isolation of synaptosomes directly from an S1 fraction: homogeneity and morphology of subcellular fractions. BRAIN RES., 441, 59-71.

Eccles, J.C., Fatt, P. & Koketsu, K. (1954). Cholinergic and inhibitory synapses in a pathway from motor-axon collaterals to motoneurones. J. PHYSIOL. (LOND.), 126, 524-562.

Eckenstein, F. & Sofroniew, M.V. (1983). Identification of central cholinergic neurons containing both choline acetyltransferase and acetylcholinesterase and of central neurons containing only acetylcholinesterase. J. NEUROSCI., 3, 2286-2291.

Egan, T.M. & North, R.A. (1986). Actions of acetylcholine and nicotine on rat locus coerulus neurons in vitro. NEUROSCI., 19, 565-571.

Eisenthal, R. & Cornish-Bowden, A. (1974). The direct linear plot. A new graphical procedure for estimating enzyme kinetic parameters. BIOCHEM. J., 139, 715-720.

Ellman, G.L., Courtney, K.D., Andres, V. Jr. & Featherstone, R.M. (1961). A new and rapid colorimetric determination of acetylcholinesterase activity. BIOCHEM. PHARMACOL., 7, 88-95.

Endemann, G. & Brunengraber, H. (1980). The source of acetyl coenzyme A for acetylcholine synthesis in the perfused rat phrenic nerve hemi-diaphragm. J. BIOL. CHEM., 255, 11091-11093.

Eterovic, V.A. & Bennett, E.L. (1974). Nicotinic cholinergic receptor in brain detected by binding of $\alpha[^{3}H]$bungarotoxin. BIOCHIM. BIOPHYS. ACTA, 362, 346-355.

Flynn, D.D. & Mash, D.C. (1986). Characterisation of L-[^{3}H]nicotine binding in human cerebral cortex: comparison between Alzheimer's disease and the normal. J. NEUROCHEM., 47, 1948-1954.

Fonnum, F. (1967). The "compartmentation" of choline acetyltransferase within the synaptosome. BIOCHEM. J., 103, 262-270.

Fonnum, F. (1969). Isolation of choline esters from aqueous solutions by extraction with sodium tetraphenylboron in organic solvents. BIOCHEM. J., 113, 291-298.

Fonnum, F. (1975). A rapid radiochemical method for the determination of choline acetyltransferase. J. NEUROCHEM., 24, 407-409.

Foy, M.R., Stanton, M.E., Levine, S. & Tompson, R.F. (1985). Stress impairs long term potentiation in rodent hippocampus. SOC. NEUROSCI. ABSTR., 11, A225.18.

Freund, R.K., Jungschaffer, D.A., Collins, A.C. & Wehner, J.M. (1988). Evidence for modulation of GABAergic neurotransmission. BRAIN RES., 453, 215-221.

Fried, R.C. & Blaustein, M.P. (1978). Retrieval and recycling of synaptic vesicle membrane in pinched-off nerve terminals (synaptosomes). J. CELL BIOL., 78, 685-700.

Gil, D.W. & Wolfe, B.B. (1986). Pirenzepine distinguishes between muscarinic receptor-mediated phosphoinositide breakdown and inhibition of adenylate cyclase. J. PHARMACOL. EXP. THER., 232, 608-616.

Gilman, A.G. (1984). G proteins and dual control of adenylate cyclase. CELL, 36, 577-579.

Goldberg, A.M. & McCaman, R.E. (1973). The determination of picomole amounts of acetylcholine in mammalian brain. J. NEUROCHEM., 20, 1-8.

Goldman, D., Deneris, E., Luyton, W., Kochhar, A., Patrick, J. & Heinemann, S. (1987). Members of a nAChR gene family are expressed in different regions of the mammalian CNS. CELL, 48, 965-973.

Gray, E.G. & Whittaker, V.P. (1962). The isolation of nerve endings from brain. An electron microscopic study of cell fragments divided by homogenisation and centrifugation. J. ANAT. (LOND.), 96, 79-88.

Grewaal, D.S. & Quastel, J.H. (1973). Control of synthesis and release of radioactive acetylcholine in brain slices from the rat: effects of neurotrophic drugs. BIOCHEM. J., 132, 1-14.

Guy, H.R. (1984). A structural model of the acetylcholine receptor channel based on partition energy and helix packing calculations. BIOPHYS. J., 45, 249-261.

Guy, H.R. & Hucho, F. (1987). The ion channel of the nicotinic acetylcholine receptor. TRENDS NEUROSCI., 10, 318-321.

Guyenet, P., Lefresne, P., Rossier, J., Beaujouan, J.C. & Glowinski, J. (1973). Inhibition by hemicholinium-3 of [^{14}C]acetylcholine synthesis and [^{3}H]choline high-affinity uptake in rat striatal synaptosomes. MOL. PHARMACOL., 9, 630-639.

Guyenet, P.G., Lefresne, P., Beaujouan, J.C. & Glowinski, J. (1975). The role of newly taken up choline in the synthesis of acetylcholine in rat striatal synaptosomes. In: Cholinergic Mechanisms. (Waser, P.G. ed.) Raven Press, New York, pp 137-144.

Haas, H.L. (1982). Cholinergic disinhibition in hippocampal slices of the rat. BRAIN RES., 233, 200-204.

Hadhazy, P. & Szerb, J.C. (1977). The effect of cholinergic drugs on [^{3}H]acetylcholine release from slices of rat hippocampus, striatum and cortex. BRAIN RES., 123, 311-322.

Haga, K. & Haga, T. (1985). Purification of the muscarinic acetylcholine receptor from porcine brain. J. BIOL. CHEM., 260, 7927-7935.

Haga, T. & Noda, H. (1973). Choline uptake systems of rat brain synaptosomes. BIOCHIM. BIOPHYS. ACTA, 291, 564-575.

Hall, Z.W. (1987). Three of a kind: the β adrenergic receptor, the muscarinic acetylcholine receptor and rhodopsin. TRENDS NEUROSCI., 10, 99-101.

Hammer, R. & Giachetti, A. (1982). Muscarinic receptor subtypes: M_1 and M_2 biochemical and functional characterisation. LIFE SCI., 31, 2991-2998.

Hammer, R., Berrie, C.P., Birdsall, N.J.M., Burgen, A.S.V. & Hulme, E.C. (1980). Pirenzepine distinguishes between different subclasses of muscarinic receptors. NATURE (LOND.), 283, 90-92.

Hardy, J., Adolfsson, R., Alafuzoff, I., Bucht, G., Marcusson, J., Nyberg, P., Perdahl, E., Wester, P. & Winblad, B. (1985). Transmitter deficits in Alzheimer's disease. NEUROCHEM. INT., 7, 545-563.

Harris, K.M. & Teyler, T.J. (1983). Age differences in a circadian influence on hippocampal LTP. BRAIN RES., 261, 69-73.

Heaton, G.M. & Bachelard, H.J. (1973). The kinetic properties of hexose transport into synaptosomes from guinea pig cerebral cortex. J. NEUROCHEM., 21, 1099-1108.

Hemsworth, B.A. & Morris, D. (1964). A comparison of the N-alkyl group specificity of choline acetyltransferase from different species. J. NEUROCHEM., 11, 793-803.

Henke, H. & Lang, W. (1983). Cholinergic enzymes in neocortex, hippocampus and basal forebrain of non-neurological and senile dementia of Alzheimer-type patients. BRAIN RES., 267, 281-291.

Hollander, E., Mohs, R.C. & Davis, K.L. (1986). Cholinergic approaches to the treatment of Alzheimer's disease. BRIT. MED. BULL., 42, 97-100.

Hulme, E.C., Birdsall, N.J.M., Burgen, A.S.V. & Metha, P. (1978). The binding of antagonists to brain muscarinic receptors. MOL. PHARMACOL., 14, 737-750.

Hunt, S. & Schmidt, J. (1979). The relationship of αbungarotoxin binding activity and cholinergic termination within the rat hippocampus. NEUROSCI., 4, 585-592.

Hunter, A.J., Murray, T.K., Jones, J.A., Cross, A.J. & Green, A.R. (1989). The cholinergic pharmacology of tetrahydroaminoacridine in vivo and in vitro. BR. J. PHARMACOL., 98, 79-86.

Hyman, B.T., van Hoesen, G.W., Damasio, A.R. & Barnes, C.L. (1984). Alzheimer's disease: cell specific pathology isolates the hippocampal formation. SCI. (USA), 225, 1168-1170.

Johnson, M.K. (1960). The intracellular distribution of glycolytic and other enzymes in rat brain homogenates and brain mitochondrial preparations. BIOCHEM. J., 77, 610-618.

Johnson, M.K. & Whittaker, V.P. (1963). Lactate dehydrogenase as a cytoplasmic marker in brain. BIOCHEM. J., 88, 404-409.

Jope, R.S. (1979). High affinity choline transport and acetyl CoA production in brain and their roles in the regulation of acetylcholine synthesis. BRAIN RES. REV., 1, 313-344.

Kang, J., Lemaire, H.-G., Unterbeck, A., Salbaum, J.M., Masters, C.L., Grzeschick, K.-H., Multhaup, G., Beyreuther, K. & Muller-Hill, B. (1987). The precursor of Alzheimer's disease amyloid A4 protein resembles a cell-surface receptor. NATURE (LOND.), 325, 733-736.

Karlin, A., Kao, P.N. & DiPaola, M. (1986). Molecular pharmacology of the nicotinic acetylcholine receptor. TRENDS PHARMACOL. SCI., 7, 304-308.

Kasa, P. & Morris, D. (1972). Inhibition of choline acetyltransferase and its histochemical localisation. J. NEUROCHEM., 19, 1299-1304.

Kauer, J.A., Malenka, R.C. & Nicoll, R.A. (1988). NMDA application potentiates synaptic transmission in the hippocampus. NATURE (LOND.), 334, 250-252.

Kellar, K.J., Whitehouse, P.J., Martino-Barrows, A.M., Marcus, K. & Price, D.L. (1987). Muscarinic and cholinergic binding sites in Alzheimer's disease cerebral cortex. BRAIN RES., 436, 62-68.

Kerlavage, A.R., Fraser, C.M. & Venter, J.C. (1987). Muscarinic cholinergic receptor structure: molecular biological support for subtypes. TRENDS PHARMACOL. SCI., 8, 426-431.

Koelle, G.B. (1955). The histochemical identification of acetylcholinesterase in cholinergic, adrenergic and sensory neurons. J. PHARMACOL. EXP. THER., 114, 167-184.

Kokmen, E. (1984). Dementia-Alzheimer type. MAYO. CLIN. PROC., 59, 35-42.

Krnjevic, K. (1974). Chemical nature of synaptic transmission in vertebrates. PHYSIOL. REV., 54, 418-540.

Kunysz, E.L., Michel, A.D. & Whiting, R.L. (1988). Functional and direct binding studies using subtype selective muscarinic receptor antagonists. BR. J. PHARMACOL., 93, 491-500.

Kurokawa, M.T., Sakamoto, M.T. & Kato, M. (1965). Distribution of sodium-plus-potassium-stimulated adenosine-triphosphatase activity in isolated nerve-ending particles. BIOCHEM. J., 97, 833-844.

Lagercrantz, H. & Pertoft, H. (1972). Separation of catecholamine storing synaptosomes in colloidal silica density gradients. J. NEUROCHEM., 19, 811-823.

Lang, W. & Henke, H. (1983). Cholinergic receptor binding and autoradiography in brains of non-neurological and senile dementia of Alzheimer-type patients. BRAIN RES., 267, 271-280.

Lapchak, P.A., Araujo, D.M., Quirion, R. & Collier, B. (1989). Effect of chronic nicotine treatment on nicotinic autoreceptor function and N-[^{3}H]methylcarbamylcholine binding sites in the rat brain. J. NEUROCHEM., 52, 483-491.

Lefresne, P., Beaujouan, J.C. & Glowinski, J. (1978). Origin of the acetyl moiety in rat striatal synaptosomes: a specific pyruvate dehydrogenase involved in ACh synthesis? BIOCHIMIE, 60, 479-487.

Lehmann, J. & Fibiger, H.C. (1979). Acetylcholinesterase and the cholinergic neuron. LIFE SCI., 25, 1939-1947.

Lewis, P.R., Shute, C.C.D. & Silver, A. (1967). Confirmation from choline acetylase of a massive cholinergic innervation to the rat hippocampus. J. PHYSIOL. (LOND.), 191, 215-224.

Loring, R.H. & Zigmond, R.E. (1988). Characterisation of neuronal nicotinic receptors by snake venom neurotoxins. TRENDS NEUROSCI., 11, 73-78.

Lowry, A., Rosebrough, N.J., Farr, A.L. & Randall, R.J. (1951). Protein measurement with the Folin phenol reagent. J. BIOL. CHEM., 193, 265-275.

Lynch, G. & Baudry, M. (1984). The biochemistry of memory: a new and specific hypothesis. SCI. (USA), 224, 1057-1063.

MacAllan, D.R.E., Lunt, G.G., Wonnacott, S., Swanson, K., Rapoport, H. & Albuquerque, E.X. (1988). Methyllycaconitine and anatoxin-a differentiate between nicotinic receptors in vertebrate and invertebrate nervous systems. FEBS lett., 226, 357-363.

MacIntosh, F.C. & Collier, B. (1976). Neurochemistry of cholinergic terminals. In: Handbook of Exptl. Pharmacol., 42, The neuromuscular junction. (Zaimis, E. ed.), Springer Verlag, Heidelberg, pp 99-228.

Malinow, R., Madison, D.V. & Tsien, R.W. (1988). Persistent protein kinase activity underlying long-term potentiation. NATURE (LOND.), 335, 820-824.

Mann, D.M.A., Lincoln, J., Yates, P.O., Stamp, J.E. & Toper, S. (1980). Changes in the monoamine containing neurones of the human CNS in senile dementia. BRIT. J. PSYCHIAT., 136, 533-541.

Marchbanks, R.M. (1967). Osmotically sensitive potassium and sodium compartments of synaptosomes. BIOCHEM. J., 104, 148-157.

Marchbanks, R.M. (1982). Biochemistry of Alzheimer's dementia. J. NEUROCHEM., 39, 9-14.

Marchbanks, R.M. & Israel, M. (1971). Aspects of acetylcholine metabolism in the electric organ of Torpedo marmorata. J. NEUROCHEM., 18, 439-448.

Marchi, M., Paudice, P. & Raiteri, M. (1981). Autoregulation of acetylcholine release in isolated hippocampal nerve endings. EUR. J. PHARMACOL., 73, 75-79.

Marchi, M., Paudice, P. & Raiteri, M. (1983). Choline uptake, acetylcholine synthesis and regulation of acetylcholine release through autoreceptors in the aging rat cortex. In: Aging of the Brain, 22, (Samuel, D., Algeri, S., Gershon, S., Grimm, V.E. & Toffano, G., eds.) Raven Press, New York, pp 191-195.

Markwell, M.A.K., Haas, S.M., Bieber, L.L. & Tolbert, N.E. (1978). A modification of the Lowry procedure to simplify protein determination in membrane and lipoprotein samples. ANAL. BIOCHEM., 87, 206-210.

Marinozzi, V. (1963). The role of fixation in electron staining. J. ROYAL MICROSCOPICAL SOC., 81, 141-154.

Mash, D.C., Flynn, D.D. & Potter, L.T. (1985). Loss of M_2 muscarine receptors in the cerebral cortex in Alzheimer's disease and experimental cholinergic denervation. SCI. (USA), 228, 1115-1117.

Mateyko, G.M. & Kopac, M.J. (1963). Cytophysical studies on living normal and neoplastic cells. ANN. NY. ACAD. SCI., 105, 185-218.

McGeer, P.L. (1984). The 12th J.A.F. Stevenson memorial lecture: Aging, Alzheimer's disease and the cholinergic system. CAN. J. PHYSIOL. PHARMACOL., 62, 741-754.

McIntosh, C.H.S. & Plummer, D.T. (1976). The subcellular localisation of acetylcholinesterase and its molecular forms in pig cerebral cortex. J. NEUROCHEM., 27, 449-457.

McLennan, M. & Hicks, T.P. (1978). Pharmacological characterisation of the excitatory cholinergic receptors of rat central neurones. NEUROPHARMACOL., 17, 329-334.

Meyer, E.M.Jr., Engel, D.A. & Cooper, J.R. (1982). Acetylation and phosphorylation of choline following high or low affinity uptake by rat cortical synaptosomes. NEUROCHEM. RES., 7, 749-759.

Miledi, R. (1973). Transmitter release induced by injection of calcium ions into nerve terminals. PROC. R. SOC. LOND. B., 183, 421-425.

Mills, A. & Wonnacott, S. (1984). Antibodies to nicotinic acetylcholine receptors used to probe the structural and functional relationships between brain α-Bungarotoxin binding sites and nicotinic receptors. NEUROCHEM. INT., 6, 249-257.

Misgeld, U. & Frotscher, M. (1982). Dependence of the viability of neurons in hippocampal slices on oxygen supply. BRAIN RES. BULL., 8, 95-100.

Mizobe, F. & Livett, B.G. (1982). Biphasic effect of eserine and other acetylcholinesterase inhibitors on the nicotinic response to acetylcholine in cultured adrenal chromaffin cells. J. NEUROCHEM., 39, 379-385.

Mizuno, Y., Oomura, Y., Hori, N. & Carpenter, D.O. (1984). Action of vasopressin on CA1 pyramidal neurons in rat hippocampal slices. BRAIN RES., 309, 241-246.

Morley, B.J., Kemp, G.E. & Salvaterra, P. (1979). α-Bungarotoxin binding sites in the CNS. LIFE SCI., 24, 859-872.

Morris, D. & Grewaal, D.S. (1971). Human placental choline acetyltransferase. Radiometric assay, inhibition by analogues of choline and acetylcholine and isotopic exchange between choline and acetylcholine. EUR. J. BIOCHEM., 22, 563-572.

Moss, S.J. & Wonnacott, S. (1985). Presynaptic nicotinic autoreceptors in rat hippocampus. BIOCHEM. SOC. TRANS., 13, 164-165.

Muller, D., Joly, M. & Lynch, G. (1988). Contributions of quisqualate and NMDA receptors to the induction and expression of LTP. SCI. (USA), 242, 1694-1697.

Murrin, L.C. & Kuhar, M.J. (1976). Activation of high affinity choline uptake in vitro by depolarising agents. MOL. PHARMACOL., 12, 1082-1090.

Nagy, A. & Delgado-Escueta, A.V. (1984). Rapid preparation of synaptosomes from mammalian brain using non-toxic isoosmotic gradient material (Percoll). J. NEUROCHEM., 43, 1114-1123.

Nestler, E.J. & Greengard, P. (1983). Protein phosphorylation in the brain. NATURE (LOND.), 305, 583-588.

Noda, M., Takahashi, H., Tanabe, T., Toyosato, M., Furutani, Y., Hirose, T., Asai, M., Inayama, S., Miyata, T. & Numa, S. (1982). Primary structure of α subunit precursor of Torpedo californica acetylcholine receptor deduced from cDNA sequence. NATURE (LOND.), 299, 793-797.

Noda, M., Takahashi, H., Tanabe, T., Toyosato, M., Kikyotani, S., Hirose, T., Asai, M., Takashima, H., Inayama, S., Miyata, T. & Numa, S. (1983). Primary structures of β and γ subunit precursors of Torpedo californica acetylcholine deduced from cDNA sequences. NATURE (LOND.), 301, 251-255.

Nordberg, A. & Winblad, B. (1986). Reduced number of [^{3}H]nicotine and [^{3}H]acetylcholine binding sites in the frontal cortex of Alzheimer brains. NEUROSCI. LETT., 72, 115-119.

Nordberg, A., Alafuzoff, I. & Winblad, B. (1986). Muscarinic receptor subtypes in hippocampus in Alzheimer's disease and mixed dementia type. NEUROSCI. LETT., 70, 160-164.

Nordberg, A., Adem, A., Hardy, J. & Winblad, B. (1988). Change in nicotinic receptor subtypes in temporal cortex. NEUROSCI. LETT., 86, 317-321.

Nordstrom, O. & Bartfai, T. (1980). Muscarinic autoreceptor regulates acetylcholine release in rat hippocampus: in vitro evidence. ACTA PHYSIOL. SCAND., 108, 347-353.

Oiki, S., Danho, W., Madison, V. & Montal, M. (1988). M2 δ, a candidate for the structure lining the ionic channel for the nicotinic cholinergic receptor. PROC. NAT. ACAD. SCI. (USA), 85, 8703-8707.

Park, T.H., Tachiki, K.H., Summers, W.K., Kling, D., Fitten, J., Perryman, K., Spidell, K. & Kling, A.S. (1986). Isolation and the fluorometric, high-performance liquid chromatographic determination of tacrine. ANAL. BIOCHEM., 159, 358-362.

Pepeu, G. (1983). Brain acetylcholine: an inventory of our knowledge on the 50th anniversary of its discovery. TRENDS PHARMACOL. SCI., 4, 416-418.

Peralta, E.G., Winslow, J.W., Peterson, G.L., Smith, D.L., Ashkenazi, A., Ramachandran, J., Schimerlik, M.I. & Capon, D.J. (1987). Primary structure and biochemical properties of a M_2 muscarinic receptor. SCI. (USA), 236, 600-605.

Perry, E.K. & Perry, R.H. (1985). New insights into the nature of senile (Alzheimer-type) plaques. TRENDS NEUROSCI., 8, 301-303.

Perry, E.K., Tomlinson, B.E., Blessed, G., Bergmann, K., Gibson, P.H. & Perry, R.H. (1978). Correlation of cholinergic abnormalities with senile plaques and mental test scores in senile dementia. BRIT. MED. J., 2, 1457-1459.

Perry, E.K., Perry, R.H., Smith, C.J., Purohit, D., Bonham, J., Dick, D.J., Candy, J.M., Edwardson, J.A. & Fairbairn, A. (1986). Cholinergic receptors in cognitive disorders. CAN. J. NEUROL. SCI., 13, 521-527.

Perry, E.K., Perry, R.H., Smith, C.J., Dick, D.J., Candy, J.M., Edwardson, J.A., Fairbairn, A. & Blessed, G. (1987). Nicotinic receptor abnormalities in Azheimer's and Parkinson's diseases. J. NEUROL. NEUROSURG. PSYCHIAT., 50, 806-809.

Perry, E.K., Smith, C.J., Court, J.A., Bonham, J.R., Rodway, M. & Atack, J.R. (1988). Interaction of 9-amino-1,2,3,4,-tetrahydroacridine (THA) with human cortical nicotinic and muscarinic receptor binding in vitro. NEUROSCI. LETT., 91, 211-216.

Perry, E.K., Smith, C.J., Perry, R.H., Johnson, M. & Fairbairn, A.F. (1989). Nicotinic ([^{3}H]nicotine) receptor binding in human brain: characterisation and involvement in cholinergic neuropathology. NEUROSCI. RES. COMMUN., 5, 117-122.

Pfaffinger, P.J., Martin, J.M., Hunter, D.D., Nathanson, M.M. & Hille, B. (1985). GTP binding proteins couple cardiac muscarinic receptors to a K^+ channel. NATURE (LOND.), 317, 536-538.

Pharmacia Fine Chemicals, Percoll reference list (1982).

Potter, L.T., Flynn, D.D., Hanchett, H.E., Kalinoski, D.L., Luber-Narod, J. & Mash, D.C. (1984). Independent M_1 and M_2 receptors: ligands, autoradiography and functions. TRENDS PHARMACOL. SCI., 5 (Suppl.), 22-31.

Quik, M. & Geertsen, S. (1988). Neuronal nicotinic α-bungarotoxin sites. CAN. J. PHYSIOL. PHARMACOL., 66, 971-979.

Raiteri, M., Leardi, R. & Marchi, M. (1984). Heterogeneity of presynaptic muscarinic receptors regulating neurotransmitter release in rat brain. J. PHARMACOL. EXP. THER., 228, 209-214.

Rapier, C., Wonnacott, S., Lunt, G.G. & Albuquerque, E.X. (1987). The neurotoxin histrionicotoxin interacts with the putative ion channel of the nicotinic acetylcholine receptors in the central nervous system. FEBS Lett., 212, 292-296.

Rapier, C.M., Lunt, G.G. & Wonnacott, S. (1988). Stereoselective nicotine-induced release of dopamine from striatal synaptosomes: concentration dependence and repetitive stimulation. J. NEUROCHEM., 50, 1123-1130.

Reid, K.H., Schurr, A., Tseng, M.T. & Edmonds, H.L. Jr. (1984). Resistance to hypoxia in the rat hippocampal slice. BRAIN RES., 302, 387-391.

Reuleuke, M. & Hucho, F. (1985). High- and low-affinity binding of [^{3}H]acetylcholine at nicotinic cholinergic receptors in rat brain. NEUROSCI. LETT., 59, 271-276.

Reynolds, E.S. (1963). The use of lead citrate at high pH as an electron-opaque stain in electron microscopy. J. CELL BIOL., 17, 208-212.

Richter, J.A. & Marchbanks, R.M. (1971). Isolation of [^{3}H]acetylcholine pools by subcellular fractionation of cerebral cortex slices incubated with [^{3}H]choline. J. NEUROCHEM., 18, 705-712.

Robinson, P.J. & Lovenberg, W. (1986). Dopamine and serotonin in two populations of synaptosomes isolated by Percoll gradient centrifugation. NEUROCHEM. INT., 9, 455-458.

Rogawski, M.A. (1987). Tetrahydroaminoacridine blocks voltage-dependent ion channels in hippocampal neurons. EUR. J. PHARMACOL., 142, 169-172.

Romano, C. & Goldstein, A. (1980). Stereospecific nicotine receptors in rat brain membranes. SCI. (USA), 210, 647-650.

Roskoski, R. Jr., Mayer, H.E. & Schmid, P.G. (1974). Choline acetyltransferase activity in guinea pig heart in vitro. J. NEUROCHEM., 23, 1197-1200.

Rossor, M.N., Emson, P.C., Mountjoy, C.Q., Roth, M. & Iversen, L.L. (1980). Reduced amounts of immunoreactive somatostatin in the temporal cortex in senile dementia of Alzheimer type. NEUROSCI. LETT., 20, 373-377.

Rovira, C., Ben-Ari, Y., Cherubini, E., Krnjevic, K. & Ropert, N. (1983). Pharmacology of the dendritic action of acetylcholine and further observations on the somatic disinhibition in the rat hippocampus in situ. NEUROSCI., 8, 97-106.

Rowell, P.P. & Winkler, D.L. (1984). Nicotinic stimulation of [^{3}H]acetylcholine release from mouse cerebral cortical synaptosomes. J. NEUROCHEM., 43, 1593-1598.

Rylett, R.J. (1989). Synaptosomal "membrane-bound" choline acetyltransferase is most sensitive to inhibition by choline mustard. J. NEUROCHEM., 52, 869-875.

Sadoshima, J., Tokutomi, N. & Akaike, N. (1988). Effects of neostigmine and physostigmine on the acetylcholine receptor-ionophore complex in frog isolated sympathetic neurones. BR. J. PHARMACOL., 94, 620-624

Sahakian, B., Jones, G., Levy, R., Gray, J. & Warburton, D. (1989). The effects on attention, information processing and short-term memory in patients with dementia of the Alzheimer type. BRIT. J. PSYCHIAT., 154, 797-800.

Sastry, B.R. (1982). Presynaptic change associated with long-term potentiation in hippocampus. LIFE SCI., 30, 2003-2008.

Schiff, S.J. & Somjen, G.G. (1985). The effects of temperature on synaptic transmission in hippocampal tissue slices. BRAIN RES., 345, 279-284.

Schuberth, J. & Sundwall, A. (1967). Effects of some drugs on the uptake of acetylcholine in cortex slices of mouse brain. J. NEUROCHEM., 14, 807-812.

Schurr, A., Reid, K.H., Tseng, M.T., Edmonds, H.L. Jr., West, C.A. & Rigor, B.M. (1986). Effect of electrical stimulation on the viability of the hippocampal slice preparation. BRAIN RES. BULL., 16, 299-301.

Schwartz, R.D., McGee, R.Jr. & Kellar, K.J. (1982). Nicotinic cholinergic receptors labeled by [^{3}H]acetylcholine in rat brain. MOL. PHARMACOL., 22, 56-62.

Segal, M. (1978). The AChR in rat hippocampus: nicotinic, muscarinic or both? NEUROPHARMACOL., 17, 619-623.

Shaw, K.-P., Aracava, Y., Akaike, A., Daly, J.W., Rickett, D.L. & Albuquerque, E.X. (1985). The reversible cholinesterase inhibitor physostigmine has channel-blocking and agonist effects on the acetylcholine receptor-ion channel complex. MOL. PHARMACOL., 28, 527-538.

Shute, C.C.D. & Lewis, P.R. (1963). Cholinesterase-containing systems of the brain of the rat. NATURE (LOND.), 199, 1160-1164.

Simon, J.R. & Kuhar, M.J. (1976). High affinity uptake: ionic and energy requirements. J. NEUROCHEM., 27, 93-99.

Simon, J.R., Atweh, S. & Kuhar, M.J. (1976). Sodium-dependent high affinity choline uptake: a regulatory step in the synthesis of acetylcholine. J. NEUROCHEM., 26, 909-922.

Sitaram, N. (1984). Cholinergic hypothesis of human memory: review of basic and clinical studies. DRUG DEV. RES., 4, 481-488.

Skrede, K.K. & Westgaard, R.H. (1971). The transverse hippocampal slice: a well defined cortical structure maintained in vitro. BRAIN RES., 35, 589-593.

Small, D.H. (1989). Acetylcholinesterases: zymogens of neuropeptide processing enzymes? NEUROSCI., 29, 241-249.

Sokolovsky, M. & Bartfai, T. (1981). Biochemical studies on muscarinic receptors. TRENDS NEUROSCI., 4, 303-305.

Sorimachi, M. & Kataoka, K. (1974). Choline uptake by nerve terminals: a sensitive and a specific marker of cholinergic innervation. BRAIN RES., 72, 350-353.

Steinbach, J.H. & Ifune, C. (1989). How many kinds of nicotinic acetylcholine receptors are there? TRENDS NEUROSCI., 12, 3-6.

Stevens, C.F. (1985). AChRs: five fold symmetry and the E subunit. NEUROSCI., 8, 335-336.

Stevens, C.F. (1989). Long term potentiation: strengthening the synapses. NATURE (LOND.), 338, 460-461.

Stevens, D.R. & Cotman, C.W. (1987). Excitatory actions of tetrahydro-9-aminoacridine (THA) on hippocampal pyramidal neurons. NEUROSCI. LETT., 79, 301-305.

Steward, O. (1976). Topographic organisation of the projections from the entorhinal area to the hippocampal formation of the rat. J. COMP. NEUROL., 167, 285-314.

Summers, W.K., Majovski, L.V., Marsh, G.M., Tachiki, K. & Kling, A. (1986). Oral tetrahydroaminoacridine in long term treatment of senile dementia, Alzheimer type. N. ENGL. J. MED., 315, 1241-1245.

Swanson, L.W., Wyss, J.M. & Cowan, W.M. (1978). An autoradiographic study of the organisation of intrahippocampal association pathways in the rat. J. COMP. NEUROL., 181, 681-716.

Swanson, K.L., Allen, C.N., Aronstam, R.S., Rapoport, H. & Albuquerque, E.X. (1985). Molecular mechanisms of the potent and stereospecific nicotinic receptor agonist (+)Anatoxin-a. MOL. PHARMACOL., 29, 250-257.

Szerb, J.C. & Somogyi, G.T. (1973). Depression of acetylcholine release from cerebral cortical slices by cholinesterase inhibition and by oxotremorine. NATURE, NEW BIOL., 241, 121-122.

Takagi, M. (1984). Actions of cholinergic drugs on cells in the interpeduncular nucleus. EXP. NEUROL., 84, 358-363.

Teyler, T.J. (1987). Long term potentiation. In: Brain slices: fundamentals, applications and implications. (Schurr, A., Teyler, T.J. & Tseng, M.T., eds.), Karger, Basel, pp 168-176.

Thorne, B., Irons, J., Lunt, G.G., Wonnacott, S & Dunkley, P.R. (1988). Comparison of methods for rapid isolation of synaptosomes from brain regions, for uptake and release studies. BIOCHEM. SOC. TRANS., 16, 309-310.

Tseng, M.T., McClure, G.D. Jr., Jackson, C.B. & Schurr, A. (1987). Functional morphology of the hippocampal CA1 subfield. In: Brain slices: fundamentals, applications and implications. (Schurr, A., Teyler, T.J. & Tseng, M.T., eds) Karger, Basel, pp 22-38.

Tucek, S. (1985). Regulation of acetylcholine synthesis in the brain. J. NEUROCHEM., 44, 11-24.

Verity, M.A. (1972). Cation modulation of synaptosomal respiration. J. NEUROCHEM., 19, 1305-1317.

Vidal, C. & Changeux, J.-P., (1989). Pharmacological profile of nicotinic acetylcholine receptors in the rat prefrontal cortex: an electrophysiological study in a slice preparation. NEUROSCI., 29, 261-270.

Vizi, V.A. & Ashley, R.H. (1987). Relation of acetylcholine release to Ca^{++} uptake and intraterminal Ca^{++} concentration in guinea-pig cortex synaptosomes. J. NEUROCHEM., 49, 1013-1021.

Wada, K., Ballivet, M., Boulter, J., Connelly, J., Wada, E., Deneris, E.S., Swanson, L.W., Heinemann, S. & Patrick, J. (1988). Functional expression of a new pharmacological subtype of brain nicotinic acetylcholine receptor. SCI. (USA), 240, 330-334.

Weintraub, M. & Standish, R. (1988). Tetrahydroaminoacridine: a possible treatment for senile dementia of the Alzheimer's type. HOSP. FORMUL., 23, 31-35.

Wesnes, K. & Warburton, D.M. (1984). Effects of scopolamine and nicotine on human rapid information processing performance. PSYCHOPHARMACOL., 82, 147-150.

Wessler, I., Scheuer, B. & Kilbinger, H. (1987). [^{3}H]Acetylcholine release from the phrenic nerve is increased or decreased by activation or desensitisation of nicotine receptors. EUR. J. PHARMACOL., 135, 85-87.

White, H.L. & Wu, J.C. (1973). Choline and carnitine acetyltransferases of heart. BIOCHEMISTRY, 12, 841-846.

Whitehouse, P.J. & Kellar, K.J. (1987). Nicotinic and muscarinic cholinergic receptors in Alzheimer's disease and related disorders. J. NEURAL. TRANSM., 24 (Suppl), 175-182.

Whitehouse, P.J., Price, D.L., Clark, A.W., Coyle, J.T. & DeLong, M.R. (1981). Alzheimer disease: evidence for selective loss of cholinergic neurons in the nucleus basalis. ANN. REV. NEUROL., 10, 122-126.

Whitehouse, P.J., Price, D.L., Struble, R.G., Clark, A.W., Coyle, J.T. & DeLong, M.R. (1982). Alzheimer's disease and senile dementia: loss of neurons in the basal forebrain. SCI. (USA), 215, 1237-1239.

Whitehouse, P.J., Martino, A.M., Antuono, P.G., Lowenstein, P.R., Coyle, J.T., Price, D.L. & Kellar, K.J. (1986). Nicotinic acetylcholine binding sites in Alzheimer's disease. BRAIN RES., 371, 146-151.

Whitehouse, P.J., Martino, A.M., Marcus, K.A., Zweig, R.M., Singer, H.S., Price, D.L. & Kellar, K.J. (1988). Reductions in acetylcholine and nicotine binding in several degenerative diseases. ARCH. NEUROL., 45, 722-724.

Whiting, P., Esch, F., Shimasaki, S. & Lindstrom, J. (1987). Neuronal nicotinic acetylcholine receptor β-subunit is coded for by the cDNA α_4. FEBS Lett.,219, 459-463.

Whittaker, V.P. (1969). The synaptosome. In: Handbook of Neurochemistry. (Lajtha, A. ed.) Plenum Press, New York, pp 327-364.

Wilcock, G.K. & Esiri, M.M. (1982). Plaques, tangles and dementia: a quantitative study. J. NEUROL. SCI., 56, 343-356.

Wilcock, G.K., Esiri, M.M., Bowen, D.M. & Smith, C.C.T. (1982). Alzheimer's disease: correlation of cortical choline acetyltransferase activity with the severity of dementia and histological abnormalities. J. NEUROL. SCI., 57, 407-417.

Wong, P.T.-H. & Prince, A.K. (1978). The membrane binding of choline acetyltransferase: uptake and acetylation of [^{3}H]choline in rabbit cortical slices. NEUROPHARMACOL., 18, 511-513.

Wonnacott, S. (1986). α-Bungarotoxin binds to low-affinity nicotine binding sites in rat brain. J. NEUROCHEM., 47, 1706-1712.

Wonnacott, S. & Marchbanks, R.M. (1976). Inhibition by botulinum toxin of depolarisation-evoked release of [^{14}C]acetylcholine from synaptosomes in vitro. BIOCHEM. J., 156, 701-712.

Wonnacott, S., Irons, J., Lunt, G.G., Rapier, C.M. & Albuquerque, E.X. (1988). α-Bungarotoxin and presynaptic nicotinic receptors: functional studies. In: Nicotinic acetylcholine receptors in the nervous system. (Clementi, F., Gotti, C. & Sher, E. eds.) Springer-Verlag, Heidelberg, pp 41-60.

Yamamoto, C. & McIlwain, H. (1966). Electrical activities in thin sections from the mammalian brain maintained in chemically defined media in vitro. J. NEUROCHEM., 13, 1333-1343.

Yamamura, H.I. & Snyder, S.H. (1972). Choline: high affinity uptake by rat brain synaptosomes. SCI. (USA), 178, 626-628.

Yamamura, H.I. & Snyder, S.H. (1973). High affinity transport of choline into synaptosomes of rat brain. J. NEUROCHEM., 21, 1355-1374.

Yamamura, H.I. & Snyder, S.H. (1974). Postsynaptic localisation of muscarinic receptor binding in rat hippocampus. BRAIN RES., 78, 320-326.